PHASE TRANSFORMATION
IN THE ELECTRODEPOSITION OF TITANIUM
FROM MOLTEN SALTS

Marco Vincenzo Ginatta

T 1342

A thesis submitted to the Faculty and the Board of Trustees of the Colorado School of Mines in partial fulfillment of the requirements for the degree of Master of Science.

Signed:_____

Marco V. Ginatta

Golden, Colorado

Date: November 23 , 1970

Approved:_____

T. Balberyszski
Thesis Advisor

_____

P. G. Herold
Head of Department
Metallurgical Engineering

Golden, Colorado

Date: December 2 ,1970

ABSTRACT

To date all refractory metals have been successfully electroplated from fused salts to any desired thickness. Only titanium has so far resisted producing a flat, smooth cathodic deposition, yielding instead a formation of dendrites and whiskers.

In this study the nature of the electrodeposition of titanium is investigated. The effects of temperature, current density, current pulsations, periodic reversed current, periodic reversed current with dead time, low frequency vibrations, and ultrasonic vibrations on the cathodic deposition of titanium are studied.

A mechanism which explains the anomalous behavior of titanium during electrodeposition is postulated.

TABLE OF CONTENTS

LIST OF FIGURES

Figure Page

Figures Page

ACKNOWLEDGMENTS

The author wishes to express his appreciation to Prof. T. Balberyszski, Department of Metallurgical Engineering, Colorado School of Mines, for his guidance and assistance throughout this investigation.

The author would like to thank Mr. J. C. Priscu, Supervisor, Process Development Division, Titanium Metals Corporation of America, and Mr. E. K. Kleespies, Research Metallurgist, United States Bureau of Mines, for their suggestions and comments during the progress of this investigation. The author would also like to express his appreciation to his colleagues, Graduate Students of the Metallurgical Engineering Department, for the stimulating discussions on the subject, which resulted in some new approaches used in this study.

The author wishes to send special thanks to his Mother for her help, encouragement and support necessary to complete this investigation.

INTRODUCTION

The cost of producing titanium by thermal reduction methods is affected by the cost of the reducing agents, Mg and Na. Electrolytic processes could reduce this cost considerably. So far the only notable advancement toward an economic replacement of the commonly used Kroll process has been made by Timet[192] which in 1967 started the first commercial facility to produce titanium sponge electrolytically. There are, nevertheless, some industrial applications of electrolytic refining of titanium, particularly for low grade sponge, titanium melting wastes and titanium based alloy scrap.

In present day practice, all refractory metals can be electroplated from fused salts to any desired thickness. In the case of titanium, however, deposits thicker than 0.1 mm are impossible to obtain without the formation of dendrites and whiskers. For this reason the present industrial practice in titanium production is complex, and consists of the following operations.

A. Electro-winning of a sponge containing approximately 50 percent salt.

B. Grinding of the sponge.

C. Leaching of the sponge with possible partial reoxidation (or vacuum distillation).

D. Electrode compacting by welding, with possible partial reoxidation.

E. First arc vacuum melting.

F. Second arc vacuum melting.

The purpose of this study is, therefore, to understand why titanium has a tendency to deposit electrolytically in the form of dendrites, whiskers, and platelets and, furthermore, to investigate the conditions for electrolytic refining of titanium which will result in a compact titanium cathode, free of dendritic growth with little, if any, entrapped electrolyte. Such a cathode would be ready for one stage arc vacuum melting to obtain titanium ingots without further metallurgical processing.

This is a comparative study between the characteristics of the deposits obtained in classic electrolytic refining, which shall be referred to as the CER deposit, and deposits obtained by the application of the following parameters:

1) High Temperature.
2) Low Current Density.
3) Current Pulsations.
4) Periodic Reversed Current.
5) Periodic Reversed Current with Dead Time.
6) Low Frequency Vibrations.
7) Ultrasonic Vibrations.

MATERIALS, EQUIPMENT, AND EXPERIMENTAL PROCEDURES

The refining of titanium, to a high degree of purity, requires rigorous procedures for establishing and maintaining pure electrolytes. One of the essential steps is the elimination of any oxygen and nitrogen. This is necessary for two reasons: Firstly, titanium metal reacts rapidly with O_2 and N_2 forming, in the case of oxygen a solid solution of TiO_x and, secondly, because the electrolyte itself will react with these gases according to:[130]

$$3TiCl_2 + N_2 \rightarrow TiN_2 + 2TiCl_3$$

Since it is not advisable[190] to expose high purity deposits (high purity is defined as less than 75 Brinell Hardness Number) to air at temperatures higher than 100°C, the electrolytic cell was built as shown in figure 1. The expanded upper section of the cell (cold chamber) permits the running of many different tests under comparable conditions; valve 5 preserves the purity of the atmosphere in contact with the surface of the bath while changing experimental parameters, and it allows the cooling of the cathode while the bath is maintained molten at a constant temperature. In this investigation, helium gas has been used, rather than argon; this is because using helium at the same

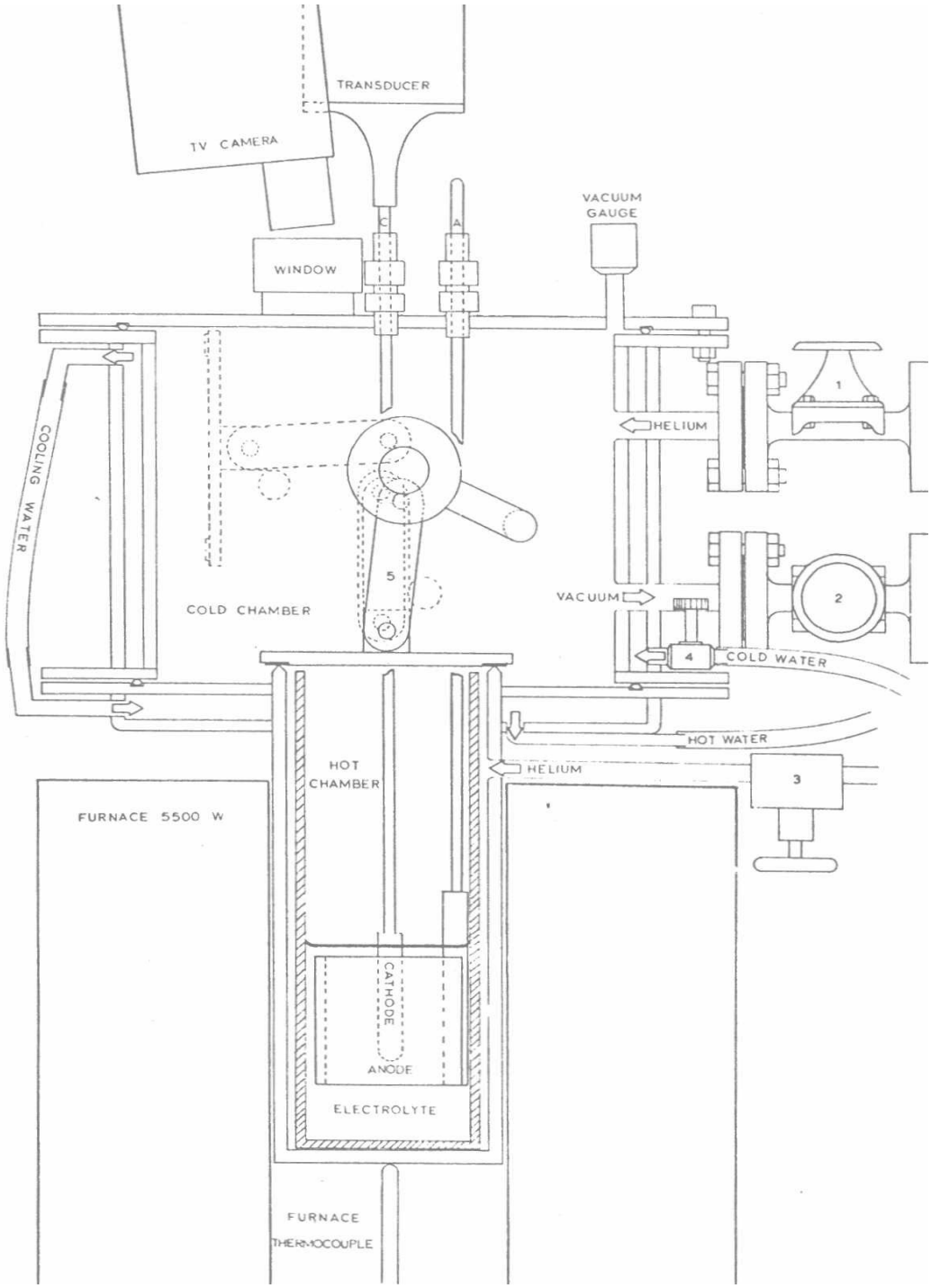

Fig. 1 – Arrangement of the electrolytic cell and auxiliary equipment

gas flow rate and temperature, a much smaller amount of salt volatized, and also because in the case of helium there is a lower heat convection loss.

The most significant chemical property affecting the technical operation of refining titanium, is the fact that at 800°C $TiCl_2$ and $TiCl_3$ have free energies of formation, per chlorine atom, that are very nearly the same (see Fig. 2). It has been experimentally found that the equilibrium

$$2TiCl_3 + Ti \overset{NaCl}{=\!=\!=\!=\!=\!=} 3TiCl_2$$

is very easily affected by contaminants in the titanium or by materials including gases, metals, elements, and compound contacting the bath.

Reactions with oxide materials such as glass, silica, thoria, etc. proceed rapidly at high temperatures and preclude the use of these materials in the construction of refining cells. The reactions with silica may be assumed to be as follows:

$$7TiCl_2 + SiO_2 \overset{NaCl}{=\!=\!=\!=\!=\!=} 2TiOCl + TiSi + 4TiCl_3$$

$$2TiOCl + Ti(anode) = 2TiO + TiCl_2$$

High density alumina can be used, but is not advisable because of the possibility of oxygen contamination.

TiCl will also react with various metals, as indicated

by the reaction:

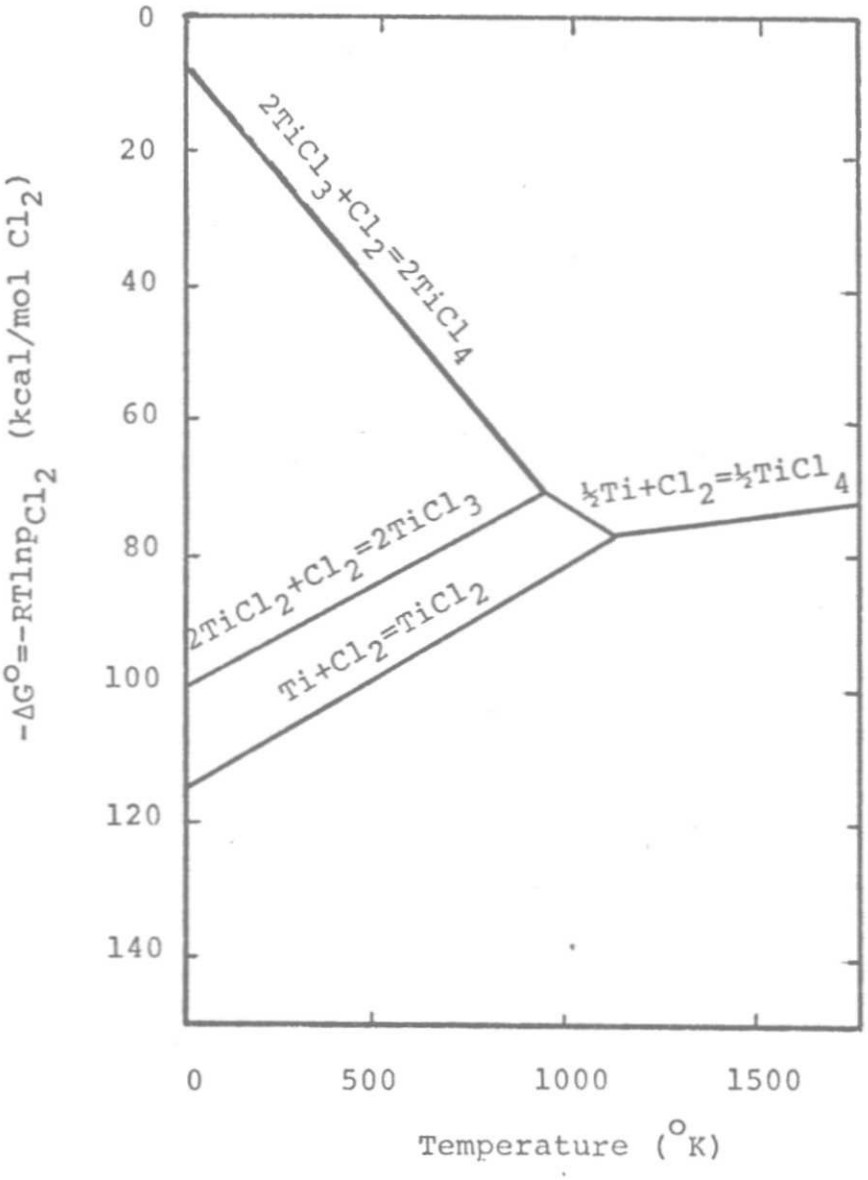

Fig. 2 - The standard free energies of formation of titanium chlorides, the standard state being the pure condensed phases and gas at 1 atm pressure. (Sinha[223])

$$2TiCl_2 + x(Cu,Al,Cr,Mn,etc.) \xrightarrow{NaCl} xMCl_{1/x} + TiCl_3 + Ti$$

These metals may be present as impurities in the anode or in the materials of construction of the apparatus. $TiCl_2$ also reacts with carbon:

$$3TiCl_2 + xC \xrightarrow{NaCl} TiC_x + 2TiCl_3$$

The mechanisms of the above reactions will be the subject of further investigations.

The most suitable material for crucibles to hold titanium electrolytes was found to be iron (mild steel with low carbon content). It forms an intermetallic compound[141] with titanium from the electrolyte, as shown by the reaction:

$$TiCl_2 + xFe \xrightarrow{NaCl} Ti(Fe)_x + TiCl_3$$

but between 750° and 850° this reaction proceeds slowly and results in stable intermetallic compounds.[131] Molybdenum and tungsten are also excellent for crucible material; however, they are expensive. The iron crucible used in these investigations had the following dimensions: 10 cm internal diameter, 28 cm height, and 0.5 cm wall thickness.

The outer lower shell (the hot chamber), valve 5, and the expanded upper section (the cold chamber), were made of stainless steel 321, tungsten-inert-gas welded. Nickel tubing was used for $TiCl_4$ and the thermocouple protection.

The metal basket holding titanium chips for $TiCl_4$ reduction should be molybdenum because of formation of intermetallic compounds with other metals. During the $TiCl_4$ reduction process which produces the electrolyte, a titanium basket of the following dimensions has been found to be suitable: internal diameter 6 cm, height 5 cm, holes 0.5 cm diameter. (Smaller holes proved to be easily clogged, thus not satisfactory for $TiCl_2$ transfer to the bath.) The electrodes, thermocouples, and $TiCl_4$ inlet nickel tube have packing glands with stainless steel 301 followers and Teflon insulating rings.

Since the present investigation is restricted to titanium electrolytic refining, the bath does not change its valency. Therefore, there is no chlorine recovery problem, no anode effect, and no need for separating anolyte and catholyte.

The system to be investigated was Na-Ti-Cl, and the electrolyte composition range was: 80-85 wt% NaCl, 20-15 wt% $TiCl_x$. The reasons for limiting the investigation to chloride systems and particularly to sodium titanium chloride are explained in the discussion section of this study.

Kroll's phase diagram for the $NaCl-TiCl_2$ and $NaCl-TiCl_3$ system is shown in Fig. 3. However, it would be more accurate to study this system as a true ternary diagram, since as can be seen from Fig. 4, the amount of titanium in the electrolyte at any composition, is greater than the

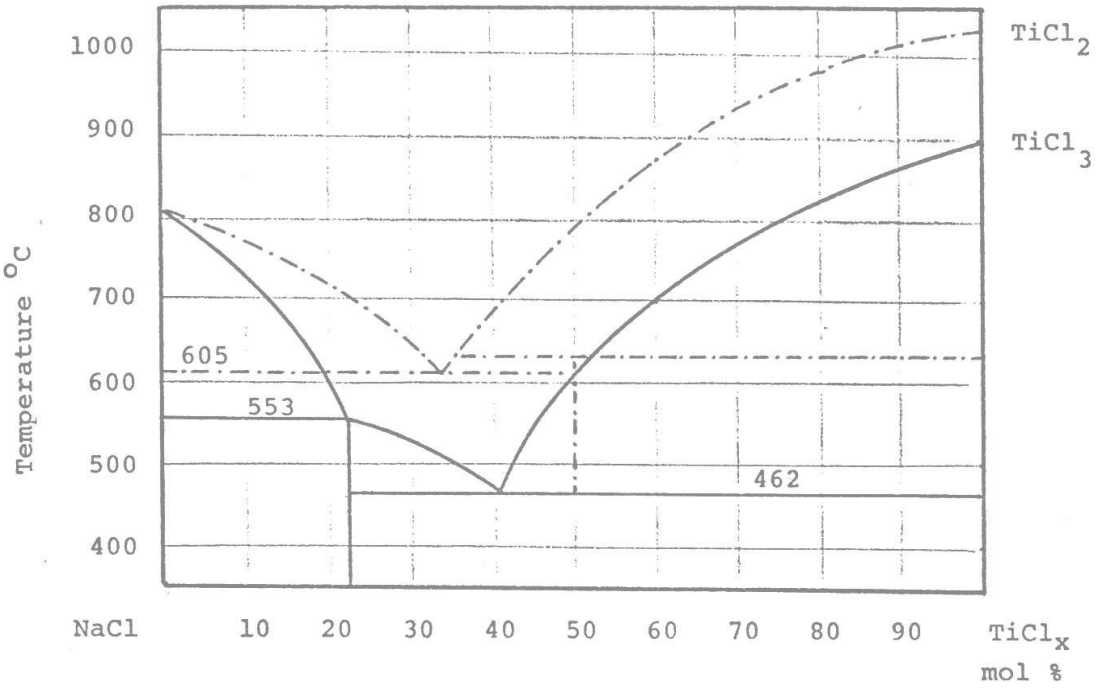

Fig. 3 - System NaCl-$TiCl_2$ NaCl-$TiCl_3$. (Kroll [141])

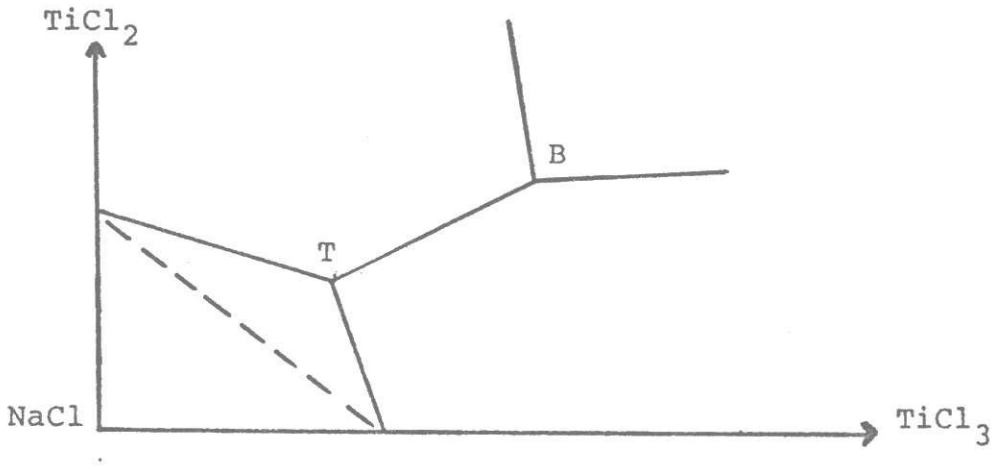

Fig. 4 - Probable configuration of the NaCl corner of the system NaCl-$TiCl_2$-$TiCl_3$; B:binary eutectic $TiCl_2$-$TiCl_3$; T ternary eutectic. (Davey [54])

amount calculated as the average from the values of $TiCl_2$ and $TiCl_3$ on the binary diagram.

Dean et. al.,[57] published a diagram for the ternary system having the components Na-Ti-Cl, that shows the single phase liquid, at 850°C, in which the homogeneous relation of a solution of sodium in fused sodium chloride and titanium chloride takes place.

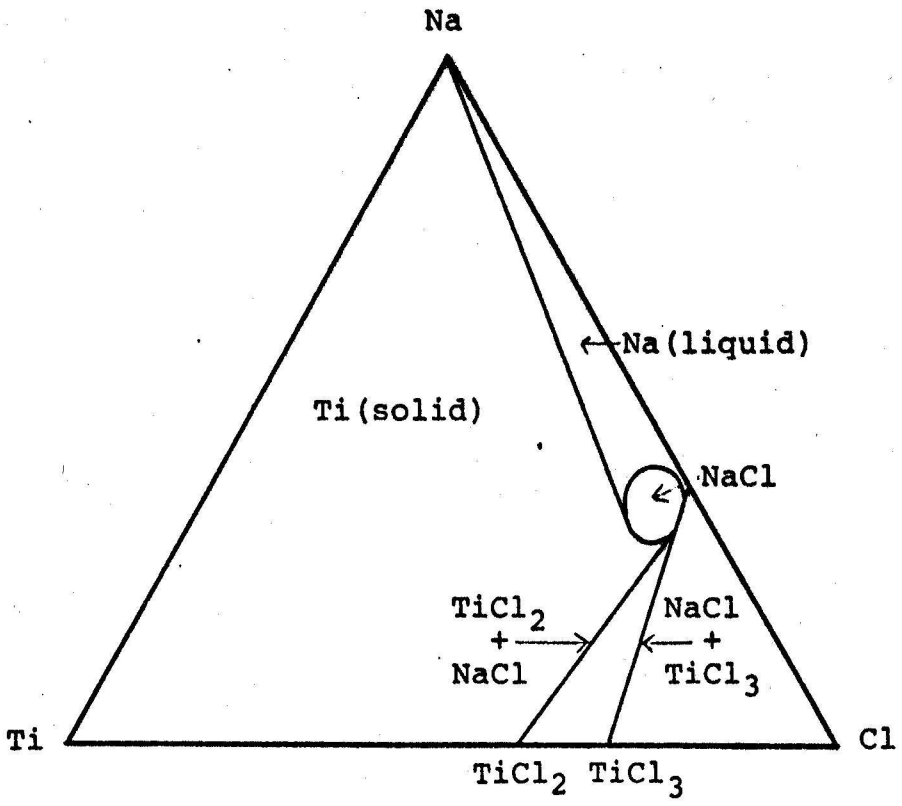

Fig. 5 - System Na-Cl-Ti at 850°C. (Dean et al. [57])

However, since the reducible species of titanium is Ti^{++}, the highest possible proportion of $TiCl_2$ has to be attained. This equilibrium has been experimentally found to be 93% $TiCl_2$ and 7% $TiCl_3$ at concentrations between 10 and 30% $TiCl_x$ at 800°C.[130]

As can be seen from Fig. 3, the assumption of a binary system introduces a little error, since we are considering the NaCl rich region with 93% $TiCl_2$ of the $TiCl_x$.

The furnace used in this study was a multiple unit, 5500 Watt, with a maximum temperature of 1050°C; it was vertically set, had a diameter of 12.5 cm inside, and height of 60 cm. The temperature was controlled by a Barber-Colman controller joined with a Alumel-Chromel Thermocouple in a quartz tube protection, that activates a 110 volt Mercury Relay to drive a 230 volt mechanical contactor.

Valve 4 is the fine control for the flowing rate of the cooling system from 0 to 2.5 l/min. Cold water enters the bottom of the cold chamber and goes out the top of it, re-enters the hot chamber and goes out from the inside ring of the hot chamber.

Valves 1, 2, 3, and 5 control the atmosphere of the cell. Valve 1 is a Grinell Stainless Steel Teflon Diaphragm for helium inlet to the cold chamber. Valve 2 is for the vacuum outlet to the ice trap, to molecular sieves for chlorine, and to the vacuum pump Duo Seal Welch.

Valve 3 is a Grove stainless steel high pressure valve for the inlet into the hot chamber of helium gas below the Vespel valve No. 5. Valve 5 is made of stainless steel 321, with Vespel gasket (DuPont High Temperature Plastic).

Thermocouple vacuum gauge CVC on top plate measures the cell atmosphere pressure.

The power supplies used in this investigation are a Udylite 50 Amp, 15 volt solid state rectifier, with a Unit-Process Assembly for periodically reversing the current, and an Electrolyzer 8 Amp, 12 volt, with a four cam Industrial Timer, for superimposing and reversing the current with dead time.

A Craig Close Circuit Television apparatus with tape-recorder is used to record the progress of the electrolytic process.

Ultrasonic Vibrations Procedure

Vibrations above 16 KHz are applied to the cathode with a molybdenum lead to carry the acoustical energy down to the titanium cathode immersed into the electrolyte.

The equipment consists of a Gulton G-1OOA high frequency generator, with a DTS-1OO transducer working at the frequency range of 16-22 KHz, with an amplitude of 0.002 in. and capable of supplying 100 watts.

A Tektronix 515 Oscilloscope is used for tuning up the cathode assembly, and for maintaining the same frequency

and amplitude of vibration throughout the period of the electrodeposition, the period in which the cathode is increasing in weight.

Since commercially pure titanium, in the 800°C temperature range, has a very low tensile elastic modulus (less than 5,000 Kg/mm^2), the cathode lead was made of molybdenum, which at 800°C has a Young's modulus of about 40,000 Kg/mm^2 and is able to carry down into the electrolytic cell most of the acoustical energy supplied by the transducer.

Because of mechanical problems in threading molybdenum, a 2 cm long, 1.25 cm diameter, stainless steel bush was interposed to connect the molybdenum rod to the transducer horn.

The cathode unit is, therefore, composed of: the transducer horn with 1.25 mm diameter stainless steel tip attached to the stainless steel bush; a molybdenum rod, 6.25 mm diameter connected to the bush, and a titanium cathode, 6 cm long, 1.25 cm diameter rod, with highly polished surface, screwed tight to the molybdenum rod. Such a cathode assembly has three mechanical junctions; that is, it has three wave reflecting surfaces that will send back a sizeable amount of acoustical energy supplied by the transducer.

Nevertheless, in tuning tests in water solutions, at 25°C (the viscosity of the electrolyte at 800°C is approximately 1.5 cp), this cathode produced a sound intensity,

measured at its tip, of about 90% the value of a solid molybdenum bar of equal dimensions.

A critical parameter to be calculated was the overall length of the cathode assembly, that is, the length of the molybdenum lead, in such a way that the immersed part of the cathode would correspond to the nodal part of the wave, to avoid irregularities and traces produced by antinodes.

For 25°C systems this critical length is easily calculated from available data using the following formulas:

$$\text{Wavespeed} = \sqrt{\frac{\text{Young's modulus}}{\text{Density}}}$$

$$\text{Wavelength} = \frac{\text{Wavespeed}}{\text{Frequency}}$$

Therefore, the lead length is the smallest multiple of the wave length that permits the installation of the transducer outside the cell vessel. It must be outside because at temperatures above 100°C the magnetostrictive properties of barium titanate are impaired.

For systems at 800°C, however, it is difficult to determine the wave length because of lack of data. Therefore, we had to proceed by trying several molybdenum leads differing by a fraction of the wave length unit. During these trials, several cathodes with a 0.625 cm diameter titanium rod lead, instead of the molybdenum rod, were tested and the results were satisfactory. This satisfactory performance was obtained due to the hot chamber cooling ring

which, being just above the electrolyte surface when the water flow rate was at 2.5 l/min, cooled most of the cathode lead environment down to about 400°C. The minimum length, that is, the length of the cathode assembly from the transducer horn to the cathode tip was found to be 52 cm.

Electrolyte Preparation

In the salts dehydration procedure the furnace is set at 200°C while the crucible is loaded with approximately 1,500 g of salts. When the thermocouple vacuum gauge measures a cell's atmosphere pressure lower than 10^{-2} Torr, the temperature is increased by 50°C. The cell's atmosphere is flushed once every hour with helium. Typical dehydration schedule for analytical reagent grade NaCl is given in Table l.

The dehydration can be further improved by flushing NaCl with $SOCl_2$ that reacts with the eventually remaining moisture:[149]

$$SOCl_2 + H_2O \rightarrow 2HCl(g) + SO_2(g)$$

The gases can be easily removed by vacuum distillation.

The melting point has to be approached slowly, to avoid boiling and evaporating the salt. Even just above the melting point, NaCl is very fluid and the difference in temperature (approximately 180°C) between the surface and the bottom of the electrolyte generates considerable convection stirring.

Table 1. Dehydration Schedule for Analytical Reagent Grade NaCl.

Time (Hr)	Furnace Temp. (°C)	Electrolyte Surface Temp. (°C)
0	200	
1	250	
2	300	
3	350	
4	400	
5	450	
6	500	
7	550	450
19	600	490
20	650	530
24	700	570
27	750	610
28	800	650
29	850	690
30	900	730
31	950	770
32	1000	810 molten

The electrolyte preparation has to be started just after the NaCl becomes molten. If it is left in the molten state, it will vaporize very quickly and condense in the colder sections of the vessel in large quantities.

A positive pressure of about 1.2 Kg/cm^2 is set above the bath surface, while the titanium basket, loaded with approximately 100 g of titanium chips of high purity (60 BHN), is lowered just above the electrolyte. By means of the nickel tube, $TiCl_4$ is injected from an external Argon pressurized flask, into the titanium chips basket. The titanium subhalides drip into the electrolyte, and finally the basket is immersed and used to stir the bath.

The electrolyte is left for twenty-four hours (soaking period) at approximately 800°C with the titanium basket immersed, to reach the equilibrium:

$$Ti + 2TiCl_3 \;\underset{7\%}{\overset{}{<=====>}}\; \underset{93\%}{3TiCl_2}$$

This equilibrium is temperature dependent. Above 800°C, $TiCl_3$ is favored and very thin platelets of titanium are found floating on the bath surface.

At the same time, the intermetallic compound starts forming on the inner iron crucible surface:

$$Fe + TiCl_x \;\overset{}{====>}\; Fe_yTi_z + TiCl_w$$

where: $x = 2.07$ $w = 2.10$

also:

$$Fe + TiCl_2 \;\overset{}{====>}\; Fe_yTi_z + TiCl_3$$

The thickness x of the diffusion layer at time t, is related according to Schlechten,[234] with the absolute temperature T at which the diffusion occurs, by:

$$\log (x^2/t) = a - b/T$$

where a and b are constants, calculated from the experimental data, different from the diffusion coefficient appearing in Fick's diffusion law.

The Gettering Electrolysis, a preelectrolysis procedure, is performed to purify the bath from Fe, Al, Sn, etc.,- and complex ions. For six hours, a current of 0.05 Amp/cm^2

(anodic) is applied between the titanium chips basket (anode) and the iron crucible, at a bath temperature of 800°C. This titanium plating of the inner surface of the crucible helps the formation of the intermetallic compound. The last step is for all particles floating on the bath surface to be removed with the basket.

Electrolysis Under CER Conditions

Since this work is a comparative study of the properties of deposits obtained in CER and with special parameter electrolysis, experiments were carried out to obtain a standard for CER deposits.

The experimental conditions for CER are as follows: 1) the electrolyte system is Na-Ti-Cl, 2) the maximum cell temperature is 850°C, 3) the starting cathodes are 0.62 cm and 1.25 cm diameter rods with highly polished surfaces, 4) interelectrode distance is up to 3 cm (see figure 6), 5) anode materials are commercially pure titanium strips and bars supplied by Titanium Metals Corp. (magnesium reduced) and by Reactive Metals Inc. (sodium reduced). The anode has a cylindrical shape of 6.5 cm inside diameter, 5.0 cm height, 0.62 cm wall thickness; its lead has to be made of a 3.0 cm diameter titanium rod to resist the bath surface corrosion (not shown in figure 6). The anode irregular cylindrical shape is due to the low ductility of the impure titanium. 6) a 5 wt% HCl aqueous solution is

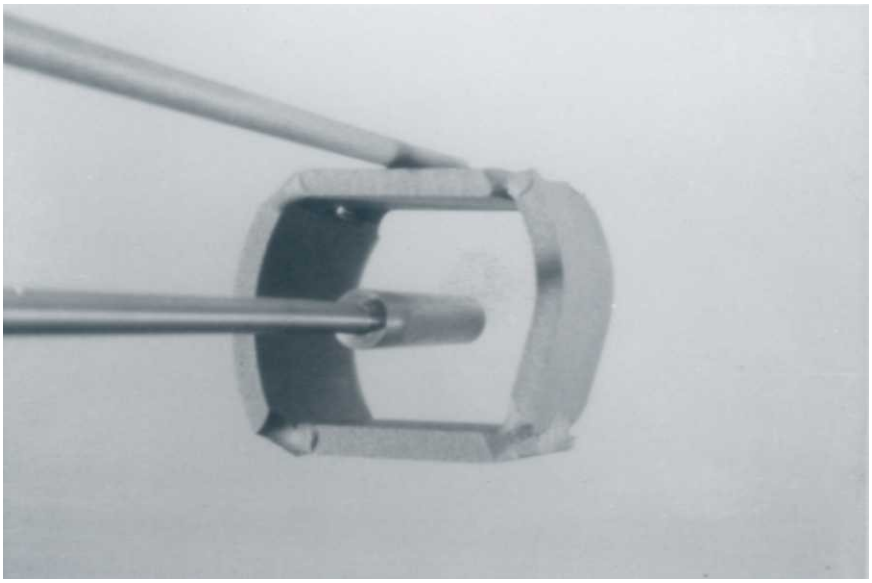

Fig. 6 - Electrodes arrangement; central cylindrical cathode surrounded by coaxial circular anode.

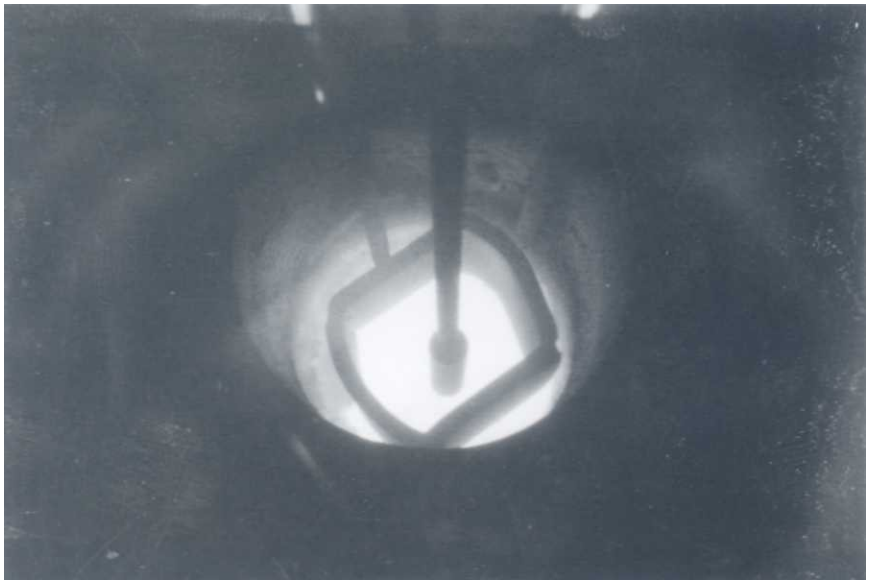

Fig. 7 - Electrolytic cell at the moment of the electrode immersion.

used to leach the entrapped salt from the cathodic deposit, 7) the power supplies deliver a total maximum current of 50 Amp. The electrolytic cell in operating conditions is shown in figure 7.

Special Parameters Electrolytic Refining

To ensure a meaningful comparative study, a number of tests were conducted with two cathodes and two anodes immersed simultaneously in the same electrolyte. One of the cathodes would be operated as a CER cathode, while the other would involve a special parameter.

However, in the experiments involving current density changes the best results (i.e., the sharpest differences from CER deposits) were obtained in the absence of the CER cathode. Clearly, the reason for this difference in deposit can be attributed to the interacting potential fields.

An important stage of the procedure is the 15 minutes immersion of the cathode in the electrolyte, in the absence of an applied potential, to remove the thin film of titanium oxide always present on the surface of titanium metal. As suggested by Schlechten et al.,[234] the titanium metallic surfaces are cleaned by the action of fused chlorides helped by the different expansion coefficient of TiOx that causes the surface oxides to break away in small particles from the solid titanium, and to be reduced by Ti lower valencies ions in the electrolyte.

EXPERIMENTAL RESULTS

Eight different sets of experiments were conducted during the progress of the investigation and their results will be presented sequentially.

Classical Electrolytic Refining

Fig. 8 shows a typical cathode obtained under what have been found to be the best conditions for producing the largest crystals by CER deposition. The crystals, as shown, are coarse up to 3 mm; microscopic observations and x-ray diffraction tests evidenced hexagonal close-packed structure.

This type of deposit was obtained with temperature ranges, at 1 cm below the bath surface, from 730 to 780°C, and at 1 cm above the cell bottom, from 780 to 830°C. The applied current densities ranged from 0.10 to 0.5 amp/cm^2, while the corresponding voltage readings varied from 0.10 to 0.5.

The initial cathodic immersed surface was highly polished and approximately 20 cm^2 in area.

The optimum electrolyte composition was: 80-85 wt% NaCl and 20-15 wt% ($TiCl_2$ + $TiCl_3$); its liquidus line temperature appeared to be about 700°C. The electrolyte was not stirred apart from natural and thermal convection.

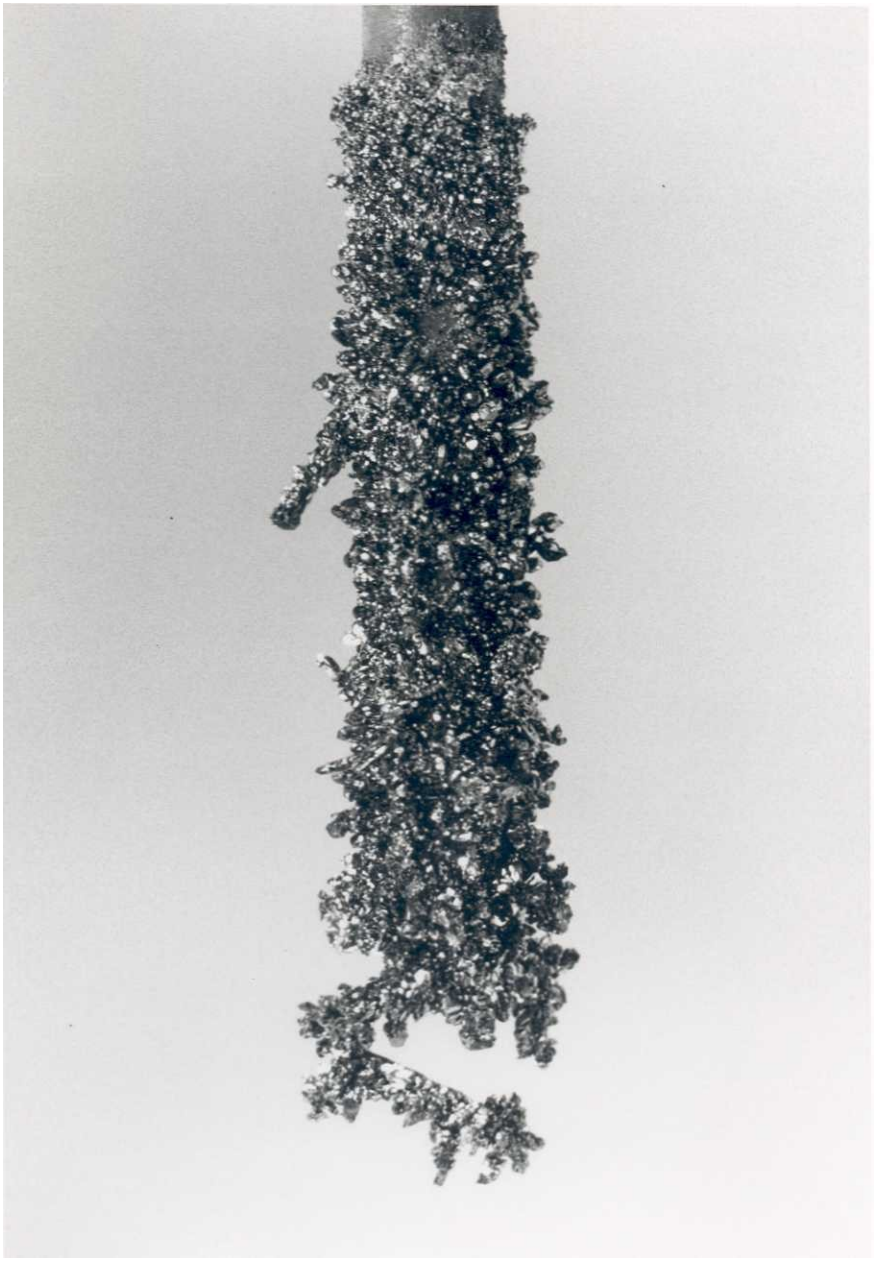

Fig. 8 - Typical deposit obtained under classical electrolytic refining conditions.

The salt dragout ratio, i.e. the weight of entrapped salt over the weight of deposited titanium, was generally less than 0.01.

The current efficiencies on the Ti^{++} bases, calculated from the cathode's weight increase, were in the 60-80% range. The dendrites lost during harvesting and leaching are not accounted for.

The leaching solution remained clear even after more than ten cathodes had been washed. A pink coloration (Ti^{+++} high concentration in solution) indicated that the value of some electrolysis parameter was upset; usually, under these conditions, a black-bluish precipitate appeared in the leaching vessel, evidencing that some sodium has been reduced and was dissolved in the electrolyte entrapped within the deposit.

High Temperature

The upper limit of the apparatus was 1050°C corresponding to 850°C at the electrolyte's surface (@ 150°C above the electrolyte's melting point). At that temperature there is a considerable evaporation of salts and the practical bath lite is much shortened. The deposit grows in form of very small crystals and mostly whiskers, as shown in Fig. 9, while the overall operating conditions, except for temperature, were exactly the same as for CER operations.

Fig. 9 - Deposit obtained at high temperature.

The calculated current efficiency values are meaningless (more than 100%) indicating that the leaching did not remove all the finely entrapped salt.

Low Current Density

At limiting small current densities (less than 0.01 amp/cm^2) very small, thin deposits were produced, but signs of corrosion were noticed on the cathodes surface.

At 0.05 amp/cm^2, with all other variables the same as for the CER state, small crystals, dendrites and whiskers were still obtained.

Current Pulsations

Fig. 10 shows a typical deposition with pulsating current, obtained under the same set of conditions as for CER depositions. (Cathodic deposition lasted for 1.5 sec, then neutral dead time for 4.5 sec,) Microscopic observations showed hexagonal crystals, and x-ray evidenced hexagonal-close-packed structure. These analyses have been carried out on the central part of the cathode.

The dendrites in evidence on the tip and bottom of the cathode are due to the edge effect and to imperfections on the polished surface; otherwise, the cathode surface is flat. A surface close up is shown in Fig. 11.

The electrolyte surface temperature was 740°C, and the cathodic current density 0.1 amp/cm2. The voltage during

Fig. 10 - Deposit resulted with pulsating current.

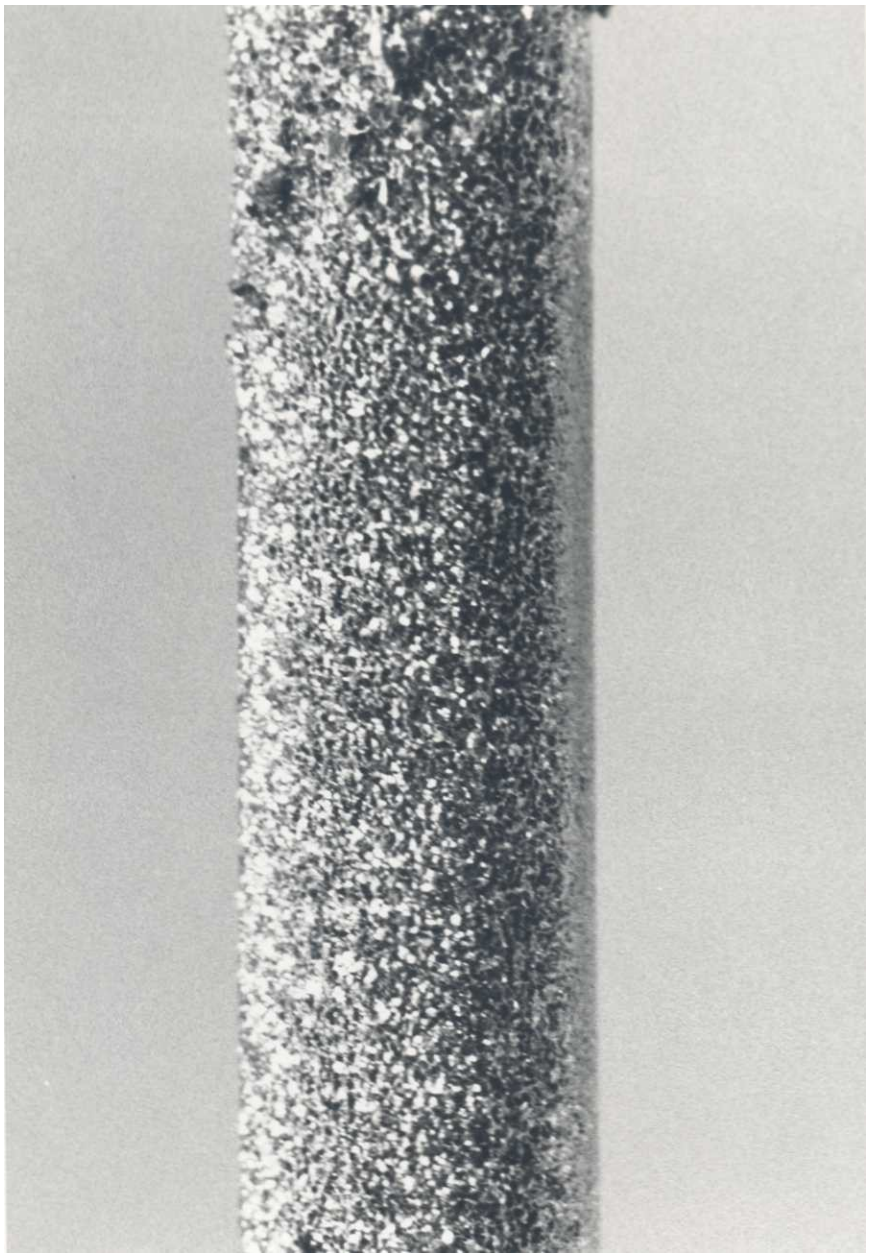

Fig. 11 - Surface close up of the deposit obtained with pulsating current.

the pulses went up to 0.08. The immersed surface area was 20 cm^2. The deposit shown on Fig. 10-11 was obtained after a period of 180 min. of electrolysis. The calculated current efficiencies were above 85%.

Periodic Reversed Current

Fig. 13 shows the type of deposit that is obtained with a direct cathodic deposition of 4.5 sec, and a reversed anodic stripping of 1.5. The operating conditions were: temperature between 775°C and 825°C at the bath surface and initial cathodic current density from 0.1 to 0.5 amp/cm^2. There was no dead time between the cathodic deposition and the subsequent anodic stripping.

The extreme whiskery character of the deposit and the very low dragout ratio are the most interesting differences from the CER cathode, deposited under comparable conditions shown in Fig. 14. The radius of the whiskers increased with increasing current density, that is the finest whiskers were obtained at 0.1 amp/cm^2.

The current efficiency was in the order of 35%, that is equivalent to a CER current efficiency for the deposition time of 70%. But again the whiskers lost in the harvesting procedure and subsequent leaching are not accounted for.

Fig. 13 - Whiskers obtained with a periodically reversed current without dead time.

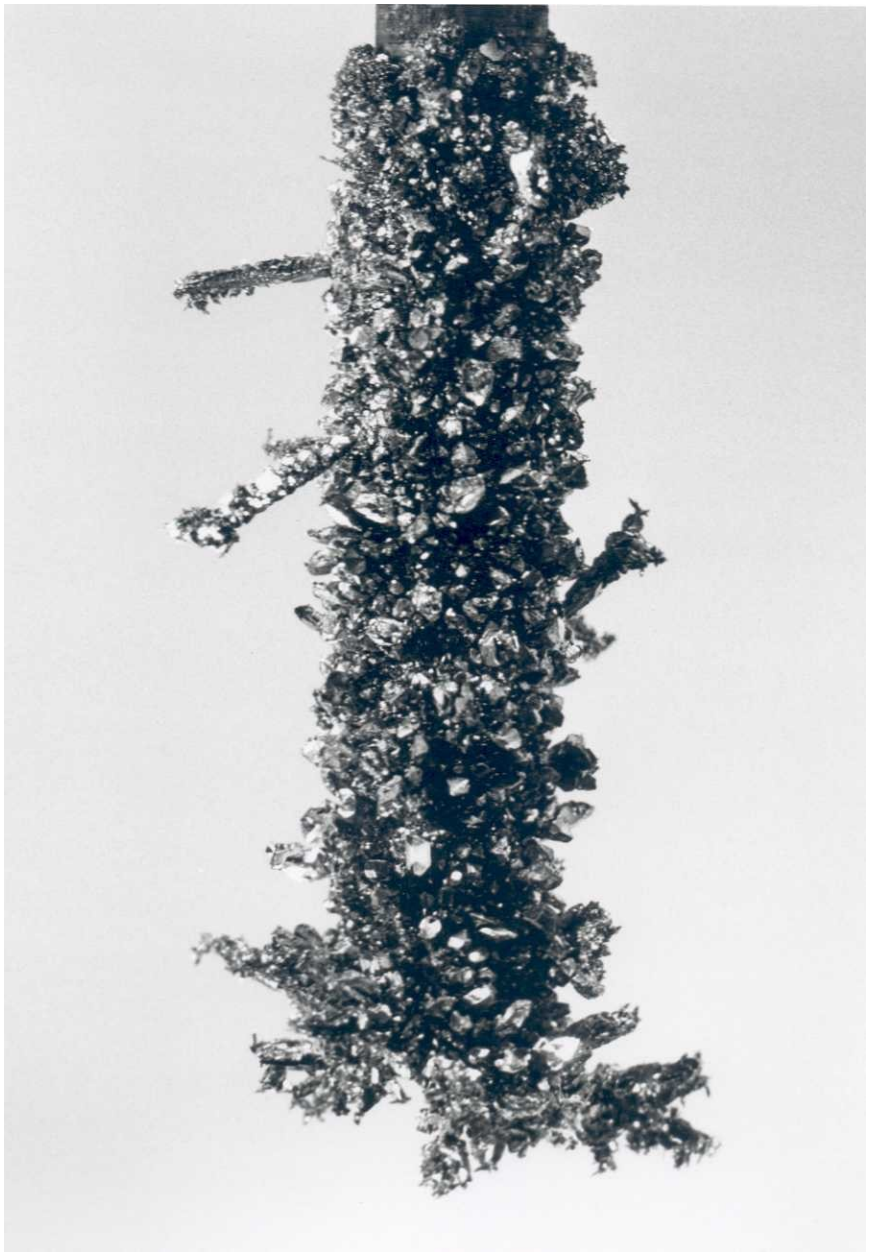

Fig. 14 - CER deposit obtained under the same conditions as for the periodic reversed one shown on Fig. 13.

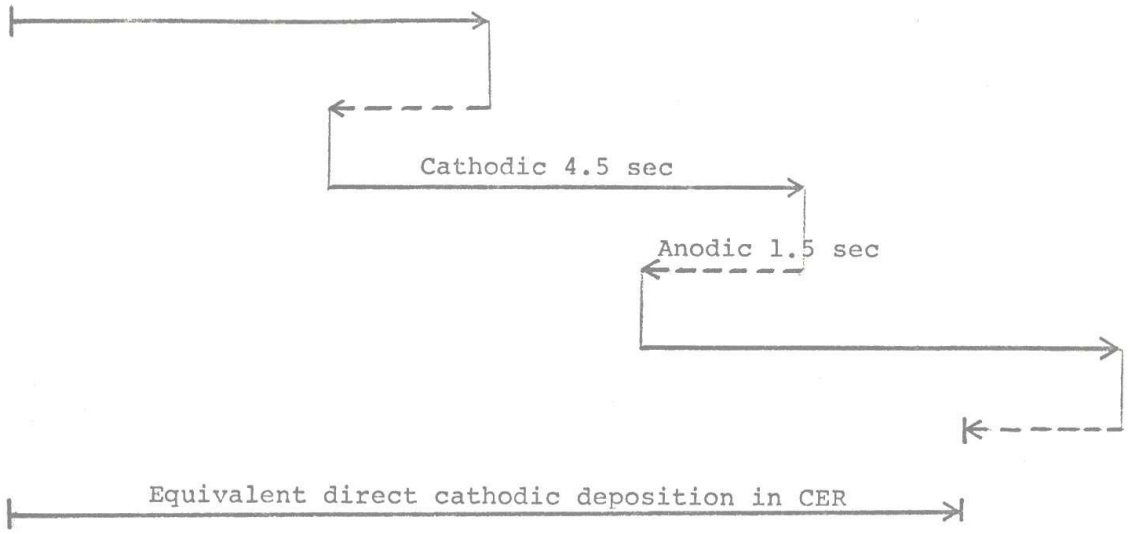

Fig. 12 - Sequence of cathodic growth with a periodic reversed current. __indicates cathode growth; --indicates reversed polarity when the cathode operates as the anode. The system efficiency corresponds to 50% of CER.

Periodic Reversed Current with Dead Time

Fig. 16 shows a typical deposit.

A cathodic deposition of 3 sec followed by 1.2 sec of neutral dead time, then anodic stripping for 0.6 is followed by another neutral time of 1.2 sec before the next cathodic deposition. See Fig.15. The operating temperature range was between 750 and 800°C at the bath surface. The current density can vary from 0.1 and 0.5 amp/cm^2.

The crystal structure obtained looks like something in between the pulsation type of deposition and the periodic reversed current - isolated dendrites on a flat background.

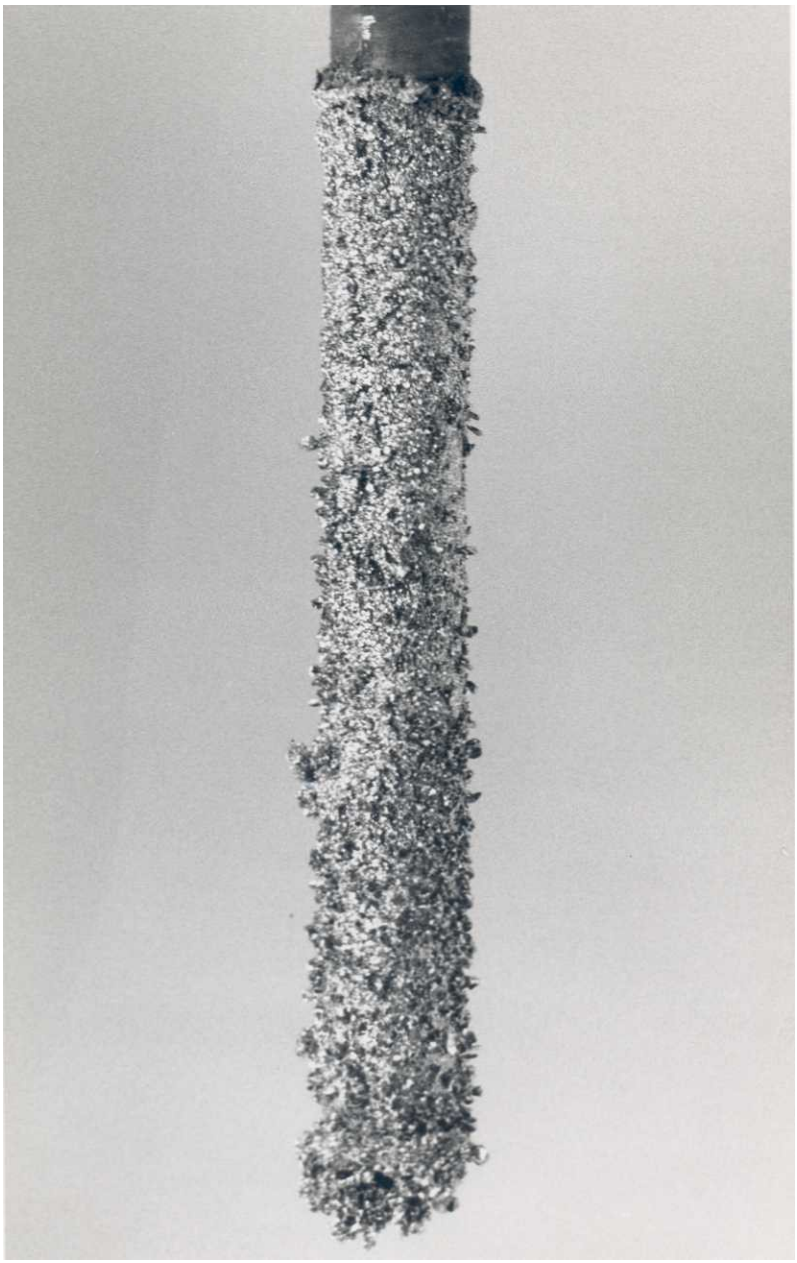

Fig. 16 - Deposit obtained under periodically reversed current with dead time.

As in all the previous sets of experiments, the starting cathode surface was highly polished.

System efficiency was 66.6% and the current efficiency approximately 50%.

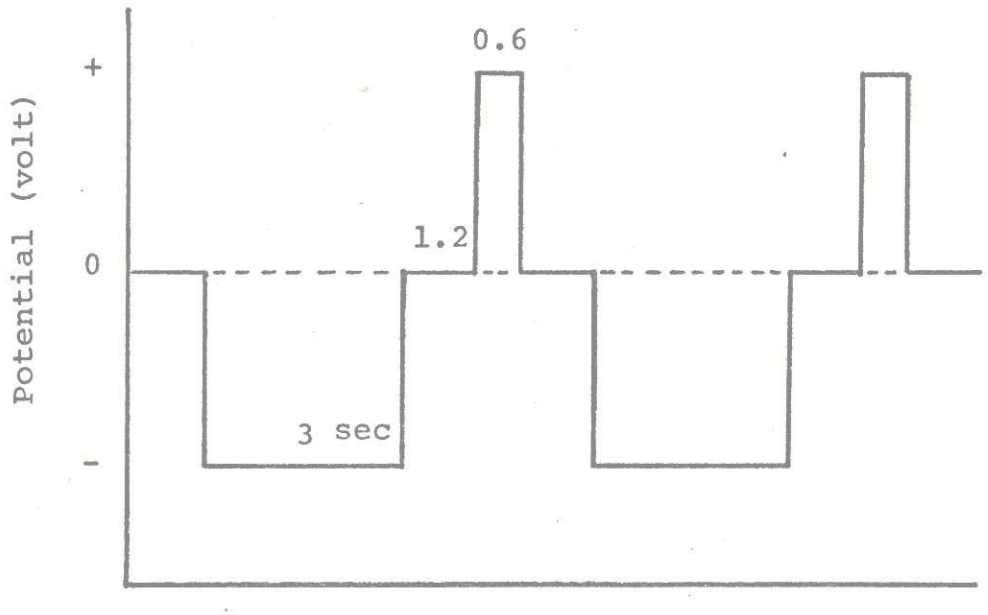

Fig. 15 - Voltage cycle for a periodic reversed current with dead time electrolysis.

Low Frequency Vibrations of the Cathode

Stirring movements applied to the cathode (axial rotation, horizontal translations) at various velocities (from O to 5,000 rpm) have always produced the type of deposit shown in Fig. 17, which is very similar to the ones obtained in CER. Vertical low frequency vibrations (less than 3,000 Hz) considerably damaged the deposit making the

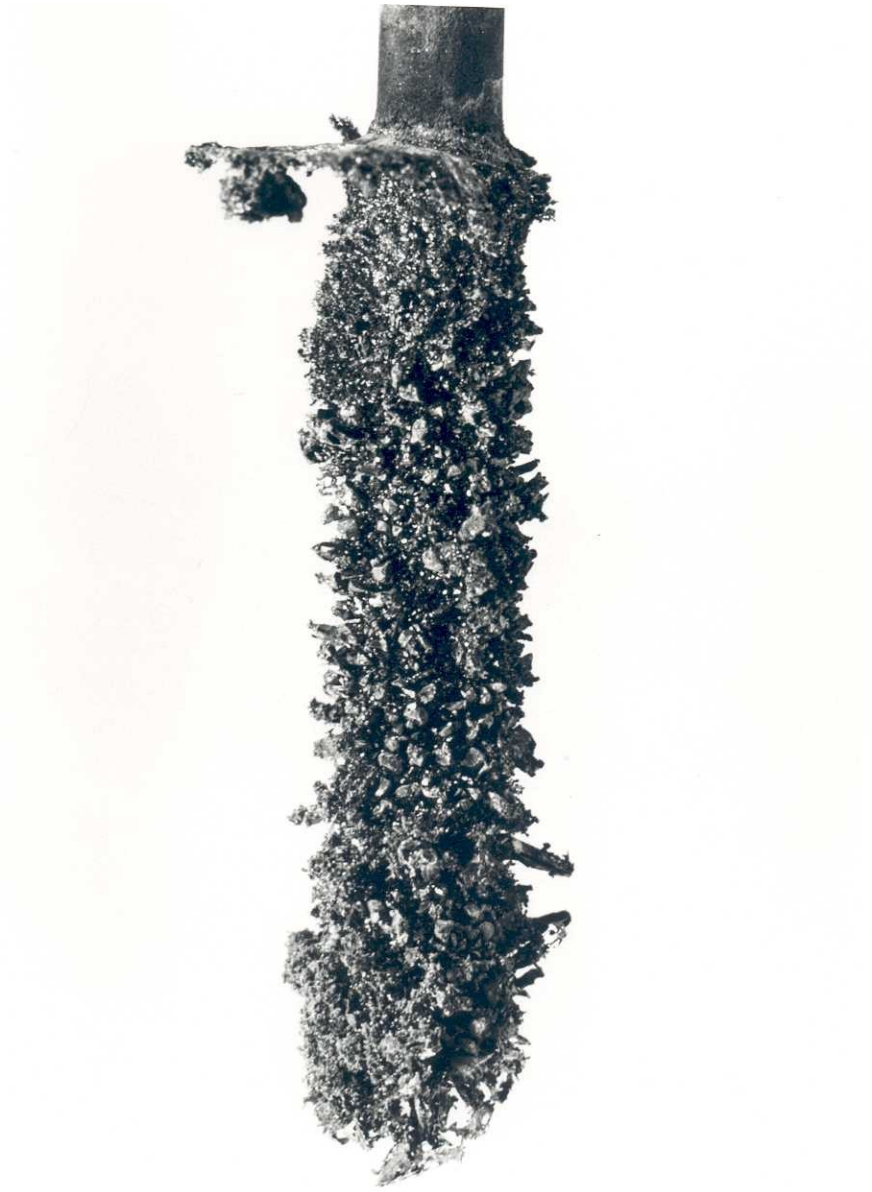

Fig. 17 - Deposit obtained applying low frequency vibrations to the cathode.

newly formed dendrites fall apart and drop to the crucible bottom; this drawback was confirmed by the unusually low current efficiency values.

The overall operating conditions were exactly the same as for the CER set of experiments.

Ultrasonic Vibrations of the Cathode

Fig. 18 shows the typical deposit obtained with 1) a titanium cathode 1.25 cm diameter, 6 cm long; 2) a titanium lead 0.62 cm diameter, 47 cm long; 3) a starting frequency 16.1 Khz, power 110 mA; 4) a final frequency 14.3 Khz, power 90 mA; 5) an initial cathodic immersed surface of 20 cm^2; 6) an initial cathodic current density of 0.3amp/cm^2; 7) an electrolyte temperature of 830°C; and 8) an initial voltage of 0.4 and a final voltage of 0.5. We can see that most of the surface is flat, compactly plated and, as usual, the dendrites on the cathode tip are generated by the edge effect, since the rod tip was not hemispherical.

It is of interest to note that the darker regions of the deposit roughly correspond to the antinodal region indicated by small bubbles adhering to the surface when the cathode was turned in water, and the clearer region corresponds to the nodal regions where these bubbles were not adhering.

Microscopic observations evidenced a cubic crystallization of the flat deposit, and x-ray indicated the existence of a mixed structure hexagonal close-packed, and

Fig. 18 - Typical deposit obtained under ultrasonic vibrations of the cathode.

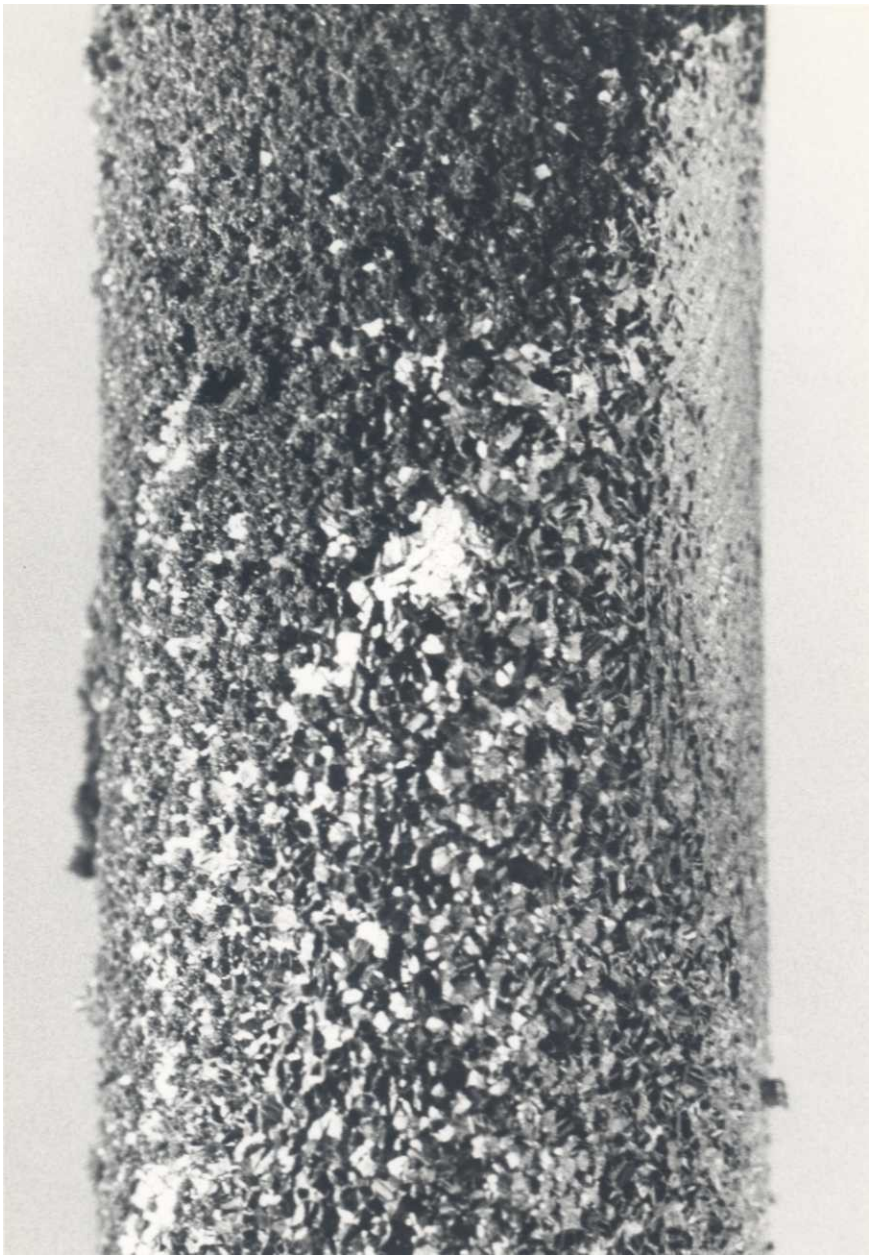

Fig. 19 - A surface close up of the deposit obtained under ultrasonic vibrations of the cathode shown in Fig. 18.

body-centered cubic. See Fig. 19. Unusually high values of current efficiency were obtained; in some instances the calculated results were higher than the theoretical 100% based on Ti^{++}.

The CER cathode deposited simultaneously with the ultra-sonic cathode is shown on Fig. 20, and it has hexagonal close-packed crystallization.

Fig. 21 shows a typical deposit obtained with an electrolyte temperature of 730°C and a 46 cm long molybdenum lead, while all other operational conditions were exactly the same as for the previous set of ultrasonic vibration electrodepositions.

This cathode appears to be similar to the CER type, but the dendrites are more compact and very strongly attached to the substrata. It was impossible to remove them by hand. The current efficiency was always better than 90%.

Fig. 20 - CER deposit obtained simultaneously with the ultrasonic vibrated cathode shown in Fig. 18.

Fig. 21 - Deposit obtained under ultrasonic vibration and low temperature.

DISCUSSION OF RESULTS

Phase Transformation of Titanium Deposit

The electrodes used in this investigation were made of commercially pure titanium. Pure titanium undergoes a phase transformation at 882.5 ± 0.5°C. Its low temperature structure (α) is hexagonal close-packed, while the (β) high temperature phase has a body-centered cubic structure. Large uncertainty among the values published in the literature relative to atomic radii and lattice parameters makes the calculation of the difference in volume between the two phases very difficult.

To eliminate the effect of thermal contraction in the process of cooling when passing from the β to the α phase, the structure parameter values are extrapolated up to 882.5 for the low temperature phase, and down to the same transformation temperature for the high temperature phase. Using these extrapolated values, the resulting difference in volume is due only to the phase transformation.
Based on the Berry and Raynor[180] (1953) lattice parameters a reduction in volume of about 2.5% is found for the isothermal transformation from β-Ti to α-Ti. On the other hand, if the Wasilewski data[180] (1961) are used, a 0.7% decrease in volume is the result.

Spreadborough and Christian[180] (1959) measured the lattice parameters by a diffractomer technique. No difference in volume is obtained if these data are used, but the authors reported an interesting finding. The a and c parameters for α-Ti at 9°C, measured at the beginning of the series of the experiments, were 2.9494 and 4.680 A°, while the same parameters measured at the end of the high temperature β-Ti measurements, when the iodide Ti sample was taken again at 9°C, were 2.9504 and 4.694. It is understood that a tensile stress is present in the material at this point.

DeBoer, MacQuillan and Wyatt[165] have measure an increase in electrical resistivity of about 10% at the transformation temperature as a result of the allotropic change β to α. By definition, an increase in resistivity in metals is an indication that the mean free path of electron movement is reduced; that is, the mobility of the electron is reduced. Therefore, it is understood that the α phase is a more dense structure than β.

Hume-Rothery, Smallman and Haworth[264] add to the complexity of this phase transformation phenomenon by reporting a measured diameter for hexagonal close-packed αTi at 25°C of 2.888 A°, and a diameter for body-centered cubic β at 900°C of 2.858. This means a large increase in diameter for the β → α transformation if we base the difference on extrapolated data at 882.5°C. This difference is theoretic-

ally true, because with more adjacent atoms (12 in HCP) compared to 8 in BCC) there is more electronic repulsion from neighboring atoms. Consequently, the interatomic distances are increased. One more contribution to the overall difference in atomic volume between α and β is given for identical spheres, between HCP (74.2%) and BCC (67.9%) by the difference in Packing Factor.

Finally, Kessler and Seagle[128] obtained a graph relating the density of pure titanium to temperature, from which, at the β to α transformation temperature of 1620°F there is an increase in density of about 0.73%. The β-Ti at 1620°F has a density of 4.35 g/cm^3, whereas the α-Ti at 1620°C has a density of 4.41 g/cm^3. Consequently we have a net volume decrease of about 1.5% of the temperature of transformation. In conclusion we can safely assume that during the transformation upon cooling from the β titanium high temperature body-centered cubic structure to the a titanium low temperature hexagonal-close-packed structure, there is a definite reduction in volume, taking place at 882.5 ±0.5°C.

Therefore, if the operational temperature range includes the transformation temperature, a tensile (or compressive) stress is introduced into the electrode surface due to the phase transformation.

The nature of the electrodeposition is dependent, primarily upon the nature and the conditions of the electrode surface, and the structure of the few layers of electrolyte

next to the electrode surface. Since the complexity of this electrolyte structure is a function of ionic composition, the understanding of multicomponent fused salt mixtures is still very limited. To avoid this complexity this investigation involved the simplest Na-Cl-Ti system.

Consideration of Electrical Multilayer in Molten Salts

The Na-Ti-Cl electrolyte used in this series of experiments is an asymmetrical mixture, with two cations of different charge structure, but with a single anion.

In a previous work[85], we have determined the partial molar quantities for each component, with the pure fused salt as the standard state at the temperature. The activity coefficients have been calculated using the Temkin definition of activity and ideal solution, based on the concept of complete ionization of molten salts. Temkin's model can be summarized as follows:[266] a) The entropy of mixing is entirely configurational, that is, the entropy increases with decreasing atomic order; b) There are two sets of positions in the molten salts, one for cations and the other for the anions; c) The cations and anions are randomly distributed aver the cation and anion positions, respectively, regardless of the magnitude of the charge, i.e., no polarization energy.

However, Temkin's model oversimplifies the actual structure of a fused salt mixture, and the results of the calculations give little indication on the nature of the

liquid.

Therefore, to reach more meaningful values, a more realistic model should be used to deduce the structure of the liquid, assuming certain ionic interactions. However, even for a binary system, a large amount of experimental information is required to specify the thermodynamic properties. Moreover, all parameters representing the free energy as a function of temperature may vary with composition. These calculations of distributions are difficult to treat mathematically.

Furthermore, not much help can be obtained by conceiving a model on the basis of similarities with aqueous electrolytic systems. Fused salt mixtures have higher diffusion and chemical reaction velocities, high ionic strength, high values of minimum capacitance, and the temperature is of greater importance.

On these bases, it is unlikely that the Diffuse Double Layer model would represent the electrode process phenomenon in fused salt melts.

Graves and Inman[93] recently proposed the idea that strong correlation between anions and cations in the melt produce an ordering of several layers of melt at the metal electrode/melt interphase, under the influence of the electric field. The excess charge on the melt side of the electrical double layer is located several ionic layers deep, the layers being alternately positively and negatively

charged.

The same authors investigated the Capacitance/Potential curves for molten chloride electrolytes, and discovered, in agreement with the Frumkin[243] research group, that these curves have a parabolic shape, with a minimum capacitance at the potential of the corresponding electrocapillarity maximum (ψ = 0 in Fig. 22). That is, the capacitance increases with potential(measured relative to the potential of zero charge).

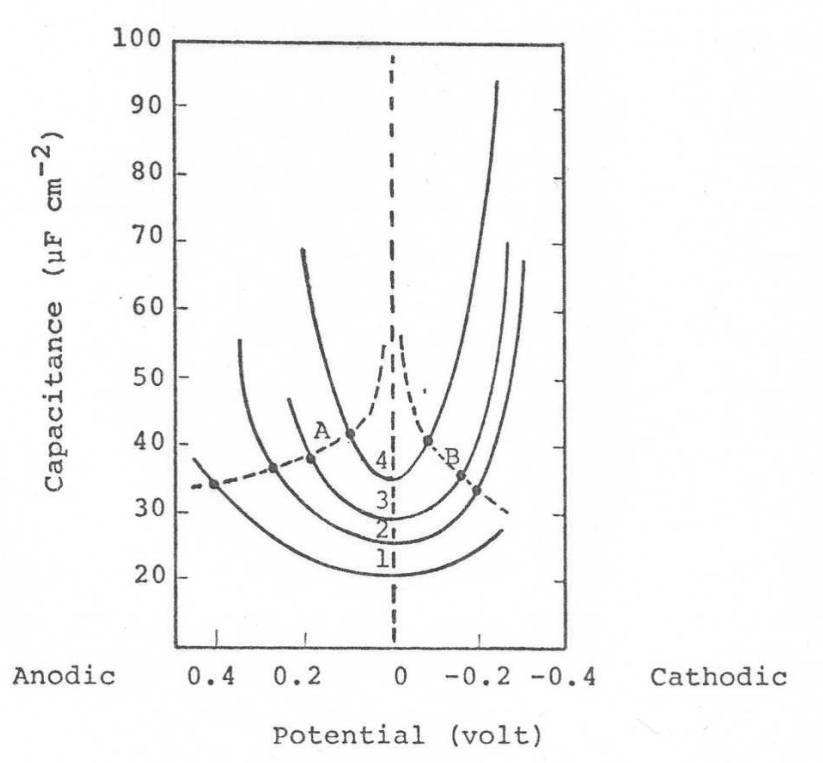

Fig. 22 - Capacitance/Potential curves of a lead electrode in an equimolar LiCl-KCl melt at : (1) 450°, (2) 600°, (3) 700°, (4) 800°C. Loci of the reversible potentials values at different temperatures are indicated by curves A and B.

It is significant not only that the minimum capacitance increases with temperature, but also that the capacitance changes more rapidly with potential at high temperatures than at low.

This phenomenon will be clearly understood when we apply the concept of Excess Energy of Electrode Processes (developed in the Appendix), to the Capacitance/Potential curves, as shown using the Inman Graves data (figure 22). In order for them to overcome the activation energy barrier the ions must be supplied with a constant amount of energy. Consequently, if these ions are at a certain energy level, the amount of energy that must be supplied from external sources is the difference between the activation energy and the actual energy of the ions.

Curves A and B in figure 22, which are obtained by connecting the points of reversible potential at different temperatures, show that at low temperatures (low energy content) a larger potential is required to make up for the extra energy needed. At high temperature (high energy content) less potential is required to reach the activation energy level.

Bakum and Ukshe[93] proposed a similar multilayer model, considering the charged layers as the plate of an infinite series of parallel plate capacitors. In determining the integral capacitance, these authors have defined the Excess Charge Factor as determined by the relative number of

positions available in the first layer of ions (pre-electrode layer) for the accomodation of the Excess Charge at a given temperature. There will be a close packed structure, but unequal number of anions and cations. Their experimental results suggest that only three layers of melts at the metal/melt interphase are ordered.

Sotnikov and Esin[93] introduced the important concept of Charged Vacancies: for a given charge density on the electrode metal, there is an equal and opposite charge density on the melt, produced by anion or cation vacancies. If in the short ranged liquid structure of the ionic atmosphere, the central ion is missing, the net charge of the vacancy is the opposite of the one of the atoms that should be in that place.

At this point it is clear why this investigation was restricted to the simplest possible system such as Na-Ti-Cl.

The Mechanism of Electrodeposition of Titanium

The Excess Energy Theory has been developed to prove that the newly reduced atoms must have an energy level equivalent to a virtual temperature of several hundred degrees centigrade higher than the electrolytic cell system.

These new titanium atom grouplets will crystallize to form a high temperature lattice structure that in the case of β titanium is body-centered cubic. This β crystallization process is facilitated by the low thermal conductivity coefficient of titanium that will allow time for local

temperature buildup.

It has been shown in the previous sections that the allotropic titanium transformation produces an isothermal reduction in volume. From the data published in the literature it is found that pure titanium, at its transformation temperature, has a low tensile elastic modulus (less than 5,000 Kg/mm^2) , and a low thermal conductivity; approximately 0.1215 W/cm°C, extrapolated from Silverman[222] data).

Since the electrode metal lattice is at the lowest energy level of the system, as the layer of body-centered cubic grows in thickness with time, the first titanium atoms crystallized in the lattice begin to transfer their extra energy to the titanium electrode metal substrate, resulting in a lowering of their temperature.

At the moment in which the temperature of the new titanium atoms layer decreases below the transformation temperature, its lattice structure becomes hexagonal-closed-packed α titanium. Since α titanium has a much denser structure than β-Ti, the phase transformation will create a tensile stress within the newly deposited titanium atom layers. The magnitude of this tensile stress will be increased by the thermal contraction due to the decrease in temperature and it will have a random orientation.

At this point, due to its low tensile elastic modulus the new titanium deposit will crack, producing a surface rouglrness with protrusions and cracks. These provide points

of high current density to nucleate dendrites and whiskers. Furthermore, the electrolyte will fill the cracks, although the throwing power is not large enough to carry Ti^{++} ions into the crevices. Meanwhile the Ti^{o} activity in the crevices is very large compared to Na^{+} activity, thus the reaction:

$$Ti + 2NaCl \Longrightarrow TiCl_2 + 2Na$$

can actually occur to make deeper crevices, and produce sodium atoms that will chemically reduce Ti^{++} in solution, away from the cathode.

The Thermodynamic Cycle for the proposed mechanism is:

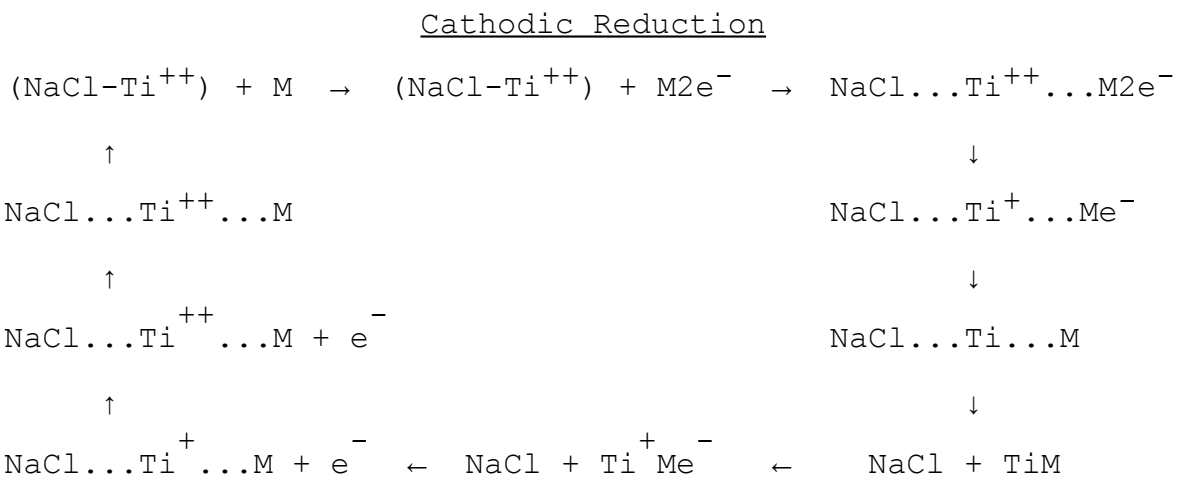

where M is the metal electrode.

Since, according to Bockris[31] the activation energy required to simultaneously transfer two electrons is much greater than that needed for one electron, the transfer of

two charges in one step is improbable. However, some evidence to the contrary may soon be available.[149]

In the light of the previous discussion it is now possible to explain the nature of the titanium deposit under the various conditions investigated.

Electrolysis Under CER Conditions

The effects of current density, Ti^{++} concentration, and temperature of the electrolyte, on the characteristics of the deposit in CER are summarized in Fig. 23.

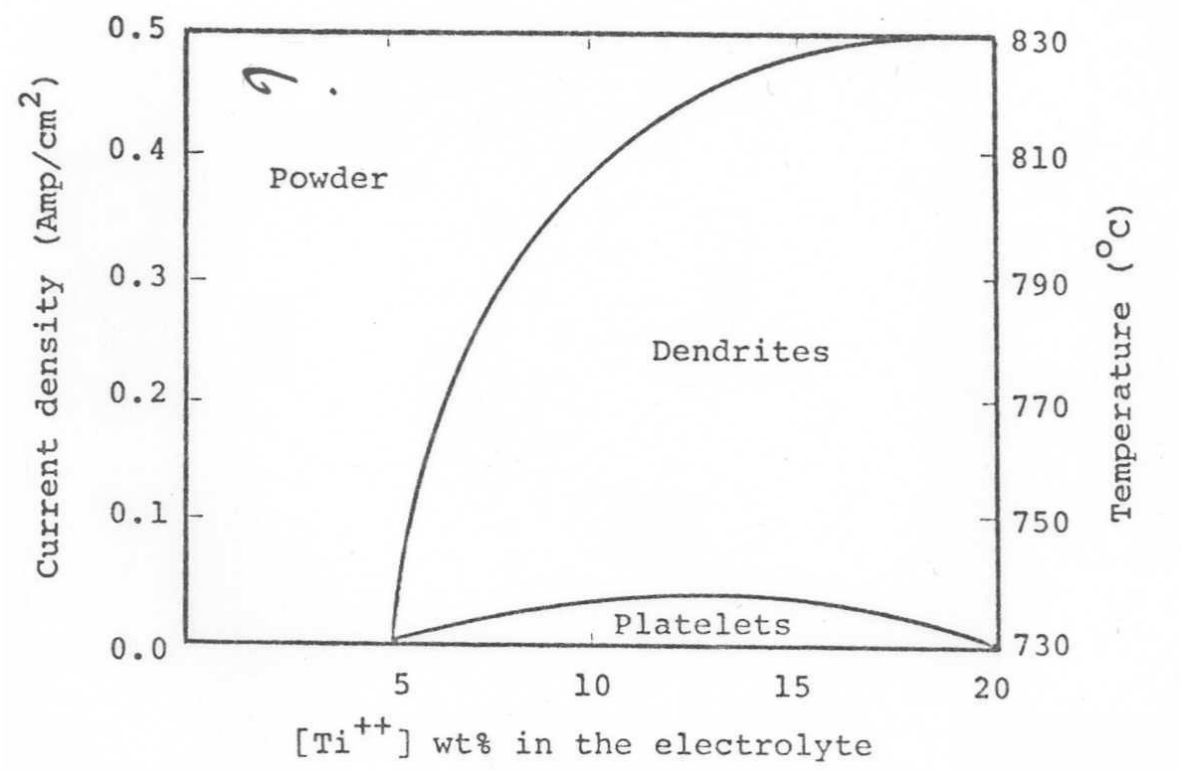

Fig. 23 - Relationship between the conditions of electrodeposition and the type of deposit.

For example, it can be seen from Fig. 23 that at a current density of 0.3 amp/cm^2, dendrites will be formed when the Ti^{++} concentration exceeds 8 wt%. Below that concentration a powder deposit will result.

The Emf dependence on temperature and concentration is the reason for the different types of deposition of titanium in our particular system.

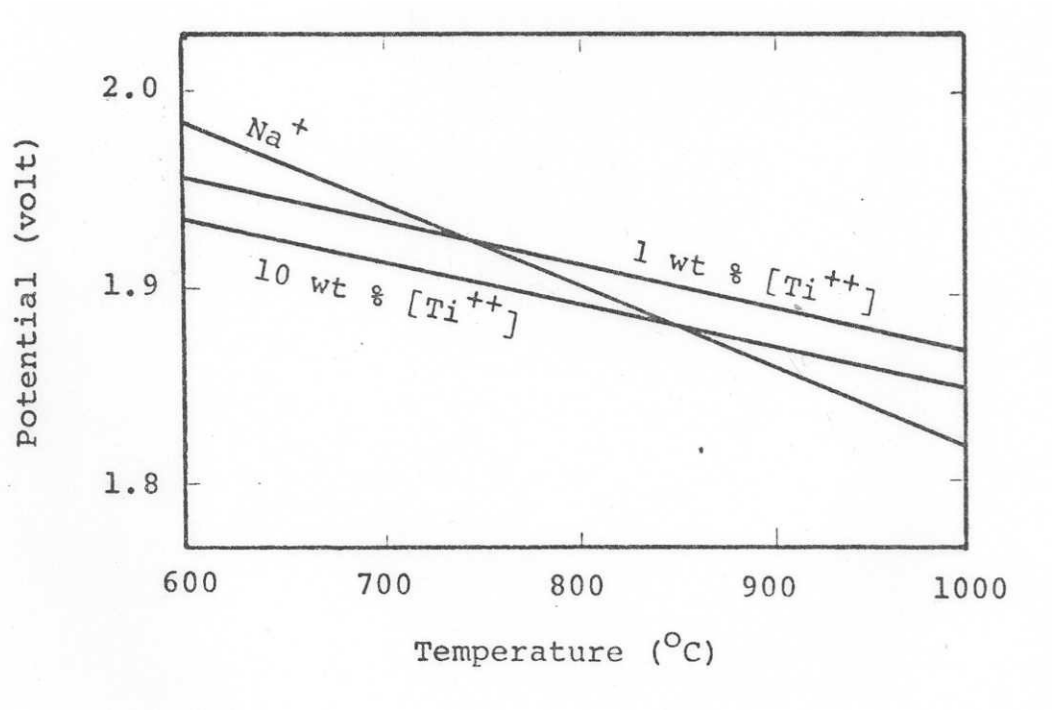

Fig. 24 - Variation of the decomposition potential with temperature and titanium divalent ions concentration.

As shown in Fig. 24, above 850°C, with a Ti^{++} concentration of 10 wt%, the decomposition potential of sodium chloride becomes lower than the titanium dichloride, therefore sodium metal starts to deposit on the cathode instead of titanium. The same phenomenon occurs at about 750°C when the Ti^{++} concentration approaches l wt%.

Furthermore, the variation in temperature of the electrolyte will displace the ideal equilibrium (Ti^{++}-Ti^{+++}) towards the trichloride direction, therefore reducing the Ti^{++} concentration. Also the sodium metal boiling point (890°C) must be taken into consideration.

It is assumed that the sodium line remains constant, within the variation range of the titanium concentration, because of the variation from ideality of both NaCl and $TiCl_2$ activity lines. However, considerable disagreement is found in the literature regarding the activity coefficient values of the two chlorides.

It can be readily seen from Fig. 25 that when varying the sodium chloride concentration between 80 and 100%, its activity does not vary significantly, therefore its decomposition potential does not vary greatly; however, when varying the titanium chloride concentration between 0 and 20%, its activity changes significantly, with a consequent change in the decomposition potential.

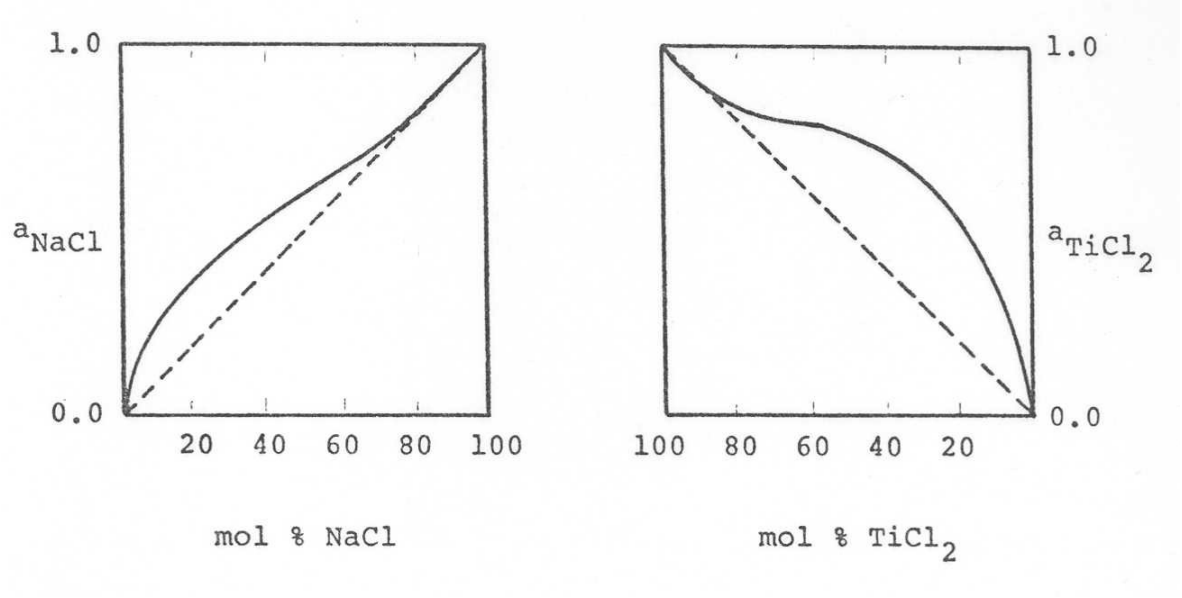

Fig. 25 - Assumed activity curves for NaCl and $TiCl_2$.

The decomposition potential versus temperature curves in Fig.24 have been qualitatively determined by the author following the general concept established by Grjotheim et al.[267] The metallic sodium having been reduced, will go back into the electrolyte to chemically reduce titanium dichloride away from the cathode surface, producing metallic titanium fog "pyrosol" of high viscosity that, with the help of some small whiskers (that are always formed) will build up a very brittle deposit that resembles cotton flock.

High current density values, since they raise the temperature of the electrical multilayer, produce essentially

the same effect as the high temperature (the high temperature effect being the formation of pseudomorphous macrostructure, multiformed, and combined cubic and hexagonal crystals).

Large depositions on base metal substrates are very similar to those on titanium, confirming that the influence of the substrate metal acts up to approximately 100 µm of thickness, within which the larger thermal conductivity coefficient of the base metal will not allow surface temperature build-up to start the mechanism of dendrite nucleation.

Several investigators report that titanium can be electroplated on titanium substrate in the form of a flat deposit, only up to a maximum thickness of 1.5 µm, whereas the smooth deposit may reach 125 µm on base metal substrates. .

In the present investigation it would have been more adequate to use cathodic rods with a diameter larger than 2.5 cm, to minimize the effect of low electrical and heat coefficient values for titanium on electrodeposition; and also to have more meaningful comparison from initial and final current densities. But a maximum of 2.5 cm was one of the limits of the experimental apparatus.

Lowering the current density, while leaving all other variables constant, results in small crystals, dendrites and whiskers. These results are in agreement with the

postulated mechanism. A lower current density corresponds to a low rate of transport of ions through the electrical multilayer. Thus, although it diminishes the rate of new atom formation, it does not prevent the build up of localized very high temperatures. These, in turn, result in the various types of deposit indicated. A limiting small current density grows a flat deposit, but will make the process impractical; and further, the corrosion on titanium on the cathode by the sodium chloride attack:

$$Ti + 2NaCl \longrightarrow TiCl_2 + 2Na$$

further diminishes the actual deposit size.

The values of current efficiency reported in the experimental results section of this work have low limits of accuracy due to the errors introduced. These are due to:

- loss of deposit in form of dendrites, whiskers, during the harvesting and leaching operations.
- amount of entrapped salt remaining in the deposit after leaching.
- large starting cathode/deposit weight ratio.
- possibility of having some Ti^{+} in solution.
- uncertainties of measuring procedures and equipment.

Current Pulsations

A pulsating current generates a repeated transient effect on the electrical multilayer, similar to that occur-

ring at the starting instant of CER at high current density. In Fig. 26 the solid curves represent the Ti^{++} and Cl^{-} concentrations at the instant of the starting of the electrolysis, while the dotted ones the steady state concentration profile of those concentrations.

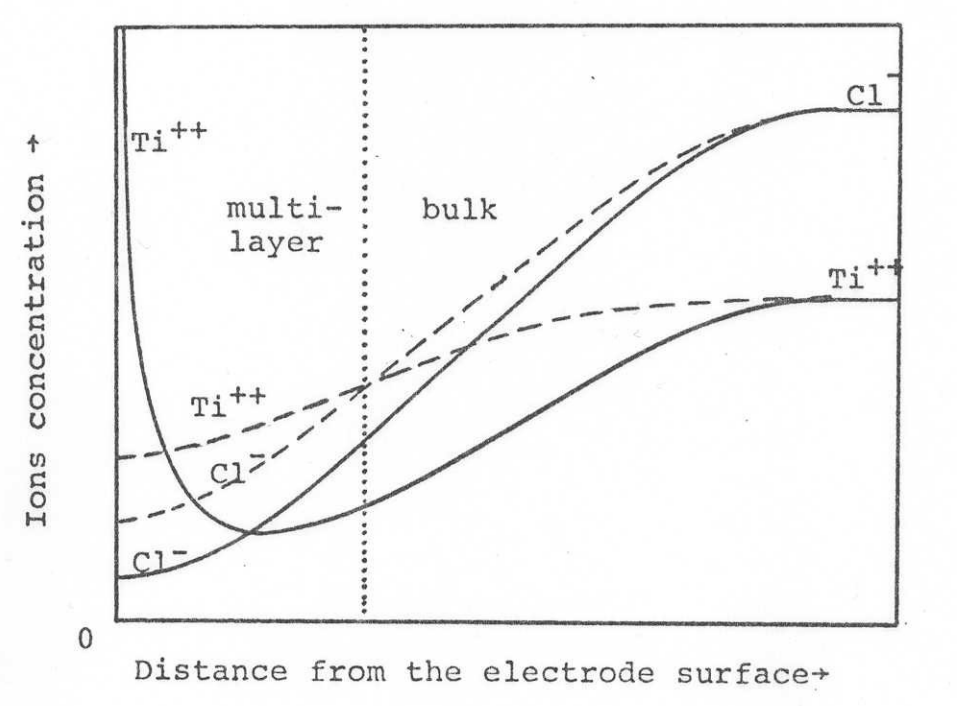

Fig. 26 - Approximate concentration profiles developed at the electrode surface by rapid charge injection, qualitatively determined by the author following Anson's work[260].

At the starting instant the deposition occurs as if there was a much higher Ti^{++} concentration in the electrolyte. After the very short initial period of time, however, the deposition continues only as a quantity of new Ti^{++} is sup-. plied by diffusion and cation mobility (in the order of 10^{-3} cm sec/volt cm).

If, after the pulse, whose length should be of the order of magnitude of one second or less, the current is interrupted for a period of three or four times the length of the pulse, then the Ti^{++} concentration next to the cathode will be restored to its previous value, ready for the next pulse. But, it is significant that there is no surface temperature build-up because of the time allowed for complete dissipation of the Ti new atoms' extra energy. Therefore the cathodic deposit will directly crystallize in hexagonal close-packed structure. This is the kind of deposit showed in Figs. 10-11. This is a confirmation of the validity of the proposed mechanism of Ti electrodeposition. This is also in agreement with the fact that titanium deposits smoothly on titanium substrate in subsequent layers of thickness up to 1.5 µm every time a cathode is reused after the dendrites produced in the previous runs have been scraped off.

Periodic Reversed Current

Experimental work carried out by Westinghouse[251] and by Nippon Mining[173] with periodic reversed current in copper electrodeposition has indicated that the surface of the electrodeposited metal has been smoother than the original base metal surface, due to the point effect during the anodic portion of the period.

What we can see on Fig. 13 is certainly not a flat

deposit. This is another confirmation of the uniqueness of the titanium electrode process. The salt dragout ratio was very low, contrary to what is expected. The fact that the diameter of the whiskers increased with increasing current density is in agreement with the concept of Corona Discharge, assuming that the tip of the whiskers has a parabolic shape.

From the above considerations, it follows that periodic reversing of the current helped to avoid the filling of the crevices on the deposit surface, but did not change the usual form of deposition of titanium; actually it worsened the characteristics of the deposit if we compare it with the CER cathode produced under comparable conditions (Fig. 14).

All this is in agreement with the postulated mechanism, because both deposition and dissolution (ionization) are processes involving activation energy. But what is very interesting is the extreme whiskery character of the periodic reversed current deposit. The explanation of this phenomenon will help us to complete the proposed mechanism for titanium electrodeposition.

From the thermodynamic point of view, according to Kushner[144], if there is an extra amount of heat (thermal energy) at the cathode, there should be a corresponding loss of heat at the anode, characterized by local cooling of a few atom layers at the surface. This would indicate that

when carrying out an electrolytic process near the melting point of the electrolyte, some solidification at the anode should take place. To show this, an attempt has been made to carry out some experiments at temperatures very near the melting point of the bath. These, however, were not successful because of the large difference in immersed area between the anode and the cathode, and a variety of other problems.

The cooling effect, referred to above, is shown by the extremely fine whiskery deposit of Fig. 13. The local refrigeration actually occurs during the anodic portion of the period. Since the anodic stripping follows immediately (no dead time), the cathodic temperature builds up, the sudden cooling of the last high temperature layer (body centered cubic) creates very high tensile stress which will tend to break up the very small grouplets of atoms.

Fig. 27 illustrates the anodic phenomenon of the decrease in surface energy level (loss of heat). The curve of the change in energy has been drawn on the same basis as for the Excess Energy Theory (see Appendix).

Rice[202] postulated the existence of a second diffuse double layer in the metallic phase characterized by a gradient in electron concentrations.

The surface refrigeration effect can be further explained by the change in energy density during the transformation of a titanium atom into a titanium ion.

Nomenclature to Figure 27

E^* = Activation energy level

E_{III} = Ground state energy level of the anode surface

E_{II} = Ground state energy level of the ions in the electrolyte at large distance from the electrodes

E_I = Ground state energy level of the cathode surface, electrons in the Fermi level of the metal

E_0 = Ground state energy level of the transient entity

ψ^+ = Galvani potential at the anode interphase, plus the Overpotential, as a function of the distance from the electrode

ψ^- = Galvani potential at the cathode interphase, plus the Overpotential, as a function of the distance from the electrode

R = Reversible potential curve as a function of the distance from the electrode

Act. = Activation energy curve as a function of the distance from the electrode surface

Dis. = Dissolution energy curve as a function of the distance from the anode surface

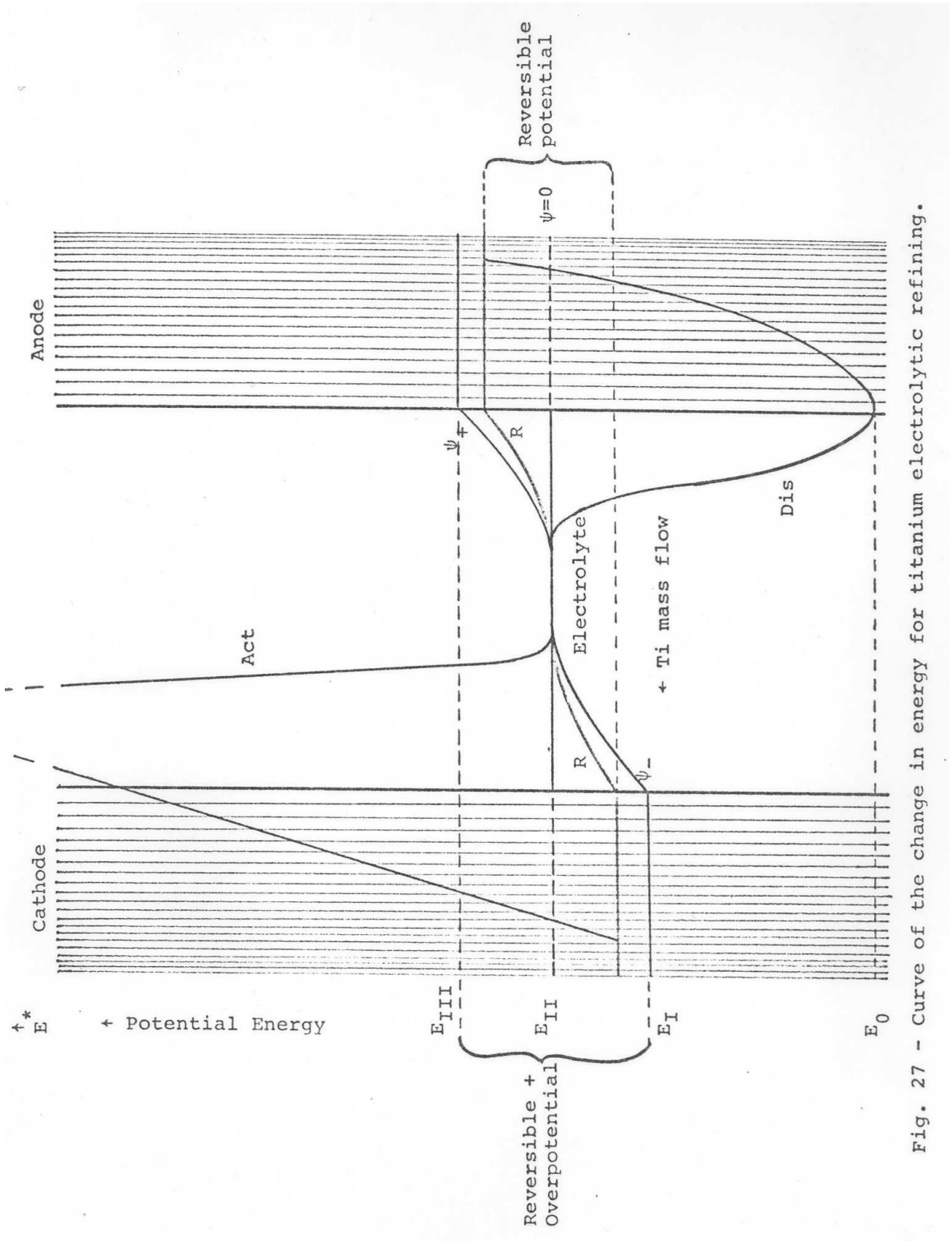

Fig. 27 - Curve of the change in energy for titanium electrolytic refining.

The various valences of Ti entities have the following radii (at room temperature):

Ti^0	1.47 A°
Ti^+	0.96
Ti^{++}	0.94
Ti^{+++}	0.76
Ti^{++++}	0.63

It can be seen that the titanium ions have a much smaller radius than atomic titanium; this is due to the fact that when one electron is removed, since the positive charge of the nucleus is constant, the other 21 electrons are pulled to orbit closer to the nucleus.

Now, when one electron is removed from the titanium atom on the surface of the anode, but the remaining electrons have not yet had time to rearrange themselves in orbits closer to the nucleus, the entity is no longer an atom, but is not yet an ion in its equilibrium electronic state. This transient entity has an energy density lower than both atom and ion, that is, a smaller number of charges per unit volume. The energy level of the above defined entity (shown in Fig. 27) is the lowest energy level of the system E_0.

At this point the physical meaning of the familiar shape of the activation energy curve clears, particularly the fact that the anodic portion of the curve curls back up into the electrode body after having passed its minimum at

the electrode surface.

The application of periodic reversed current with dead time (shown in Fig. 16) resulted in a deposit of intermediate characteristics between the one obtained with current pulse and that with periodic reversal without dead time.

In this case, the benefits of current pulse (high Ti^{++} concentration and time to dissipate the excess energy) have been added to those of reversing the current (corona discharge and point effect).

Low Frequency Vibrations of the Cathode

The purpose of stirring the solution of an electrolytic cell is to minimize the concentration polarization at the electrodes.

In the electrolyte used in this investigation a strong convection current was always present, streaming upward from the center bottom and downward along the cell's sides. This agitation, as has been stated, was generated by the large difference in temperature between the crucible bottom and the surface of the bath in contact with the helium atmosphere (a gradient of approximately 180°C when the furnace is at 1000°C) .

Therefore, various types of motion applied to the cathode (axial rotation, horizontal translation and vibration with respect to the bath surface) will not affect the deposition conditions, that is the electrical multilayer.

This is confirmed by the type of deposits obtained under low frequency conditions, Fig. 17, which was very nearly similar to the ones obtained under CER conditions.

Meanwhile, vertical low frequency vibrations (less than 3000 Hz) will considerably damage the deposit making the newly formed dendrites fall apart and drop at the crucible's bottom. This damage is also indicated by the low current efficiency value as calculated by the cathode's weight increase.

Ultrasonic Vibrations to the Cathode

The kinetics of electrode processes are largely determined by the concentration, activation and resistance polarizations. Ultrasonic vibrations affect these three polarizations differently. Strong ultrasonic fields can change the state of the ionic atmospheres and can excite the electrons in the shell of the reacting particles. Thus it should result in higher electrical conductivity of the electrolyte and a lower decomposition potential.

The overall effect of applying ultrasonic vibrations to electrolytic processes is the very high deposition rate. The accelerating effect of ultrasonic vibrations on the deposition rate is partially due to the improved mixing that enhances the uniformity of composition of the electrolyte and the diffusion at the electrode-electrolyte boundary.

When the ultrasonics are applied to the cathode, a desirable side effect will occur. Since a part of the vibrational energy applied is transformed into heat energy, the viscosity of the electrolyte next to the cathode will be lower, enhancing the escaping of the entrapped salt, making the multiple layer thinner, and helping the Cl^- substitution.

Russian workers[136] have experimented with frequencies within the range of 20 KHz to 3 MHz on electrode processes in aqueous electrolytes. No references are available to date, to our knowledge, on ultrasonic vibrations applied to fused salt systems.

Different frequencies and amplitudes within the operational range of the transducer have been tested, in an attempt to find the right values to settle titanium deposit homogeneously on the cathode surface, taking into account cavitational resonance phenomena.

Our results show that the variation of the frequency from 16 to 22 KHz does not affect the character of the deposit; that is, the results of application of ultrasonic vibrations is constant within the range.

What really affected the type of deposit, under the same conditions of ultrasonic vibrations, was the temperature. A fundamental difference between the cathode obtained at 830°C (Fig. 18) and that obtained at 730°C (Fig. 21) is observable. The fact that one has a titanium

cathode lead while the other has a molybdenum lead has been experimentally proved to have negligible effect on the deposit.

As has been pointed out earlier, the specific effect of ultrasonics on the system under investigation, besides all the beneficial effects for electrolytic processes as described for aqueous systems, is that a part of the acoustical energy applied to the titanium cathode is transformed into heat energy, on the electrode surface, primarily because of friction within the titanium cathodic rod, due to the stretching and compressing motion (because of the low Young's modulus value at 830°C) and friction between the fused salt layer close to the cathode surface and the titanium cathode surface.

The deposit of the cathode shown on Fig. 19 was found to have a cubic macrostructure, therefore, it can safely be assumed that the cathode surface temperature, during the electrodeposition, was higher than the transformation temperature of titanium. It follows that the portion of acoustical energy transformed into heat was large enough to create a cathodic surface temperature increase of more than 50°C, which was needed to exceed the transformation temperature of 882.5°C.

On the contrary, the deposit shown on Fig. 21, obtained at 730°C, proves that the application of ultrasonic vibration to the cathode under these conditions did not

alter the usual aspect of the titanium crystallization, since it is very similar to the CER one. The only difference was in the compactness and strength of attachment of the dendrites. Moreover, the crystal structure was hexagonal close-packed, typical of low temperature structure.

Consistent with what has been said above, we can assume that the portion of acoustical energy transformed into heat was not large enough to increase, and maintain the cathode surface temperature by at least 170°C required to exceed the transformation temperature. Therefore, in accordance with the proposed mechanism, the newly reduced titanium atoms crystallizing in body centered cubic structure, remained ordered in this type of lattice, when the temperature of the cathode surface is kept above the transformation temperature, producing a flat compact deposit (as shown on Fig. 19). There is no tensile stress generation and thus no dendrite nucleation.

On the other hand, when the cathode surface temperature cannot be kept above the transformation temperature, the newly reduced titanium atoms in the body centered structure in approaching the temperature of the cathode surface, transform their structure, thereby creating the effects leading to the formation of dendrites as usually occurs in CER.

An additional conclusion that can be reached from the above results is that oxide films present at the starting

surface of the electrodes are not a cause of spot nucleation of dendrites. Dendritic deposits were obtained in spite of the fact that the chemical corrosion by fused chlorides as well as the high viscosity of the electrolyte at low temperatures would remove any trace of oxide films from the cathode surface. On the other hand, flat deposits were obtained at high temperatures, at which the cleaning effect of ultrasonic vibrations was less pronounced due to the lower viscosity.

COMMENTS AND FURTHER WORK

The author's intention, in carrying out this investigation, was to gain an understanding of the complexity of electrochemistry of reactive metals. Titanium proved to be an excellent test ground with its multivalency, its position in the chloride electromotive series, the properties of its chlorides, and its solid phase transformation. As Kroll said,"when the many difficulties of titanium electrolysis will be overcome, there will be an open road for the electrolytic production and refining of a dozen plurivalent metals, which can be deposited from fused salts in a solid state."

Some of the difficulties in this study were due to the lack of data regarding physicochemical properties of titanium. Therefore, considerable research is needed in the following areas:

- Ti-Na-Cl phase diagram, Ti activity coefficients and quantitative emf values.
- reaction of $TiCl_2$ with impurities.
- multilayer capacitance for NaCl-$TiCl_2$ system.
- quantum mechanical determination of energy values of the various steps in the thermodynamic cycle of titanium electrodeposition.

- refinability parameters for various titanium alloying metals.
- effects of ultrasonic vibrations on the current efficiency of electrodeposition.
- effects of combined ultrasonic vibrations with high current density pulses on the electrodeposition of titanium.

BIBLIOGRAPHY

1. Abkowitz, S., Burke, J.J., Hiltz, R.H., Titanium in industry. Technology of structural titanium: N.Y., ed. Van Nostrand Co. (1955).

2. Agar, J. L., Thermogalvanic cells in Advances in electro-chemistry and electrochemical engineering: Interscience, v. 3, (1963).

3. Alabyshev, A. F., Lantratov, M. F., Morachevskii, A.G., Reference electrodes for fused salts: Washington, D.C., The Sigma Press (1965).

4. Alpert, M.B., Electrolytic production of titanium metal: U.S. Patent n. 3,114,685, National Lead Co. (1963).

5. Alpert, M.B., Hamilton, J.A., Schultz, F.J., Sullivan, W.F., Electrolytic preparation of titanium from fused salts; II Design of Laboratory Cells: Jour. Electrochem. Soc., v. 106, p. 142, Feb. (1959).

6. Alpert, M.B., Schultz, F.J., Sullivan, W.F., Electrolytic preparation of titanium from fused salts; I. Preliminary electrolytic studies with diaphragmed cells: J. Electrochem. Soc., v. 104, p. 555, Sept. (1957).

7. Andrews, E.W., Production of Titanium Metals: U.S. Patent n. 2,892,764, The New Jersey Zinc Co. (1959).

8. Andrews, E.W., Production of titanium: U.S. Patent n. 2,898,275, The New Jersey Zinc Co. (1959).

9. Andrews, E.W., Electrolyzing device: U.S. Patent p. 2,900, 318, The New Jersey Zinc Co. (1959).

10. Anson, F.C., Transient effects in the double layer: Conf. on the electrical double layer and its influence on electrode processes: University of Kentucky, Sept. (1970).

11. Arrhenius, S., Professor at the Univ. of Stockholm; Text-book on electrochemistry: London, Longmans, Green and Co. (1902).

12. Babikov, O.I., Ultrasonics and its industrial applications: Consultants Bureau (1960).

13. Baker, D.H., Nettle, J.R., Titanium electrorefining: cathode studies and deep bath deposition: U.S. Bureau of Mines, Report of Investigations, n. 5481 (1959).

14. Baraboshkin, A.N., Electrochemistry of molten and solid electrolytes: Inst. of Electrochemistry, Urals Academy of Science, v. 7, Physicochemical Properties of Electrolytes, Consultant Bureau, N.Y. (1969).

15. Barksdale, J., Titanium. Its occurrence, chemistry, and technology: N.Y., The Ronald Press Co. (1966).

16. Barnett, C.E., Production of titanium: U.S. Patent n. 2,908,619, The New Jersey Zinc Co. (1959).

17. Baroch, C.T., Kaczmarek, T.B., W.D. Barnes, Galloway, L.W., Mark, W.M., Lee, G.A., Titanium plant at Boulder City, Nev., its design and operations: U.S. Bureau of Mines, Report of Investigation 5141 (1955).

18. Beck, T.R., Stress corrosion cracking of titanium alloys: Electrochemistry of freshly generated titanium surfaces: Boeing Scientific Research Laboratory, NAS 7-489, Quarterly Progress Report n. 9, Nov. (1968).

19. Beck, T.R., Blackburn, M.J., Smyrl, W.H., Speidel, M.O., Stress corrosion cracking of titanium alloys: Electrochemical kinetics, SSC Studies, Polarization curves in molten salts, liquid metal embrittlement: Boeing Scientific Research Laboratory, NAS 7-489, Quarterly progress Rept. n. 14, Dec. (1969).

20. Bertorelle, E., Trattato di galvanotecnica: Milano, Hoepli, (1960).

21. Bett, F.L., Worner, H.K., Titanium research at the University of Melbourne: Proceed. Australasian Inst. Min. Met., n. 178, p. 1 (1956).

22. Blomgren, E., Inman, D., Bockris, J.O'M., Arrangement for electrochemical potential-time measurements in the millimicrosecond range: Rev. Scient. Instrum., 32, p. 11-2 (1961).

23. Bloom, H., The chemistry of molten salts: Amsterdam, Benjamin, Inc., N.Y., (1967).

24. Bloom, H., Bockris, J.O'M., Molten electrolytes in Modern aspect of electrochemistry: Butterworth, v. 2, (1959).

25. Bockris, J.O'M., Ionic absorption at the solid solution interface; Conference on electrical double layer and its influence on electrode processes: Univ. of Kentucky, Sept. (1970).

26. Bockris, J.O'M, Electrode kinetics in Modern aspects of electrochemistry: Butterworth, v. l, (1964).

27. Bockris, J.O'M., A brief summary of hydrogen electrode kinetics: J. Electrochem. Soc., v. 99, p. 366C, Dec. (1952).

28. Bockris, J.O'M., Damjanovic, A., The mechanism of the electrodeposition of metals, in Modern aspects of electrochemistry: Butterworth, v. 3, (1964).

29. Bockris, J.O'M., Matthews, D.B., The mechanism of charge transfer at electrodes: Proc. Roy. Soc. London, Ser. A 292, p. 479 (1966).

30. Bockris, J.O'M., Matthews, D.B., The mechanism of electrolytic hydrogen evolution - Evidence for the participation of Proton Tunnelling: Electrochimica Acta, v. 11, p. 143 (1966).

31. Bockris, J.O'M., Razumney, G.A., Fundamental aspect of electrocrystallization: Plenum press, N.Y. (1967).

32. Bockris, J.O'M., Srinivasan, Fuel cells: their electrochemistry: McGraw-Hill (1969).

33. Bonnemay, M., The double layer and anodic oxidation on platinum: Conf. on the electrical double layer and its effects on the electrode processes, Univ. of Kentucky, Sept. (1970).

34. Brandes, H., Elektrolytische polarisationen aus anlass von kristallwachstumshemmungen: Z. Physik. Chem. 142, 97, (1929).

35. Bratland, D., Euchem Conference on Molten Salts, Salice Terme, Italia, May (1968).

36. Breiter, M., Some problems in the study of oxygen overvoltage, in Advances in electrochemistry and electrochemical engineering: Interscience, v. l, (1961).

37. Brenner, A., Electrolysis of non-aqueous systems, in Advances in electrochemistry and electrochemical engineering: Interscience, v. 5, (1967).

38. Brown, B., Goodman, J.E., High-intensity ultrasonics, industrial applications: D. Van Nostrand Co. (1965).

39. Brynestad, J., Grjotheim, K., Krohn, C., Theoretical treatment of equilibria in fused mixtures of reciprocal salt systems: Revue Roumanie de Chimie, v. 9, p. 163 (1964).

40. Burton, R.E., Daly, J., Molecular orbital studies of ion hydration: The Faraday Soc., p. 1281 (1970).

41. Butler, J.A.V., Hydrogen overvoltage and reversible hydrogen electrode: Proc. Roy. Soc. A., 157, 423.

42. Campos, Vicente F., Kinetics of electrode processes; A review of reversible and irreversible potential: Paper presented at the Seminar on Electrometallurgy held at Colorado School of Mines, Spring (1969).

43. Castelfranchi, G., Fisica moderna atomica e nucleare: Milano, Ulrico Hoepli (1959).

44. Cattoir, F.R., Nettle, J.R., Baker, D.H., Determination of the average effective valence state of titanium in sodium chloride: U.S. Bureau Mines, Rept. Inv. 5372 (1957).

45. Charlot, G., Tremillon, B., Chemical reaction in solvents and melts: Pergamon (1969).

46. Chicago Development Corp., Summary of works on Electrolytic Titanium: (1957).

47. Clark, R.J.H., The chemistry of titanium and vanadium: Elsevier (1968).

48. Clough, W.R., Reactive metals: Metallurgical Soc. Proc., Buffalo (1958).

49. Collings, E.W., Ho, J.C., Physical properties of titanium alloys: Metal Sci. Group. Battelle Memorial Inst. International Conf. on Titanium. London, England, May (1968).

50. Conway, B.E., Proton solvation and proton transfer processes in solution, in Modern aspect of electrochemistry; Butterworth, v. 3, (1964).

51. Conway, B.E., Theory and principles of electrode process: N.Y., Ronald press, (1965).

52. Cottrell, A.H., Theoretical structural metallurgy: London, Edward Arnold, (1965).

53. Damjanovic, A., Mechanistic analysis of oxygen electrode reactions, in Modern aspects of electrochemistry: Plenum Press, v. 5, (1969).

54. Davey, T.R.A., Private Communication (1970). CSM.

55. Davis, H.Y.T., McDonald, J., Conformal solution theory of certain molten salts: Dept. of Chem. Eng., Univ. of Minnesota, Minneapolis (1968).

56. Dean, R.S., Electrolytic refining of titanium: Chicago Development Co., Light Metal Age, April (1957).

57. Dean, R.S., Gullet, W.W., McCawley, F.X., Hornstein, I., Announce a method for reduction of titanium chloride by solutions of alkalinous metals in their fused salts: Industrial Laboratories, Chicago, v. 8, n. 4 (1957).

58. Delahay, P., Advances in electrochemistry and electrochemical engineering: Interscience, v. l, (1961).

59. Delahay, P., Electrode processes without a priori separation of double-layer charging: Jour. Phys. Chem. 70, p. 2373-9 (1966).

60. Delahay, P., Double-layer perturbation without equilibrium between concentrations and potential: Jour. Phys. Chem. 71, p. 779-780 (1967).

61. Delahay, P., Susbielles, C.G., Double-layer impedance of electrodes with charge-transfer reaction: Jour. Phys. Chem. 70, p. 3150-7 (1966).

62. De Levie, R., Electrochemical oscillators: Conf. on electrical double-layer and its influence on electrode processes, Univ. of Kentucky, Sept. (1970).

63. Delimarskii, Y.K., Markov, B.F., Electrochemistry of fused salts: Sigma Press (1961).

64. Edlin, F.E., Production of refractory metals: U.S. Patent n. 2,904,427, E.I. du Pont de Nemours and Co. (1959).

65. Ellingham, H.J.T., Electrolysis: principles of plant design and operation: Trans. Institution Chem. Engin., London, v. 16, p. 77 (1938).

66. Elwell, W.T., Wood, D.F., Analysis of the new metals: Pergamon (1966).

67. Elwell, W.T., Wood, D.F., The analysis of titanium zirconium and their alloys: John Wiley & Sons, (1961).

68. Erdey-Gruz, T., Volmer, M., Zur frage der elektrolytischen metallüber spanning: Z. Physik. Chem. A 157, 165 (1931).

69. Faber, M., Darnell, A.J., Disproportionation and vapor pressure of $TiCl_2$: J. Chem. Phys., v. 25, n. 3, p. 526 (1956).

70. Fermi, Enrico, Dispersion and absorption of sound by molecular processes: Scuola Internazionale di Fisica, XVII Corso (1963).

71. Fitts, D.D., Nonequilibrium thermodynamics: McGraw-Hill (1964).

72. Fleischmann, M., Thrisk, H.R., Metal deposition and electrocrystallization, in Advances in electrochemistry and electrochemical engineering: Interscience, v. 3 (1963).

73. Fogler, H.S., Effect of ultrasonic waves on the mass transfer of selected fluids: Ph.D. Thesis, Univ. of Colorado (1965).

74. Frederick, J.R., Ultrasonic engineering: John Wiley & Sons, Inc. (1965).

75. Frumkin, A.N., Hydrogen overvoltage and adsorption phenomena. Part I, Mercury, in Advances in electrochemistry and electrochemical engineering: Interscience, v. l (1961).

76. Frumkin, A.N., Hydrogen overvoltage and adsorption phenomena. Part II, in Advance in electrochemistry and electrochemical engineering: Interscience, v. 3, (1963).

77. Frumkin, A.N., Note on B. Kamienski's parer, The nature of the electric potential at the free surface of aqueous solutions: Electrochimica Acta, v. 2, p. 351 (1960).

78. Frumkin, A.N., Damaskin, B.B., Chizmadzhev, Y.A., Comments on, Structure of the double-layer (electric) at the metal-solution (interface) boundary: Sov. Electrochem., 2, 813 (1966).

79. Gathje, J.C., Potentiometry, Alternating current polarography and amperometry: Parer presented at the Seminar on Electrometallurgy held at Colorado School of Mines, Spring (1969).

80. Gerischer, H., Uber den ablauf von redoxreaktionen an metallen und an halbleitern: z. Physik. Chem. Frankfurt Neue Folge, v. 26, 223-247, 325 (1960); v. 27, 48 (1961).

81. Gilchrist, J.D., Extraction metallurgy: Pergamon Press, (1967).

82. Gileadi, E., Electrosorption: N.Y., Plenum Press (1967).

83. Gileadi, E., Conway, B.E., The behavior of intermediates in electrochemical catalysts, in Modern aspect of electrochemistry: Butterworth, v. 3, (1964).

84. Gill, C.B., Straumanis, M.E., Schlechten, A.W., Corrosion of titanium in fused chlorides. Formation of pyrosols: Jour. Electrochem. Soc., v. 102, p. 42, Jan. (1955).

85. Ginatta, Marco V., Fused salt electrolysis. A review of the theory and few of the most recent developments: Paper presented at the Seminar on Electrometallurgy held at Colorado School of Mines, Spring (1969).

86. Goldman, R., Ultrasonic technology: Reinhold Publ. Corp., (1962).

87. Grady, L.D., Methods of separating titanium crystals: U.S. Patent n. 2,875,033, The New Jersey Zinc Co. (1959).

88. Grady, L.D., Production of titanium: U.S. Patent n. 2,821,468, The New Jersey Zinc Co. (1958).

89. Graves, A.D., Private Communication at The Double Layer Conf. at the Univ. of Kentucky, September (1970).

90. Graves, A.D., Ph.D. Thesis, University of London, The Nuffield Research Group, (1967).

91. Graves, A.D., The electrical double layer in molten salts. Part I. The potential of zero charge: J. Electroanal. Chem., 25, 349 (1970).

92. Graves, A.D., Hills, G.J., Inman, D., Electrode processes in molten salts, in Advances in electrochemistry and electrochemical engineering: Interscience, v. 4, p. 117 (1966).

93. Graves, A.D., Inman, D., The electrical double layer in molten salts. Part 2. The double-layer capacitance: J. Electroanal. Chem., 25, 357 (1970).

94. Graves, A.D., Inman, D., Electron transfer processes at the liquid metal-molten alkali halide interface, in Electromotive force measurements in high-temperature system: Proc. of Nuffield Research Group, The Institution of Mining and Metallurgy, London, American Elsevier, p. 183 (1968).

95. Gray, J.J., Carter, A., Chemistry and metallurgy of titanium production: London, Royal Institute of Chemistry, (1958).

96. Greene, N.D., Experimental electrode kinetics: Troy, N.Y., Rensselaer Polytechnic Inst., (1965).

97. Grjotheim, K., High temperature chemistry: Semmering, Hungary, Euchem Conf., Oct. (1967).

98. Grjotheim, K., Krohn, C., The application of molten salts electrolysis in modern technology: Cleveland, Ohio, Paper presented at the Extractive Metallurgy Symposium on Electrometallurgy, Dec. (1968).

99. Grjotheim, K., Krohn, C., Toguri, J.M., Thermodynamic evaluation of activities in molten mixtures of reciprocal salts systems: Transaction of the Faraday Soc., v. 57, n. 467, Part II, Nov. (1961).

100. Grjotheim, K., Toguri, J.M., Thermodynamic treatment of disproportionation equilibria involving complex ion formation in molten salts: TMS, v. 215, p. 403.

101. Guggenheim, E.A., Applications of statistical mechanics: Oxford, Clarendon Press, (1966).

102. Guidelli, R., Thermodynamic considerations of the various contribution to overpotential: The Faraday Soc., p. 1185 (1970).

103. Gurney, R.W., The quantum mechanics of electrolysis: London, Proc. Roy. Soc., A, 134, p. 137 (1931).

104. Hart, P.F., Hills, A.D.W., Tomlinson, J.W., Electrorefining using molten salt electrolysis. Refinability parameter, in Advances in extractive metallurgy: London, Proc. Symp., Elsevier Publishing Co., p. 624, April (1967).

105. Hamer, W.J., Fifty years of electrochemical theory: J. Electrochem. Soc., v. 99, n. 12, 331C, Dec. (1952).

106. Haver, F.P., Baker, D.H., Development of a 10,000 amp cell for electrorefining titanium: U.S. Bureau of Mines, Rept. of Inv. n. 5805 (1961).

107. Head, R.B., The lower chlorides of titanium: their production and reduction to titanium sponge by electrical energy: Proc. Australasian Inst. Min. Met., n. 178, p. 21 (1956).

108. Head, R.B., Electrolytic production of sintered titanium from titanium tetrachloride at a contact cathode: J. Electrochem. Soc., v. 108, p. 806, Aug. (1961).

109. Henrie, T., Baker, D., Electrometallurgy: Cleveland, Ohio, Proc. Extractive Metallurgy Symp. on Electrometallurgy, Dec. (1968).

110. Henrie, T.A., Baker, D.H., A theory on the reduction of titanium chlorides by metallic sodium, in Physical chemistry of process metallurgy, Part 2: Pittsburgh Conf., (1959).

111. Hickman, B.S., Willis, G.M., Titanium carbide anodes for electrodeposition of titanium: Proc. Australasian Inst. Min. Met., n. 178, p. 29 (1956).

112. Hirschhorn, I.S., Commercial production of rare earth metals by fused electrolysis: J. of Metals, p. 19, March (1968).

113. Hoar, T.P., The anodic behavior of metals, in Modern aspect of electrochemistry: Butterworth, v. 2 (1959).

114. Holub, K., Tessari, G., Delahay, P., Electrode impedance without a priori separation of double-layer charging and faradaic process: J. Phys. Chem. 71, p. 2612-8, (1967).

115. Homme, V.E., Wong, M.M., Methods for producing titanium lower chlorides: U.S. Bureau of Mines, Rept. of Inv. 6360 (1964).

116. Ibl, N., Application of mass transfer theory: The formation of powdered metals deposits, in Advances in electrochemistry and electrochemical engineering: Interscience, v. 2, (1966).

117. Inman, D., Bockris, J.O'M., Blomgren, E., The single pulse galvanostatic method applied in the millimicrosecond range to the determination of the exchange current density of $Ag/AgNO_3$-$NaNO_3$-KNO_3 (molten) system: Jour. Electroanal. Chem., 2, p. 506-14, (1961).

118. Ives, D.J.G., Janz, G.J., Reference electrodes. Theory and practice: Academic Press, (1961).

119. Jacobson, H.W., Method of coating and bonding refractory base metal articles: U.S. Patent 3,263,325, E.I. du Pont de Nemours, Wilmington, Del., Aug. 2, (1966).

120. Janz, G.J., Molten salts handbook: Academic Press (1967).

121. Janz, G.J., Dampier, F.W., Lorenz, P.K., Lakshminarayanan, G.R., Tomkins, R.P.T., Molten salts: Volume l, Electrical conductance, density, and viscosity data: NSRDS-NBS l5, U.S. Dept. of Commerce, National Bureau of Standards (1968).

122. Janz, G.J., Reevs, R.D., Molten-salt electrolysis: Transport properties, in Advances in electrochemistry and electrochemical engineering: Interscience, v. 5, (1967).

123. Johnson, R.L., Production of titanium: U.S. Patent n. 3,054,735, The New Jersey Zinc Co.

124. Kardos, O., Gardner, Foulke D., Applications of mass transfer theory: electrodeposition on small-scale profiles, in Advances in electrochemistry and electrochemical engineering: Interscience, v. 2, (1966).

125. Kelley, K.K., Alla D. Mah, Metallurgical thermochemistry of titanium: U.S. Bureau of Mines, Rept. of lnv. 5490, (1959).

126. Kellog, H.H., Duby, P., An improved method of transport numbers measurement in pure fused salts: J. Phys. Chem., p. 191, Jan. (1962).

127. Kenji, Nakano, Namiuchi-Machi, Method for electrolytic manufacture of titanium and aluminum: V.S.. Patent n. 3,213,007 (1965).

128. Kessler, H.D., Titanium and its alloys: Metal Engineering Inst., American Soc. Metals (1968).

129. Kittelberger, W.W., Production of titanium: U.S. Patent n. 2,789,943, The New Jersey Zinc Co. (1957).

130. Kleespies, E., Private Communication.

131. Kleespies, E.K., Henrie, T.A., Reaction rate of titanium-iron alloys and titanium trichloride in molten sodium chloride: U.S. Bureau Mines, Rept. Inv. 7039 (1967).

132. Kleespies, E.K., Henrie, T.A., Electrolytic methods for producing titanium and titanium alloys: U.S. Bureau Mines, Rept. Inv. 6875, (1966).

133. Kleespies, E.K., Henrie, T.A., Preparation of titanium nitride: U.S. Bureau Mines, Rept. Inv. 6447 (1964).

134. Kleespies, E.K., Henrie, T.A., Transfer of selected metals in titanium electrorefining: U.S. Bureau Mines, Rept. Inv. 6437 (1964).

135. Kleespies, E.K., Jackson, J., Henrie, T.A., Reaction rates of the titanium-oxygen alloy system and titanium chlorides in molten sodium chloride: U.S. Bureau Mines, Rept. Inv. 7005, (1967).

136. Kochergin, S.M., Vyaseleva, G.Y., Electrodeposition of metals in ultrasonic fields: N.Y., Consultant Bureau, (1966).

137. Kornilov, I.I., Titanium and its alloys: London, Oldbourne press, n. 10, (1966).

138. Kortum, G., Treatise on electrochemistry: Elsevier (1965).

139. Krishtalik, L.I., Hydrogen overvoltage and adsorption phenomena: Part III. Effect of the adsorption energy of hydrogen on overvoltage and the mechanism of the cathodic process, in Advances in electrochemistry and electrochemical engineering: John Wiley & Sons, v. 7, p. 283 (1970).

140. Kroll, W.J., The present state of titanium extractive metallurgy: Trans. AIME, v. 215, 546 (1959).

141. Kroll, W.J., The fusion electrolysis of titanium: Chemistry and Industry, p. 1314, Oct. 22 (1960).

142. Krol1, W.J., Method for manufacturing titanium and alloys thereof: U.S. Patent 2,205,854, June 25 (1940).

143. Krupp, Fried., GMBH Schmiede und Giesserei, Titan Tikrutan, Blatt 10.6309, 11.6409, 21.6303, 22.6412, 31.6303, 32.6303 (1968).

144. Kushner, J.B., Stress in electroplated metals: Metal prog., p. 88, February (1962).

145. Laitinen, H.A., Gaur, H.C., Impedance and polarization measurements in fused lithium chloride-potassium chloride: Jour. Electrochem. Soc. 104, p. 730-7 (1957).

146. Laitinen, H.A., Randles, J.B., Anomalous faradaic admittance of an electrode due to adsorption of the reactants: Trans. Faraday Soc. 51, p. 54-62 (1955).

147. Laitinen, H.A., Tischer, R.P., Roe, D.K., Exchange current measurements in KU-LiU eutectic melt: Jour. Electrochem. Soc. 107, p. 546-55, (1960).

148. Latimer, W.M., Oxidation potential: N.J., Prentice-Hall (1952).

149. Lawson, F.M., Private Communication, (1970). CSM.

150. Leone, O.Q., Observations in the development of titanium-refining cells: U.S. Bureau Mines, Rept. Inv. 6432, (1964).

151. Leone, O.Q., Nettle, J.R., Baker, D.H., Electrorefining titanium using an internally heated cell: U.G. Bureau Mines, Rept. Inv. 5494, (1959).

152. Levich, V.G., Present state of the theory of oxidation-reduction in solution (bulk and electrode reaction) , in Advances in electrochemistry and electrochemical engineering: Interscience, v. 4, (1966).

153. Lingane, J.J., Electroanalytical chemistry: Interscience Pub., N. Y., (1966).

154. Livanov, V.A., Bukhanova, A.A., Kolachev, B.C., Hydrogen in titanium: N.Y., Daniel Davey Co., (1965).

155. Lorenz, W., Zur allgemeinen theorie des impedanzspektrums potewtialabhangiger phasengrenz reaktionen: Z. Physk. Chem., 218, p. 272-6, (1961).

156. Lorenz, W., Salie, G., Zum mechanismus der elektrochemischen phasengrenz reaktion: Z. Physk. Chem. 218, p. 259-71, (1961).

157. Lowenheim, F.A., Modern electroplating: J. Wiley & Sons, (1963).

158. Luks, K.D., Davis, H.T., Law of corresponding states for the transport properties of molten salts: Minneapolis, Dept. of Chem. Eng., Univ. of Minn., (1966).

159. Luks, K.D., Davis, H.T., On certain recent statistical mechanics theories of the thermodynamics properties of molten salts: Minneapolis, Dept. of Chem. Eng., Univ. of Minn., May (1967).

160. Lumsden, J., Thermodynamics of molten salts mixtures: Academic Press, (1966).

161. Mah, A.D., Kelley, K.K., Gellert, N., King, E.G., O'Brien, C.J., Thermodynamic properties of titanium-oxygen solutions and compounds: U.S. Bureau of Mines, Rept. Inv. 5316, (1957).

162. Mantell, C.L., Electrochemical engineering: McGraw-Hill, (1960).

163. Mashovets, V.P., Revazyan, A.A., Soviet electrochemistry of fused salts: Copsultant Bureau, v. 2, (1961).

164. Matthews, D.B., Ph.D. Thesis, The Electrochemical Laboratory, Univ. of Pennsylvania, (1964).

165. McQuillan & McQuillan, Titanium: Metallurgy of the rarer metals: Butterworths Scientific Publication, n. 4, (1956).

166. Mellgren, S., Opie, W., Equilibrium between titanium metal, titanium dichloride, and titanium trichloride in molten sodium chloride-strontium chloride: Jour. of Metals, v. 9, p. 266, Feb. (1957).

167. Miller, J.A., Titanium; a material survey: U.S. Bureau Mines, Inf. Circ. 7791, (1957).

168. Mohilner, D.M., Thermodynamic treatment of the electro-capillary curve for reversible electrodes and properties of the double layer: Jour. Phys. Chem. 66, p. 724-6, (1962).

169. Molchanova, E.K., Phase diagram of titanium alloys: N.Y., Daniel Davey, (1965).

170. Nettle, J.R., Baker, D.H., Wartman, F.S., Electrorefining titanium metal: U.S. Bureau Mines, Rept. Inv. 5315, (1957).

171. Nettle, J.R., Hill, T.E., Baker, D.H., Electrorefining of titanium from binary alloys: U.S. Bureau of Mines, Rept. Inv. 5410, (1958).

172. Myhren, A.J., Kelton, E.H., Johnson, R.L., Snow, G.E., Grady, L.D., AJldrews, E.W., Reimert, L.J., Barnett, C.E., Electrolytic titanium pilot plant: J. of Metals, p. 38, May (1968).

173. Nippon Mining Co., Copper electrolytic refining with periodic reversed current: U.S. Patent.

174. Nosov, V.A., Ultrasonic in the chemical industry: Consultants Bureau (1965).

175. Nozdreva, V.F., Ultrasound in industrial processing and control: Consultants Bureau, (1966).

176. Ogden, H.R., Titanium, in Rare metals handbook, ed. Hampel, A.C., Reinhold, (1967).

177. Ollard, E.A., Smith, E.B., Handbook of industrial electroplating: American Elsevier (1964).

178. Olson, C.M., Titanium metal production: U.S. Patent n. 2,917,440, DuPont (1959).

179. Opie, W.R., Moles, O.W., A basket cathode electrolytic cell for production of titanium metal: Trans. Met. Soc. AIME , v. 218, p. 646, Aug. (1960).

180. Parson, W.B., Handbook of lattice spacings and structure of metals: Pergamon, v. 1 & 2, (1967).

181. Parsons, R., Equilibrium properties of electrified interphases, in Modern aspect of electrochemistry, Bockris and Conway: Butterworth, v. 1, (1954).

182. Parsons, R., The structure of the electrical double-layer and its influence on the rates of electrode reactions, in Advances in electrochemistry and electrochemical engineering: Interscience, v. 1, (1961).

183. Parsons, R., The kinetics of electrode reactions and the electrode material: Surface Science 2, 418 (1964).

184. Pavan, F., L'applicazione degli ultrasuoni in galvanotecnica: Galvanotecnica, anno XIX, n. 5, p. 83 (1968).

185. Payne, R., The electrical double layer in nonaqueous solutions, in Advances in electrochemistry and electrochemical engineering: ed. P. Delahay: Interscience Publishers, v. 7, (1970).

186. Payne, R., Fundamental problems of the double layer at mercury: Conf. on the electrical double layer and its effects on electrode processes, Univ. of Kentucky, Sept. (1970).

187. Perkins, R.S., Andersen, T.N., Potentials of zero charge of electrodes, in Modern aspects of electrochemistry: Plenum Press, v. 5, (1969).

188. Plonski, I.H., Overvoltage of two stepwise-proceeding electrode reactions under transient conditions: J. Electrochem. Soc., v. 116, p. 944, July (1969).

189. Potter, E.C., Electrochemistry. Principles and applications: London, Cleaver-Hume Press, (1961).

190. Priscu, J.C., Private Communication.

191. Priscu, J.C., Titanium electrowinning cell: Paper presented at the Extractive Metallurgy Symposium on Electrometallurgy held in Cleveland, Ohio on Dec. 2, (1968).

192. Priscu, J.C., Electrolytic cell for the production of titanium: U.S. Patent n. 3,282,822, Titanium Metals Corp. of America (1966).

193. Prisekina, T.N., Kuznetsov, V.A., Malyutina, N.P., Influence of temperature on the zero-charge potentials of certain metals in molten lithium and potassium chlorides: Sov. Electrochem, 2, 1194 (1966).

194. Rand, M.J., Reimert, L.J., Electrolytic titanium from $TiCl_4$: J. Electrochem. Soc., v. III, n. 4, p. 429, April, (1964).

195. Randles, J.E.B., White, W., Reaction of metal ions at mercury electrodes in fused salts: Z. Elektrochem., 59, p. 666 (1955).

196. Raney, B.B., Titanium group metals: U.S. Patent n. 3,152,885, Chicago Development Co., (1964).

197. Raub, E., Muller, K., Fundamentals of metals deposition: Elsevier, (1967).

198. Reed-Hill, R.E., Physical metallurgy principles: Princeton, Van Nostrand, (1966).

199. Reimert, L.J., Fatzinger, E.A., Production of titanium: U.S. Patent n. 2,975,111, The New Jersey Zinc Co., (1961).

200. Reimert, L.J., Production of titanium: U.S. Patent n. 3,082,159, The New Jersey Zinc Co., (1963).

201. Reimert, L.J., Fatzinger, E.A., Electrolytic production of metallic titanium: U.S. Patent n. 2,843,397, The New Jersey Zinc Co., (1958).

202. Rice, System of two diffuse double layers: Phys. Rev., 35, 1051 (1928); Z. Phys. Chem., v. 30, 1501, (1926).

203. Rose, R.M., Shepard, L.A., Wulff, J., The structure and properties of materials; Vol. IV, Electronic Properties: John Wiley & Sons, (1966).

204. Rossini, F.D., Thermodynamics and physics of matter: Princeton Univ. Press, (1955).

205. Rozenberg, L.D., Kazantsev, V.F., Makarov, L.O., Yakhimovich, D.F., Ultrasonic cutting: N.Y., Consultant Bureau, (1964).

206. Sacher, E., Laidler, K.J., Theories of elementary homogeneous electron-transfer reactions, in Modern aspect of electrochemistry: Butterworth, v. 3, (1964).

207. Schaefer, J.C., Preparation of titanium by flouride electrolysis: J. Electrochem. Soc., p. 700, Dec. (1955).

208. Schlain, Electrodeposition of high temperature materials: Paper presented at AIME, Denver Annual Mtg., Feb. (1970).

209. Schlechten, A.W., Straumanis, M.E., Gill, C.B., Deposition of titanium coating from pyrosols: J. Electrochem. Soc., v. 102, p. 81 (1955).

210. Schuldiner, S., Hydrogen overvoltage on bright platinum: J. Electrochem. Soc., v. 99, p. 488, Dec. (1952).

211. Schultz, F.J., Buck, T.M., Electrolytic method for refining titanium metal: U.S. Patent n. 2,904,427, National Lead Co., (1959).

212. Senderoff, S., Electrodeposition of refractory metals: Metallurgical Reviews, v. 11, p. 97 (1966).

213. Senderoff, S., Brenner, A., Electrolytic titanium: J. Electrochem. Soc., v. 99, p. 223C, Aug. (1952).

214. Senderoff, S., Mellors, G.W., Electrodeposition of coherent deposits of refractory metals. I. Niobium: J. Electrochem. Soc., v. 112, p. 266, Mar. (1965).

215. Senderoff, S., Mellors, G.W., The electrodeposition of coherent deposits of refractory metals. II. The electrode reaction in the deposition of tantalum: J. Electrochem. Soc., v. 112, p. 840, Aug. (1965).

216. Senderoff, S., Mellors, G.W., The electrodeposition of coherent deposits of refractory metals. III. Zirconium: J. Electrochem. Soc., v. 113, p. 60, Jan. (1966).

217. Senderoff, S., Mellors, G.W., The electrodeposition of coherent deposits of refractory metals. IV. The electrode reactions in the deposition of niobium: J. Electrochem. Soc., v. 113, p. 66, Jan. (1966).

218. Sheng-Tai, Shih, Hydrogen overvoltage on titanium: Ph.D. Thesis, Univ. of Missouri, (1954).

219. Shih, S.T., Straumanis, M.E., Schlechten, A.W., Deposition of titanium from titanium-oxygen alloys on copper, iron, and mild steel: J. Electrochem. Soc., v. 103, p. 395 (1956).

220. Sibert, M.E., Production of titanium: U.S. Patent 2,974,092, Horizon Titanium Corp., Princeton, N.J., Mar. 7, (1961).

221. Sibert, M.E., Steinberg, M.A., Electrodeposition of titanium on base metals: J. Electrochem. Soc., v. 102, p. 641, Nov. (1955).

222. Silverman, L., Thermal conductivity data presented for various metals and alloys up to 900°C: J. Metals, N.Y., v. 5, 631 (1953).

223. Sinha, H. N., A method of preparing titanium trichloride: Proc. Australasian Inst. Min. Met., n. 178, p. 7, (1956).

224. Slatin, H.L., Electrolytic production of multivalent metals from refractory oxides: U.S. Patent n. 2,861,030 (1958).

225. Sluyters-Rehbach, M., Sluyters, J.H., On impedance of galvanic cells: Rec. Trav. Chim., 83, p. 967-975, (1964).

226. Sluyters-Rehbach, M., Timmer, B., Sluyters, J.H., On impedance of galvanic cells: Rec. Trav. Chim., 82, p. 553-564, (1963).

227. Snow, G.E., production of titanium: U.S. Patent n. 2,898,276, The New Jersey Zinc Co., (1959).

228. Snow, G.E., Electrolytic cell for production of titanium: U.S. Patent n. 2,998,373, The New Jersey Zinc Co., (1961).

229. Snyder, L.E., Electrolytic production of titanium: U.S. Patent n. 3,274,083, Titanium Metals Corp. of America, (1966).

230. Socci, M., Zuliani, G., Cristofanelli, G., Metallurgia primaria del titanio con particolare riguardo alla fabbricazione di polveri per sinterizzazione: Milano, Giornata di studio sul Titanio. Centro di studio per le leghe leggere. Associazione Italiana di Metallurgia. Sept. (1969).

231. Steinberg, M.A., Carlton, S.S., Wainer, E., Preparation of titanium by flouride electrolysis: J. Electrochem. Soc., p. 332, June (1955).

232. Stetkewicz, J.D., Studies on the hydrolysis of titanium sulfate solutions by means of refractive index and viscosity measurements: Columbia University, Ph.D. Thesis, (1939).

233. Staumanis, M.E., Cheng, C.H., Schlechten, A.W., Hydrogen evolution from dissolving titanium-oxygen alloys in hydrofluoric acid and the constitution of Ti-O alloys: J. Electrochem. Soc., v. 103, p. 439, (1956).

234. Straumanis, M.E., Shih, S.T., and Schlechten, A.W., The mechanism of deposition of titanium coatings from fused salt baths: J. Electrochem. Soc., v. 104, p. 17, Jan. (1957).

235. Sundheim, B.R., Fused salts: McGraw-Hill, (1964).

236. Svanstrom, K.A., Opie, W.R., Electrolytic production of titanium: U.S. Patent n. 2,749,295, National Lead Co., (1956).

237. Thomas, N.T., Nobe, Ken, Kinetics of the hydrogen evolution reaction on titanium: Jour. of Electrochem. Soc., v. 117, p. 622, May (1970).

238. Timax Associates, Electrolytic process for production of titanium metal: U.S. Patent n. 3,137,541, Slatin, H.L., (1964).

239. Titanium Metals Corporation of America, Engineering bulletins.

240. Townsend, D., The fluoride plating process for niobium: Paper presented at AIME, Denver Mtg., Feb. (1970).

241. Ukshe, E.A., Investigation of the electric double layer in salts melts: Electrochim. Acta. 9, p. 431-9, (1964).

242. Ukshe, E.A., Bukun, N.G., Measurements of capacitance of electrical double layer in molten salts: Russian Jour. of Physical Chem., v. 37, 890 (1963).

243. Ukshe, E.A., Bukun, N.G., Leikis, D.I., Frumkin, A.N., Investigations of the electric double-layer in salts melts: Electrochimica Acta., v. 9, p. 431, (1964).

244. Van Rysselberghe, Some aspects of the thermodynamic structure of electrochemistry, in Modem aspects of electro- chemistry: Plenum Press, v. 4, (1966).

245. Van Vlack, L.H., Elements of materials science: Addison-Wesley, (1967).

246. Vermilyea, D.A., Anodic films, in Advances in electro-chemistry and electrochemical engineering: Inter-science, v. 3, (1963).

247. Vetter, K.J., Electrochemical kinetics. Theoretical and experimental aspects: Academic Press, (1967).

248. Wagner, C., The electromotive force of galvanic cells involving phases of locally variable composition, in Advances in electrochemistry and electrochemical -- engineering: Interscience, v. 4, (1966).

249. Wahl, A.C., Chemistry by computer: Scientific American, p. 54, April (1970).

250. Weir, W.D., Enke, C.G., The current-impulse relaxation technique and the kinetics of rapid electrochemical reactions: Jour. Phys. Chem., 71, p. 275-9, (1967).

251. Westinghouse, Electrorefining of copper in periodic reversed current: U.S. Patent.

252. Westinghouse, Ultrasonics: Westinghouse.

253. White, R.L., Thermal conductivity of molten salts: Univ. of Minn., Ph.D. Thesis, July, (1967).

254. White, L.R., Davies, H.T., Thermal conductivity of molten alkali nitrates: J. Chem. Phys., v. 47, n. 12, 5433, Dec. 15, (1967).

255. Williams, S.C., Report on titanium. The ninth industrial metal: Ann Arbor, Mich., Edwars Brothers, Inc., (1965).

256. Wong, M.M., Campbell, R.E., Fleck, D.C., Baker, D.H., Electrolytic methods of preparing cell feed for electrorefining titanium: U.S. Bureau Mines, Rept. Inv. 6161 (1963).

257. Worner, H.W., Technology of titanium: Proc. Australasian Inst. Min. Met., N.S. n. 158-159, p. 89 (1950).

258. Worner, H.W., Cordner, The extraction of titanium: Proc. Australasian Inst. Min. Met., N.S. vol., n. 158-159, p. 65 (1950).

259. Wurm, J.G., Gravel, L., Potvin, J.A., The mechanism of titanium production by electrolysis of fused halide baths containing titanium salts: J. Electrochem. Soc., v. 104, p. 301, May (1957).

260. Yarnitzky, C., Anson, F.C., Mechanism of charging and discharging ionic double layers at electrodes: J. Phys. Chem., v. 74, n. 16, p. 3123, (1970).

261. Young, L., Zobel, F.G.R., Anodic and electronic currents at high fields in oxide films, in Modern aspects of electrochemistry: Plenum Press, v. 4, (1969).

262. Zelikman, A.N., Krein, O.E., Samsonov, G.V., Metallurgy of rare metals: Oldbourne Press, (1966).

263. Ziman, J.M., Electrons in metals: London, Taylor & Francis Ltd., (1962).

264. Hume-Rothery, W., Smallman, Haworth, Structure of metals and alloys: The Metal and Metallurgical Trust, London (1969).

265. Hampel, C.A., Rare Metals Handbook: Reinhold Publishing Co. London (1967).

266. Temkin H., Acta Physicochim., 20 (1945) 411.

267. Grjotheim.,K., Krohn,C., Nebell,H., Petrucci,S., The relative electrochemical potentials of aluminum and sodium in molten alkali halides: Institute of Inorganic Chemistry The Technical University of Norway, Trondheim, Norway, (1965)

268. Rosental, K.Y, Veselowskiy, V.Y., Dokl. Akad. Nauk SSSR 111, 637 (1956). [See also Vetter pag. 631].

269. Baker D. H., Neelameggham R., Some observations of factor in encing the electrolytic plating of Titanium: Paper presented at the A.I.M.E 1970 Feb., Denver, Colorado,meeting.

270. "Physical chemistry of molten salts and slags" Proceedings Academy of science USSR, Nov. 1960, USA-tr-5948

APPENDIX

THE ANODIC OXIDATION OF TITANIUM

INTRODUCTION

The literature regarding the anodization of titanium metal in aqueous electrolytes is quite extensive, but the authors appear to be divided into two groups, as far as the interpretation of the nature of the titanium surface layer is concerned.

One group supports the belief that the cause of the change in color of the anodically treated Ti surface is due merely to an optical phenomenon produced by the rearranging in orientation of the metal atoms of the surface in presence of an electric field.

The other group, mainly Russian researchers,[268] are suggesting the idea that the colored surface layer is a titanium oxide; however, they do not bring a forward convincing explanation for this.

To gain a better understanding of the electrode reactions, the Hydrogen Overpotential theories will be briefly reviewed, and a physical concept for the Activation Energy Barrier will be proposed.

HYDROGEN OVERVOLTAGE

Experimental Procedure

The electrolyte was a 2N H_2SO_4 solution in triple distilled water, 500 ml total volume. The Pb anode had 40 cm^2 of immersed area facing the cathode (the anode back was masked). The materials used as cathodes were: Cu, Al, Fe, Pb, and PbO_2 and masked to obtain 10 cm^2 of total immersed area facing the anode. The interelectrode distance was 25 mm. The electrolyte temperature was kept constant at 27 ± 0.5°C.

A one hour preelectrolysis was performed before each experiment, in order to allow the formation of a thick film of lead oxide on the Pb anode surface. The cathode metal surface roughnesses were equivalent to a cold-worked 1/16 in. sheet.

A periodically reversed electrolysis was performed on each of the cathodes in order to activate their surfaces and eliminate some impurities from the surfaces. Then, varying the current density from 0.002 to 0.1 Amp/cm^2, the respective values of cell voltages were recorded. This was repeated five times for each of the different cathodes. The above procedure has been repeated, varying the temperature, with an aluminum cathode. The results are summarized in figures 1A - 6A.

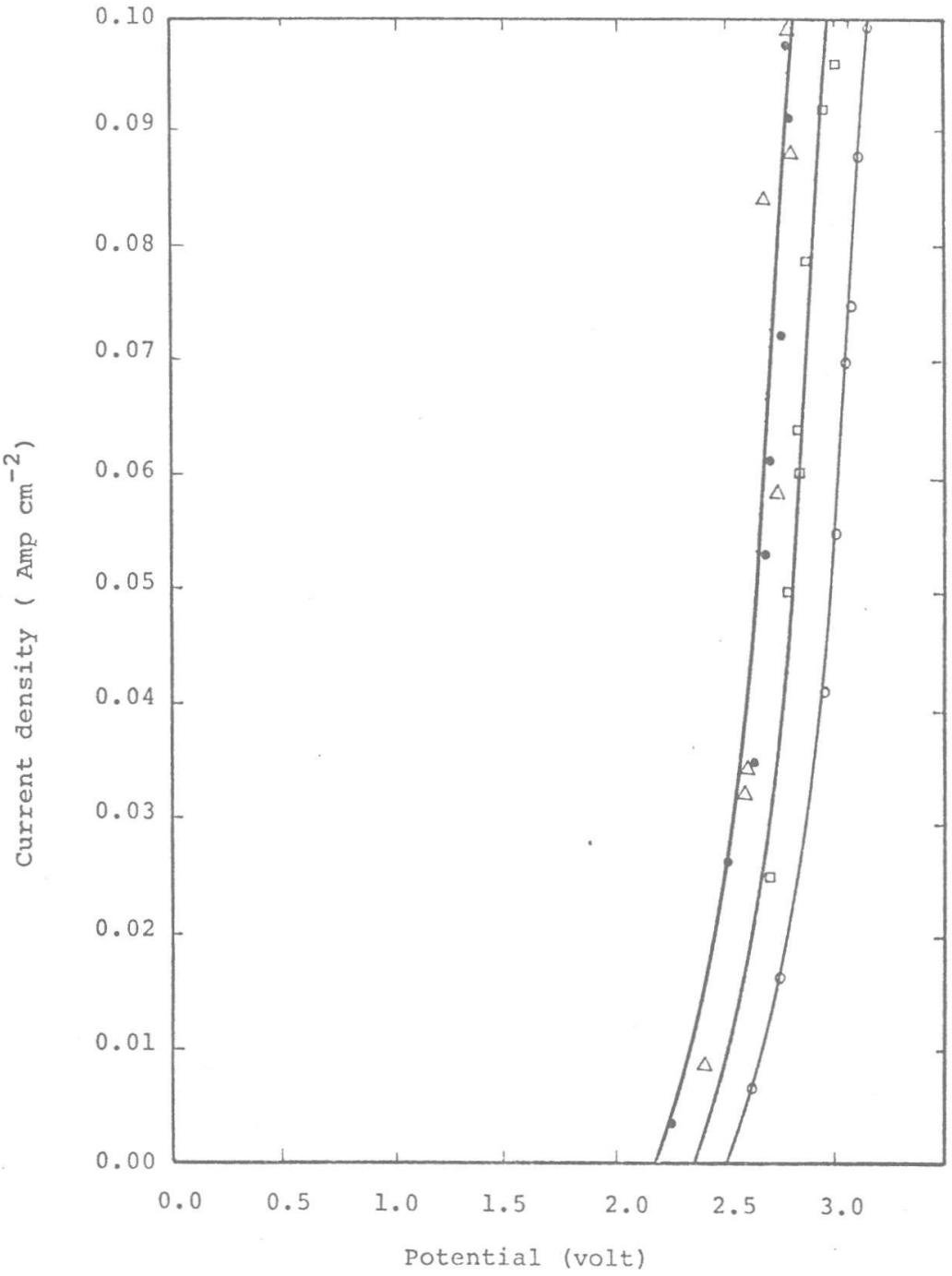

Fig. 1A - Effect of the cathode materials and of current density on hydrogen overpotential; where Pb ○ , Al □ , Fe △ , Cu ●

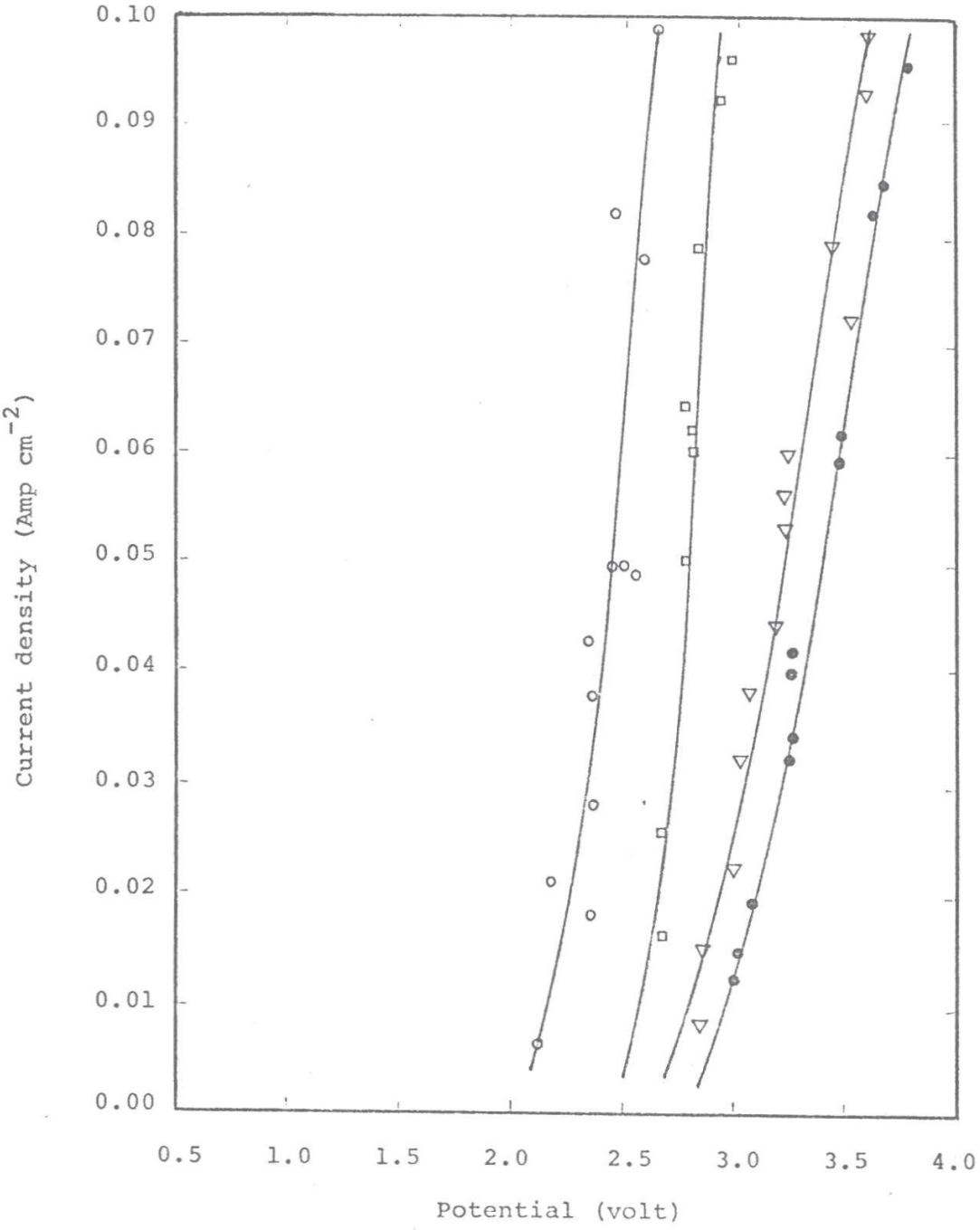

Fig. 2A - Effect of temperature changes with Al cathode; where ○(55-40), △(40-20), □(20-5), ●(5-0.5)°C

indicate four temperature ranges.

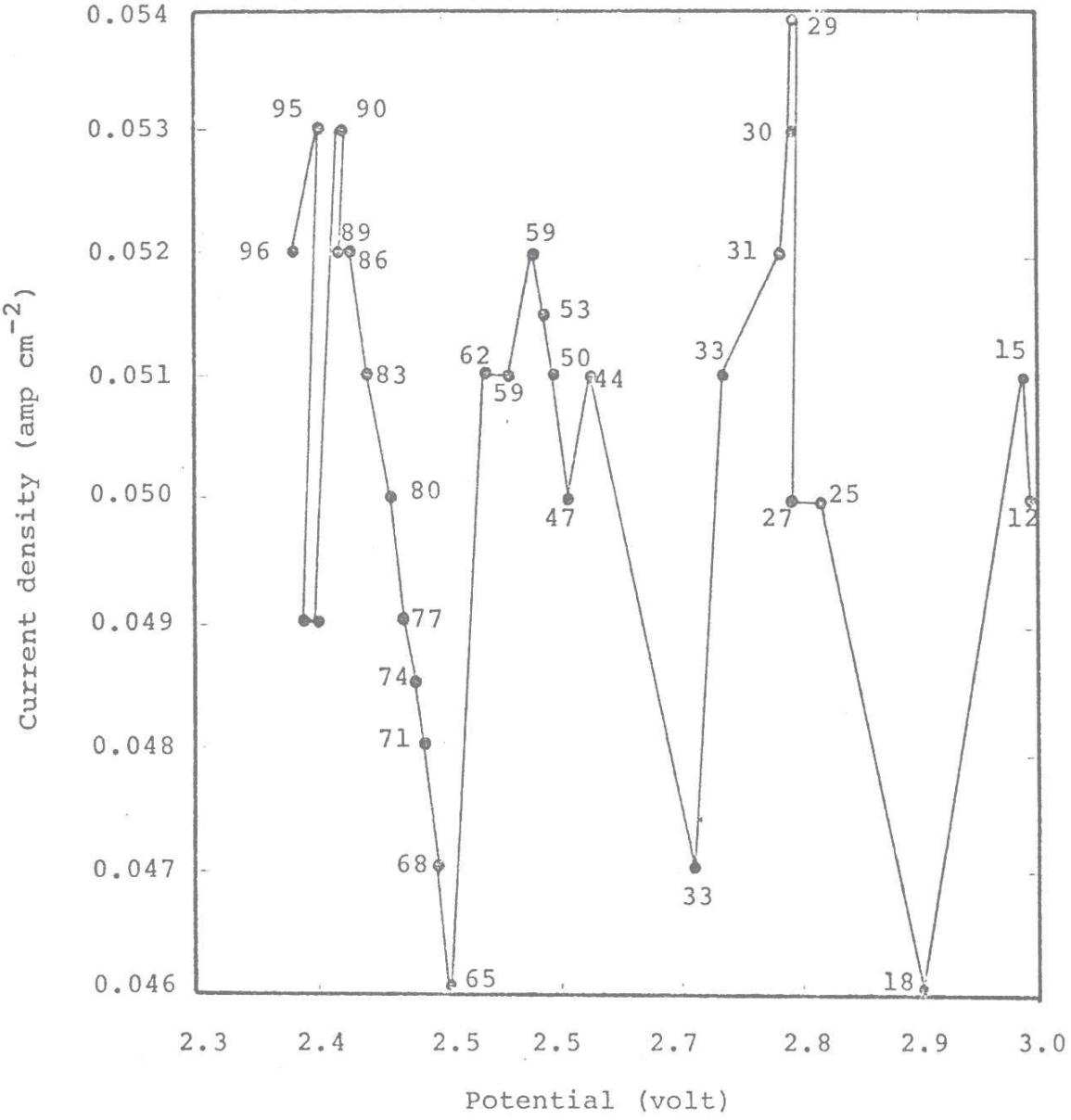

Fig. 3A - Effect of temperature change from 100 to 10°C with Al cathode. The numbers are temperatures in degree centigrade.

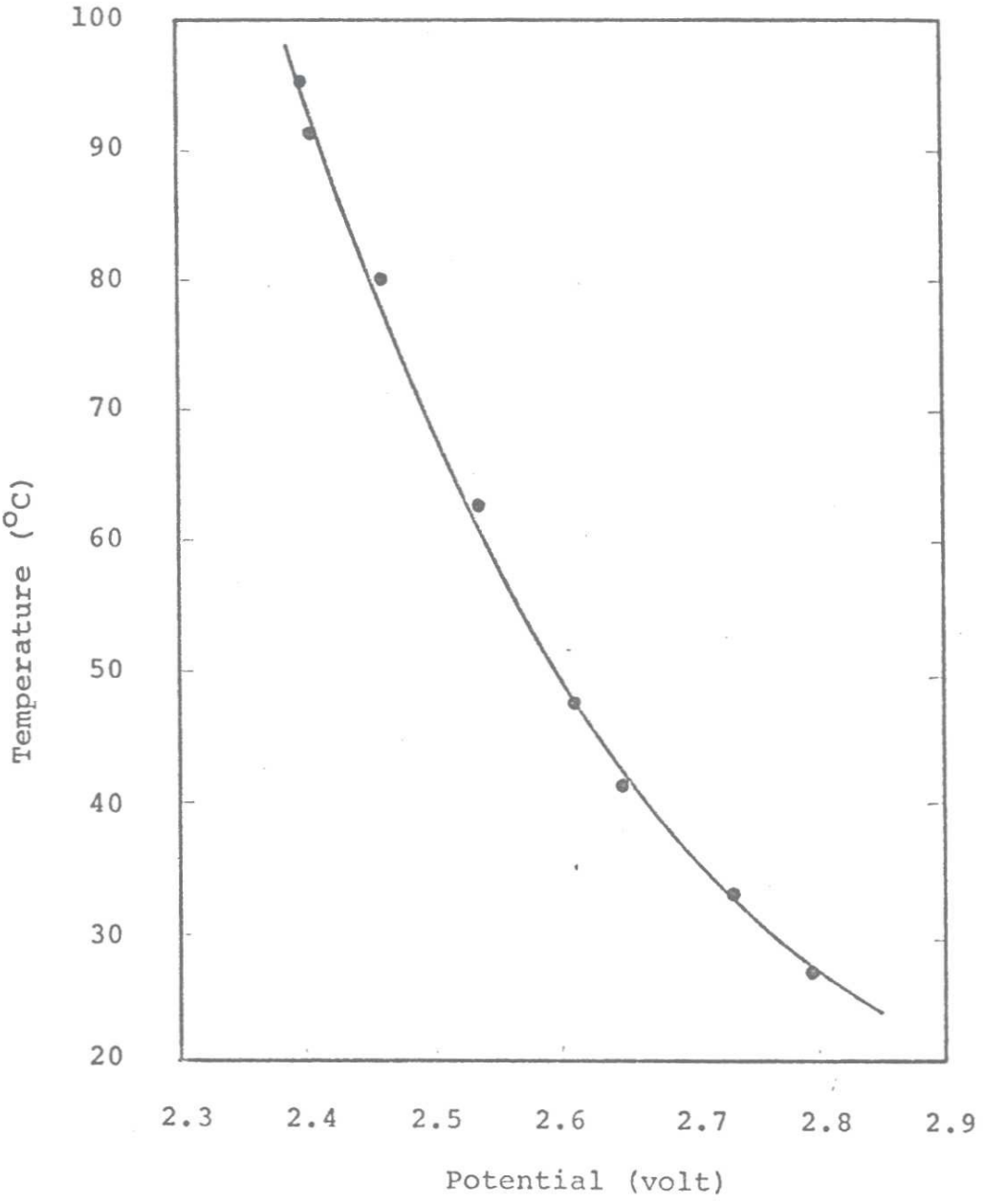

Fig. 4A - Elimination of the current density change effect from the data of Fig. 2A and 3A. The curve represents the relationship between overpotential and temperature at a constant current density (0.05 amp cm^{-2})

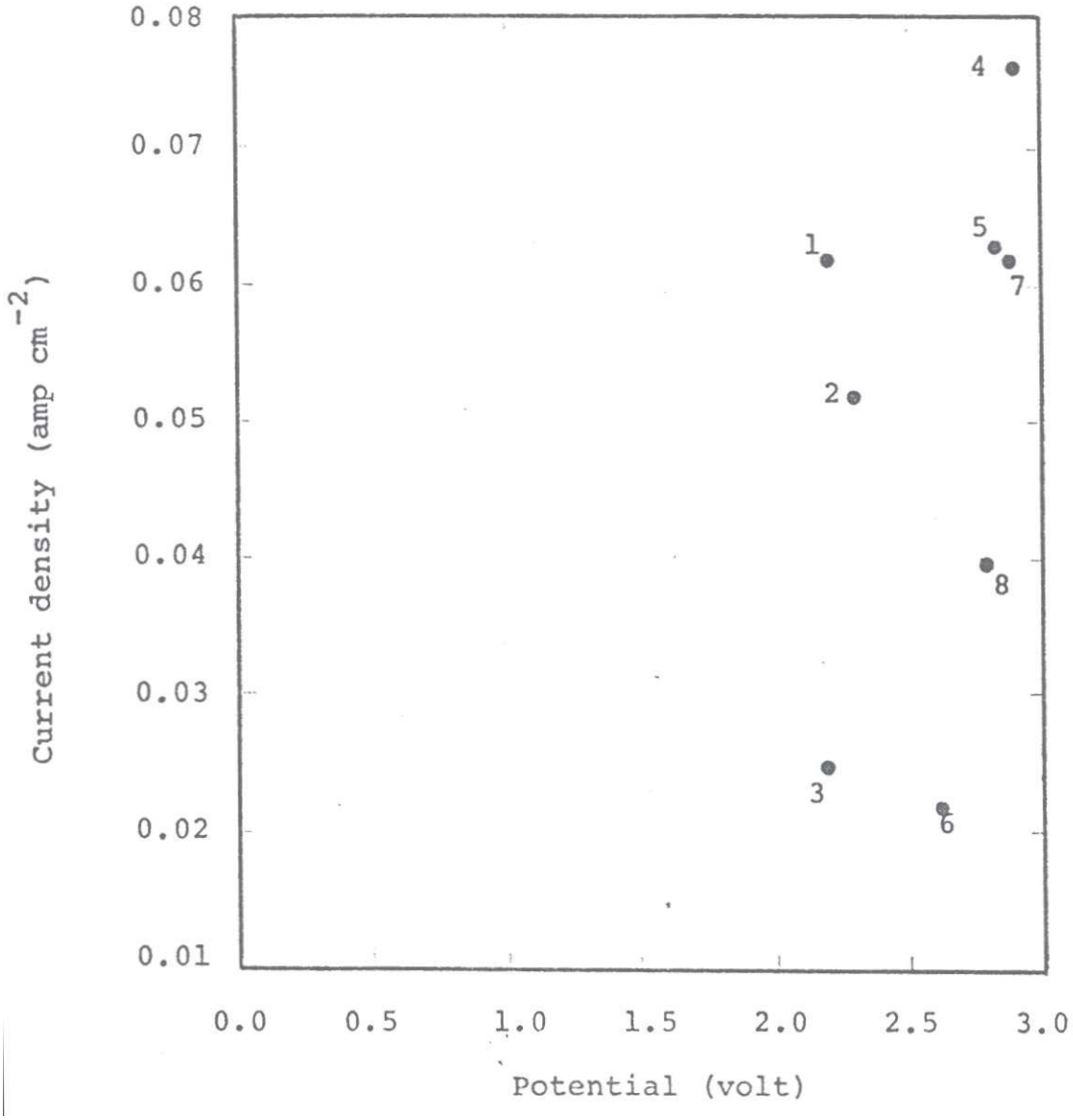

Fig. 5A - Effect of oxide on cathode's surface (PbO_2). The numbers indicate the time sequence of the readings as the oxide reduction proceeds.

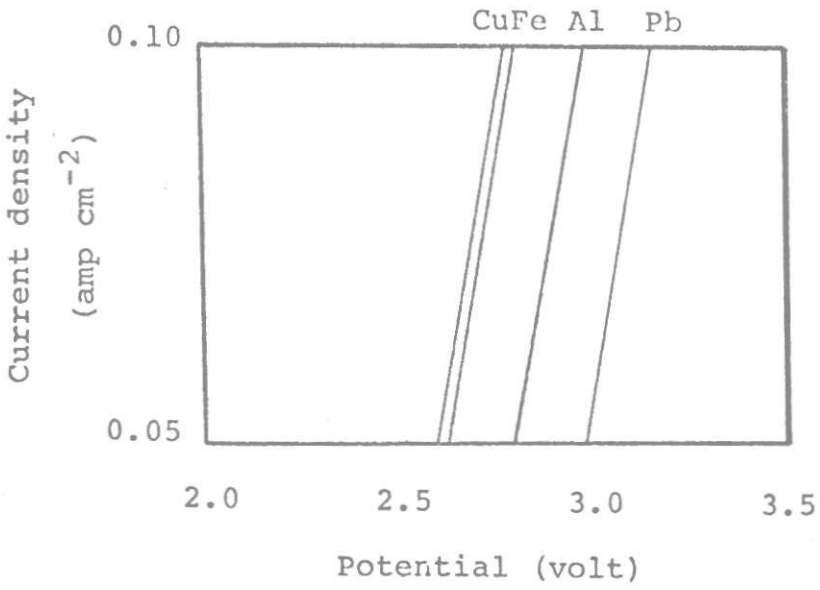

Total cell voltage readings from this investigation.

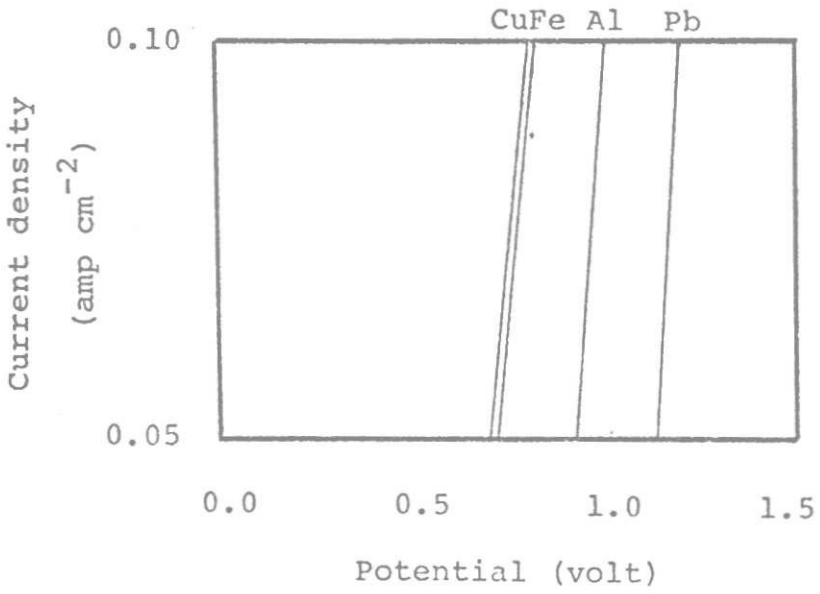

Fig. 6A - Average of literature values of hydrogen overvoltage.

Discussion

1) Effect of Cathode Materials and Current Density on Hydrogen Overpotential

Maximum attention has been paid to keep all conditions constant during the period of the experiments, except for the nature of the cathode and the current density. Therefore, we can be sufficiently certain that voltage variations at a given current density are entirely due to Hydrogen Overpotential on different metals. To analyze the experimental results, since the HOP is a dynamic phenomenon, we have to choose a suitable current density to allow the electrolysis to occur at a "practical" rate.

If a current density of 0.05 Amp/cm2 is chosen, fig. 1A shows that, under the conditions studied, the maximum overpotential can be obtained on a lead cathode. The aluminum cathode readings follows at about 0.2 Volt less than Pb. Copper and iron are almost on the same path at approximately 0.2 Volt less than Al.

Comparing these results to those collected by Mantell[162] from various literature sources (figure 6A good agreement is obtained. Hence, it is seen that the Hydrogen Overpotential is a function of the cathode material and of current density.

2) Effect of Temperature on Hydrogen Overpotential

The results shown on Fig. 2A-3A have been obtained using the aluminum cathode, under the same overall conditions,

only varying the temperature. Aluminum was chosen because of its mechanical properties, its surface reproducibility and because it is representative of the reactive metals. Fig. 2A represents the low temperature range: 0.5-55.0°C. Fig. 3A represents the high temperature range: 25.0-96.0°C.

The tendency of HOP to decrease with increasing temperature is clearly evident if the effect of current density change is eliminated from the experimental data. This is shown on fig. 4A in which choosing a constant current density of 0.05 Amp/cm^2 the temperature dependence of HOP can be fully appreciated. This is another very important fact that will be used in the development of the mechanism that follows.

3) Effect of Oxide Layer on Cathode Surface

This experiment has been performed in a cell in which both the anode and the cathode were initially of Pb electrolytically coated with a film of lead oxide. All other conditions were the same as in the previous experiments. The readings shown in fig.5A have been taken at almost constant intervals of about 30 sec. At the end of the work period the surface of the cathode has been found to be of clean Pb while the anode was still coated with lead oxide. These readings are in sequence with increasing voltage, starting from the initial of 2.2 Volt (lead oxide on cathode) to the final of 2.9 Volt (clean Pb cathode), with a current density of 0.062 Amp/cm^2. Hence, there is a difference of 0.7 Volt to

be accounted for. This effect can be explained as follows:

a) Lead oxide reduction:	ε°	$n\varepsilon^\circ$
a.r. $2H_20 \rightarrow O_2 + 4H^+ + 4e^-$	-1.229	-4.92
c.r. $Pb0_2 + 4H^+ + 2e^- \rightarrow Pb^{++} + 2H_20$	+1.46	+2.92
c.r. $Pb^{++} + 2e^- \rightarrow Pb$	-1.263	-2.526
Cell $Pb0_2 \rightarrow O_2 + Pb$	-1.131 Volt	-4.526

The corresponding calorimetric data (National Bureau of Standards, Selected Values of Chemical Thermodynamic Properties) for the reaction are:

$Pb0_2(s) = Pb(s) + O_2(g)$ $\quad \Delta G^\circ_{298} = 52{,}340$ cal

since $\Delta G^\circ_{298} = -nF\varepsilon^\circ$

$$\varepsilon^\circ = \frac{52.340 cal}{2\, equiv.(23{,}060 cal/equiv.volt)} = -1.131 Volt$$

which confirms that the above reaction truly represents the electrolytic reduction of lead oxide, previously obtained by electrolytic oxidation of Pb metal. If we compare this to the electrolysis of water:

a.r. $H_2O \rightarrow 1/2O_2 + 2H^+ + 2e^-$ = 1.229 Volt

c.r. $2H^+ + 2e^- \rightarrow H_2$ = 0.0

a) first difference (-1.229) - (1.131) = 0.098 Volt appears.

b) At the beginning almost no evolution of hydrogen has been observed, because H^+ was reducing the lead oxide. This is the main reason for the difference of 0.7 Volt, because as

shown on fig. 1A the HOP on Pb is very high. Then gradually, the voltage readings increase proportionally to the decrease of the amount of lead oxide left on the cathode surface, and the hydrogen starts a visible evolution; thus the HOP has an increasing contribution to the total voltage.

At the end of the experiment, after 4 minutes of electrolysis, the last reading shows a voltage close to that of the cell with Pb cathode in fig.1A (approximately 3 volts at 0.062 Amp/cm^2) proving that the cathode surface is of almost pure Pb, but there is still some oxide left.

c) There is also an effect that, on the contrary, tends to lower the voltage as far as the reaction proceeds: it is inherent to the semiconducting properties of the oxide film; that is, the resistance through the film is progressively reduced with the reduction of its thickness.

Considerations of Electrode Processes

In spite of the wealth of information available, it is still impossible to arrive at a clear definition of HOV. A multitude of approaches have been suggested. According to Bockris[27], "The physical meaning of the hydrogen overpotential observed at a given current density is that, when multiplied by αF, it is the amount by which the free energy of activation of the reaction at the reversible potential has to be decreased to make the overall reaction occur at the given rate."

Conway[51] defines the hydrogen overpotential as the extra potential beyond the reversible value required to drive the electrode process at the net rate "i" faster than the forward direction of the process at the reversible potential. Potter[189] points out that, "It is this remarkable sensitivity of hydrogen overpotential to electrode poisoning which explains the diversity of published values for hydrogen overpotential. Moreover, two misconceptions have added to the confusion.

First, it has been insufficiently realized that HOP varies considerably with current density and second, HOP has sometimes been wrongly identified with the excess potential over the reversible value at which bubbles of gas begin to be observed." Latimer[148] on the contrary says that, "In the electrolytic reduction of hydrogen at the cathode, it is possible to measure the excess voltage, over the reversible potential, which is required to liberate hydrogen. This excess voltage is termed overvoltage. The net effect of the overvoltage phenomenon is to cause the hydrogen ion to act as though it were a much less powerful oxidizing agent and hydrogen gas as though it were a much less powerful reducing agent, than the reversible potential would indicate." Schuldiner and Carl Wagner[210] postulate, "The overall mechanism of HOV on platinum cathode would therefore be two parallel reactions; a) a catalytic controlled reaction (double-layer concept), and b) a slow discharge reac-

tion, both of which take place at all current densities. If we conclude that virtual maximum rate of discharge of proton from water molecules < virtual maximum rate of combination of hydrogen atoms < virtual maximum rate of discharge of protons from hydronium ions ...."

This scientific understanding of the HOP can be best summarized with a statement by Bockris[28] who said, "... a much described process for which little mechanism evaluation has been attempted." The main reason for these difficulties in visualizing electrolytic phenomena is due to the failure of classic thermodynamics in explaining such concepts as the Activation Energy barrier, Electric Double Layer, Neutralization conditions. This is because thermodynamics give valuable information only for the initial and final state of the process, being unable to account for the actual path followed by the entities undergoing the process.

We find, in the literature, abuses of Tafel equation concept and misuses of the double layer model to try to present an explanation of electrode processes. But everything fails against such difficulties as:

- reproducibility of solid electrode surfaces (*)
- purity of the electrolyte (**)

---

* The degree of roughness is inversely proportional to the HOP; little can be done to achieve the same degree of roughness on different electrode materials.

** All author's have been careful in achieving the cleanest possible system with all kinds of pretreatments and pre-electrolysis; nevertheless the presence of impurities on the electrode surface, that increase significantly the HOP, cannot be avoided even using analytical grade reagents.

- true electrode area determination (***)

The concept of sorption (ad and ab) have added to the confusion giving rise to definition of such flimsy entities as adion, adatom, embryos, etc., that can eventually be transferred through a relatively long path on the electrode surface. (In this case, how can the growth of a whisker be possible?)

Recent literature, however, has taken a more scientific approach, adopting concepts of Quantum Mechanics, that proved to be very effective in accounting for the unsolved problems of high complexity mentioned above. Following the pioneering work of Gurney[103], Caspari[247], Erdey-Gruz[68], Volmer[247], Brandes[34], Butler[41], Horiuti[29], Polanyi, a few of the researchers in the field such as Gerischer[80], Bocris[29], Mattews[164], and Guidelli[102], have proposed very interesting mechanisms giving precise physical meanings and evaluations to the concept of Activation Energy, Charge Transfer, Double Layer, and Overpotential. Matthews' Ph.D. Thesis[164] (1965) is a representative work of the present level of understanding and will be briefly discussed.

He begins by saying, "In the theory of metal deposition the tendency has been a preoccupation with the relative movements of the ions and its hydration sheaths, neglecting the part played by the electron and omitting to consider the

---

*** The most used method, is the Grahame's double-layer capacitance measurement.

charge on the activate state. On the other end, in the realm of redox reactions one finds a preoccupation with the electron, with ion movement playing a secondary and sometimes negligible role."

The different possible ways of Neutralizing an Ion are:

1) Classical Electron Transfer, over an Energy Barrier, to a Proton in its ground state; but it has been shown that it occurs with a very high energy of activation.

2) The electron has a finite probability of being transferred by quantum mechanical tunnelling, from the metal to the Proton, providing there is an empty electron level of suitable energy to accept the electron. The Standard Heat of reaction ΔH° for electron transfer becomes the Effective Standard Activation Energy by quantum mechanical tunnelling.

3) Activation of H^{+}--OH_2 Bond. To activate in the sense of adding energy $\Delta\varepsilon$ which results in stretching the H^{+}--OH_2 bond. This requires a comparatively lower amount of energy.

In Fig. 7A we superimposed the two Matthews' curves (figures 3 and 4 respectively for electron transfer and proton transfer) to be able to visualize the net effect of the two simultaneous transfer processes. Bearing in mind the Frumkin Double-layer correction, that takes into account both the driving force due to H^{+} and the driving force due

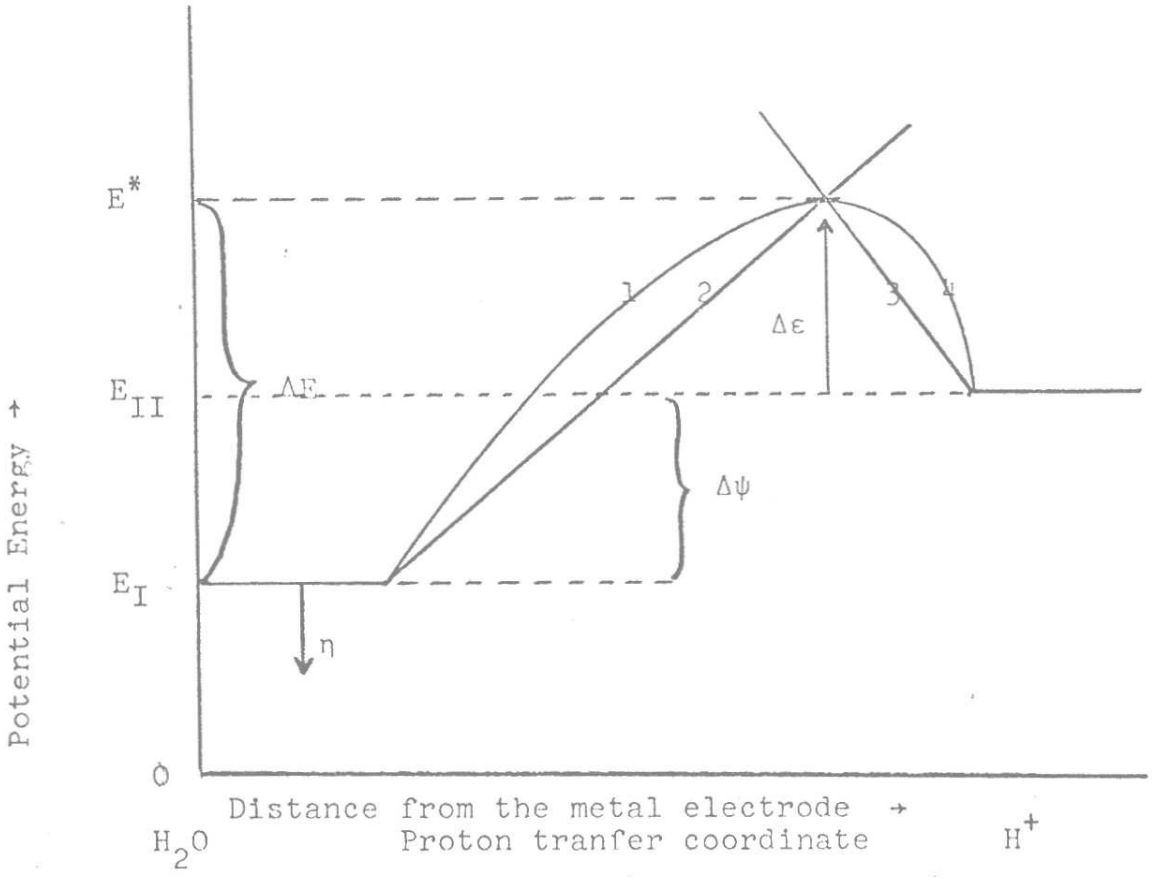

Fig. 7A - Combined Proton and Electron transfer.

Nomenclature

E^* = ground state energy level of activated species for electron transfer.

E_{II} = ground state energy level of final state, electron on energy level of ion.

E_I = ground state energy level of initial state, electron on Fermi level of Metal.

1 = change in potential energy as the electron moves away from the metal phase electrode surface.

2 = potential energy change by stretching H^+--OH_2 bond.

3 = potential energy of interaction between H_2O and H°.

4 = change in potential energy as the electron approaches a ion.

$\Delta\psi$ = reversible standard potential.

$\Delta\varepsilon$ = extra energy added to H^+--OH_2 stretching.

η = hydrogen overpotential.

to the electron, and if we weigh them with the respective charge/mass ratios, it is easy to realize that the maximum of the Activation Energy curve gives the value of the distance from the electrode at which the ion neutralization actually occurs.

The Rate of Proton Discharge depends on:

a) Electron distribution in the metal; i.e., the number of electrons with energy between E and E+ΔE which strike a unit area of the surface in unit time from within the metal.

b) Electron Tunnelling Probability, at energy level E_I. Matthews calculated, using the w.k.b. approximation (Moelyn Hughes), a value of 0.011.

c) Distribution of protons with energy E corresponding to the energy level E_{II} in the H_3O^+ ion. For each vibra-rotational state there will be a corresponding neutralized state E (M..H..H_2O) where the energy depends on ε.

Matthews' Thermodynamic Cycle is:

$(H_3O^+)dl + Me^-$ → Discharge → $(M..H..H_2O)dl$

↑ ↓ Repulsive forces

$M^- + H^+$ (g) + H_2O + aq. M...H + $(H_2O)aq$

↑ ↓ Attractive forces

$M + H^+$ (g) + e^- + H_2O + aq. ← M + H(g) + H_2O + aq

Ionization

assuming that there is no specific adsorption of the H_3O^+ ion and that there is no diffuse double layer.

At this point the literature gives almost no information regarding the additional data needed to draw the Activation curve. In particular, such information as what is the height of the Activation Energy Barrier, that is, what is the value of the energy level that the ion has to reach, before undergoing to Neutralization. Therefore, how much energy, ΔE, has to be supplied?

The aim of this study is precisely to find an answer to that question, or at least to propose a mechanism that explains and visualizes the physical meaning of the above process.

Proposed Method for Calculating the Level of the Activation Energy Barrier

From Fig.4A it can be seen that the cell voltage decreases with increasing temperature and that the relationship is not linear (using only values at temperature above 32°C to avoid the influence of the water's peculiar liquid structure at low temperature). BHy the curve fitting method it is found that the expression representing the cell voltage versus temperature relationship, is a Hyperbole of the form

$$y = \pm(33/31.6)\sqrt{x^2-(31.6)^2}$$

Using the above equation for the hyperbole, the voltage will reach a value of zero at 4,500°C, where:

y = (Voltage + Temperature)/$\sqrt{2}$

x = (Voltage - Temperature)/$\sqrt{2}$

Analyzing more carefully the various contributions to the total voltage we can see that all its components decrease with increasing temperature: Standard emf, IR drop of the electrolyte, Overvoltage.

Now, when a decomposition reaction starts to occur with zero applied potential, we say that the reaction does not need any activation energy, i.e., it is spontaneous at that temperature. Therefore, when $\varepsilon^\circ=0$, $\Delta G^\circ=0$, because $-\Delta G^\circ=nF\varepsilon^\circ$. If one extrapolates the $2H_2 + O_2 = 2H_2O$ line on the Ellingham diagram for the Standard Free Energy of formation of oxides to $\Delta G^\circ=0$, a temperature of 4,200°C will be obtained.

Checking the calorimetric data against the electrochemical data if we use for the reaction of water decomposition $\varepsilon^\circ = -1.229$, for H^+, n = 4, at 25°C:

$\Delta G^\circ_{298} = -4.92 \times 23.060 = -113.5$ kcal/mole O_2

The corresponding Ellingham value for $\Delta G^\circ_{298} = -110.0$ kcal/mole O_2. If we use the electrochemical value, the water decomposition line is shifted by approximately 3.5 kcal in the negative direction, and the temperature for $\Delta G^\circ=0$ is 4,400°C.

Conclusions

The Activation Energy Barrier is a High Temperature Energy Level (in the case of Hydrogen equivalent to 4,400°C) which must be attained by the ionic species involved in

order to force an electron from, or into, an established electronic configuration, so that it can form an atom, at that temperature level.

Since the electrode surface remains at a low (ambient) temperature the heat of the neutral species will be dissipated through the metal as soon as it reaches its surface. Should the thermal conductivity of the surface be low, instantaneous high surface temperatures will result.

This concept will now be used to explain the formation of a titanium oxide at 25°C

ANODIC OXIDATION OF TITANIUM

Experimental Procedure

The electrolyte was a 2N H_2SO_4 solution in triple distilled water. Anolyte volume of 1,300 ml, was separated from the 1,300 ml volume Catholyte, by a liquid junction of approximately 1 cm^2 cross section. The Pb cathode was a flat strip, of about 300 cm^2 of immersed area, 4 cm wide. The Ti anode was a cylindrical bar, commercially pure, with a diameter of 2.85 cm, and approximately 300 cm^2 of immersed area. The electrolyte temperature was kept constant: 26 ± 0.5°C.

The Anodization of Titanium was performed at a potential of 15 Volts, with a current density of 0.003-0.00003 Amp/cm^2. The total current through the liquid junction was 1.0 - 0.01 Amp. The liquid junction was used to slow the rate of anodization of titanium in order to distinguish the various stages of anodization. A cooling coil around the liquid junction, protected the electrolyte from temperature changes. Periodically the Ti anode was extracted from the electrolyte, washed with methyl alcohol, and a color picture of it was taken. At the same time a sample of the anolyte was analyzed. X-ray, Electron diffraction, microprobe analysis and polaroid glasses observations were performed on the anodized titanium surfaces.

At the end of each anodization the Ti bar was cathodically treated reversing the polarity of the cell, to produce a new fresh Ti surface.

Results

The color photographs are representative of the experimental results of this series of experiments.

Figure 8	A taken after	5 minutes at	13 Volts and	0.3 Amp
9	A	60	14	0.16
10	A	180	14.5	0.12
11	A	600	14.5	0.10
12	A	1,000	15.0	0.07
13	A	3,000	15.0	0.05

Fig. 14 A shows the Anolyte color after approximately 1,000 minutes from the beginning of the experiment (yellow).
Fig. 15 A shows the fresh surface of the Ti bar after being cathodically treated for a period of 1,000 min. during which the voltage was constantly at 15, while the current increased with time up to 0.50 Amp at the end of the period. Considerable evolution of hydrogen was noted in the titanium section of the cell, while the yellow colored electrolyte moved on the lead section (anolyte at this stage). Oxygen evolution on Ti surface during anodization was in the form of a single layer of approximately 1 mm diameter bubbles moving upward at a velocity of 0.2 cm/sec. Fig.16A shows on the left-hand side the electron microprobe counts of

Fig. 8A – After 5 minutes at 13 volt and 0.3 amp.

Fig. 9A – After 60 minutes at 14 volt and 0.16 amp.

Fig. 10A – After 180 minutes at 14.5 volt and 0.12 amp.

Fig. 11A – After 600 minutes at 14.5 volt and 0.10 amp.

Fig. 12A – After 1,000 minutes at 15 volt and 0.07 amp.

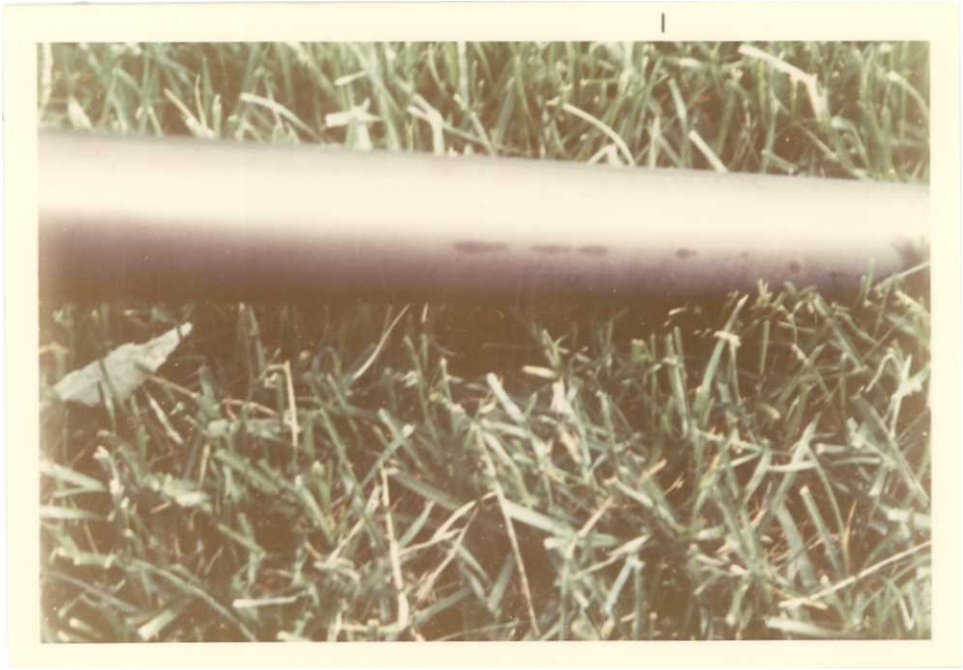

Fig. 13A – After 3,000 minutes at 15 volt and 0.05 amp.

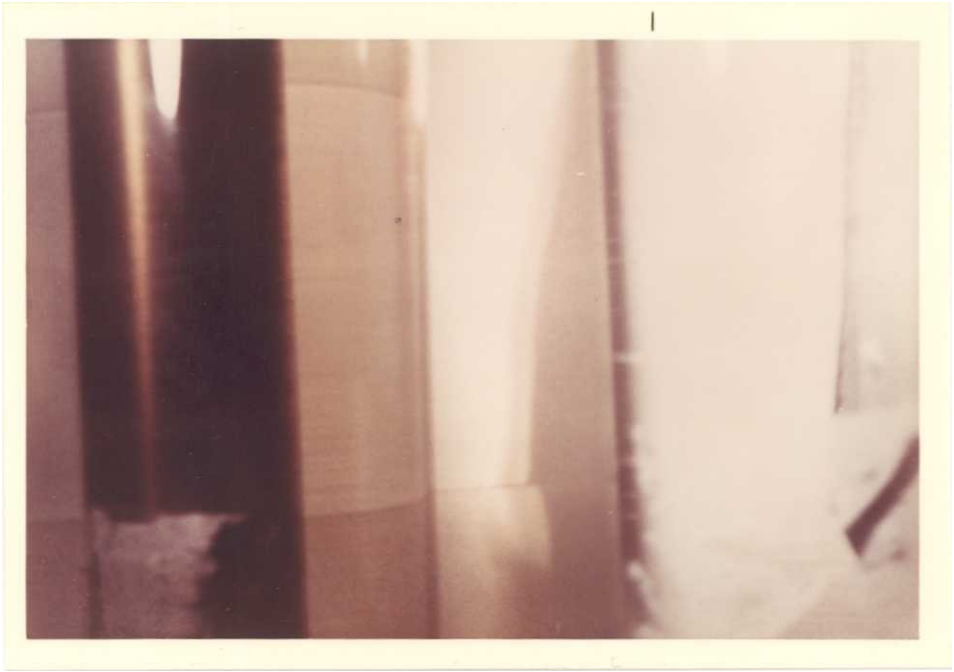

Fig. 14A – On the left is the yellow colored anolyte.

Fig. 15A – Cathodically reduced surface.

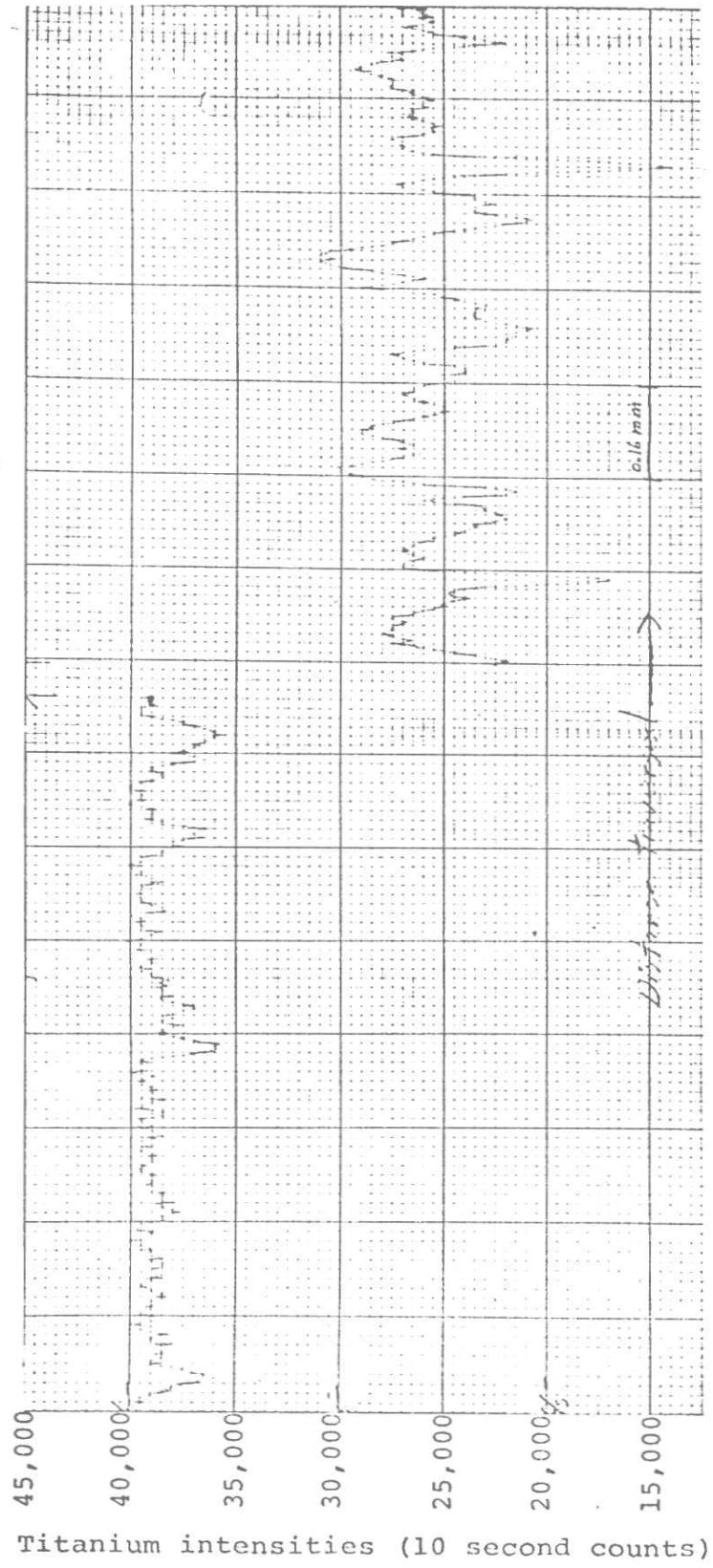

Fig. 16A - Electron microprobe counts of titanium intensities for metallic titanium on the left end side and for anodically treated titanium surface on the right.

surface intensities for fresh Ti from Fig. 15A. On the right-hand side are shown the count intensities for the anode of Fig. 11A. The depth of penetration of 99% of the electrons was (6.5 µm/density of the material) approximately 1.44 µm (14,000 °A).

For the purpose of comparison thermal oxidation of titanium was carried out. A section of the commercially pure Ti bar used for the anodization experiments has been heated in an oxygen atmosphere. The color of the surface of the bar changed with increasing temperature. The sequence of the colors, and the colors themselves, were exactly the same as for anodization with increasing time.

Discussion

The information given by this series of experiments strongly support the titanium oxide view. The reasons are:

1) The titanium thermal oxidation showed the same surface colors and in the identical sequence with respect to the energy build-up process (temperature and current, respectively).

2) The substance giving the yellow color at the Ti anolyte after approximately 1,000 min. of electrolysis, was found to be titanium peroxide hydrated ($TiO_3 \cdot xH_2O$).

3) The electron microprobe counted considerably less titanium atoms on the anodically treated surfaces. Since the instrument used was not sensitive to oxygen there is no

true proof for saying that the remaining atoms were oxygen, but considering the actual conditions of the experiments, we can assume that only oxygen may combine with the metal of the electrode. Furthermore, we cannot determine the stoichiometry of the oxide by looking at Fig. 16A because the microprobe counts all titanium atoms down to a depth of about 14,000 A°, therefore it averages the amount of Ti of the different layers; however, we can be sure that the electrode beam reached well inside the pure titanium metal substrate (thus increasing the apparent amount of Ti) because of the insulating properties of the titanium oxides, i.e., we can be sure that the oxide layer thickness is less than 1.4 μm.

Thus, sufficient evidence has been provided to prove the presence of an oxide layer on the surface of titanium anodes in aqueous acid solution electrolytes.

Barksdale[15] gives the following minimum temperatures for the formation of the various titanium oxides in the presence of oxygen:

TiO	Gold color	150°C
Ti_2O_3	Violet "	250 "
Ti_3O_5	Blue "	350 "
TiO_2	White "	500 "

The question ought to be asked, therefore, how can high temperature compounds, such as various titanium oxides, be formed at 25°C? To answer this question the Excess Energy theory will be proposed. Fig. 17A illustrates grafically the

Nomenclature for Figure 17A

E_{II}= ground state energy level of the ions in the electrolyte at large distance from the electrodes.

E_{I} = ground state energy level of the cathode surface, electrons in the Fermi level of the metal.

E_{III}= ground state energy level of the anode surface.

Ψ^{+} = Galvani potential at the anode interphase, plus the oxygen overpotential, as a function of the distance from the anode.

Ψ^{-} = Galvani potential at the cathode interphase, plus the hydrogen overpotential as a function of the distance from the cathode.

E* = Activation energy level.

AH = activation energy curve for the proton as a function of the distance from the cathode.

AO = activation energy curve for the oxygen ion as a function of the distance from the anode.

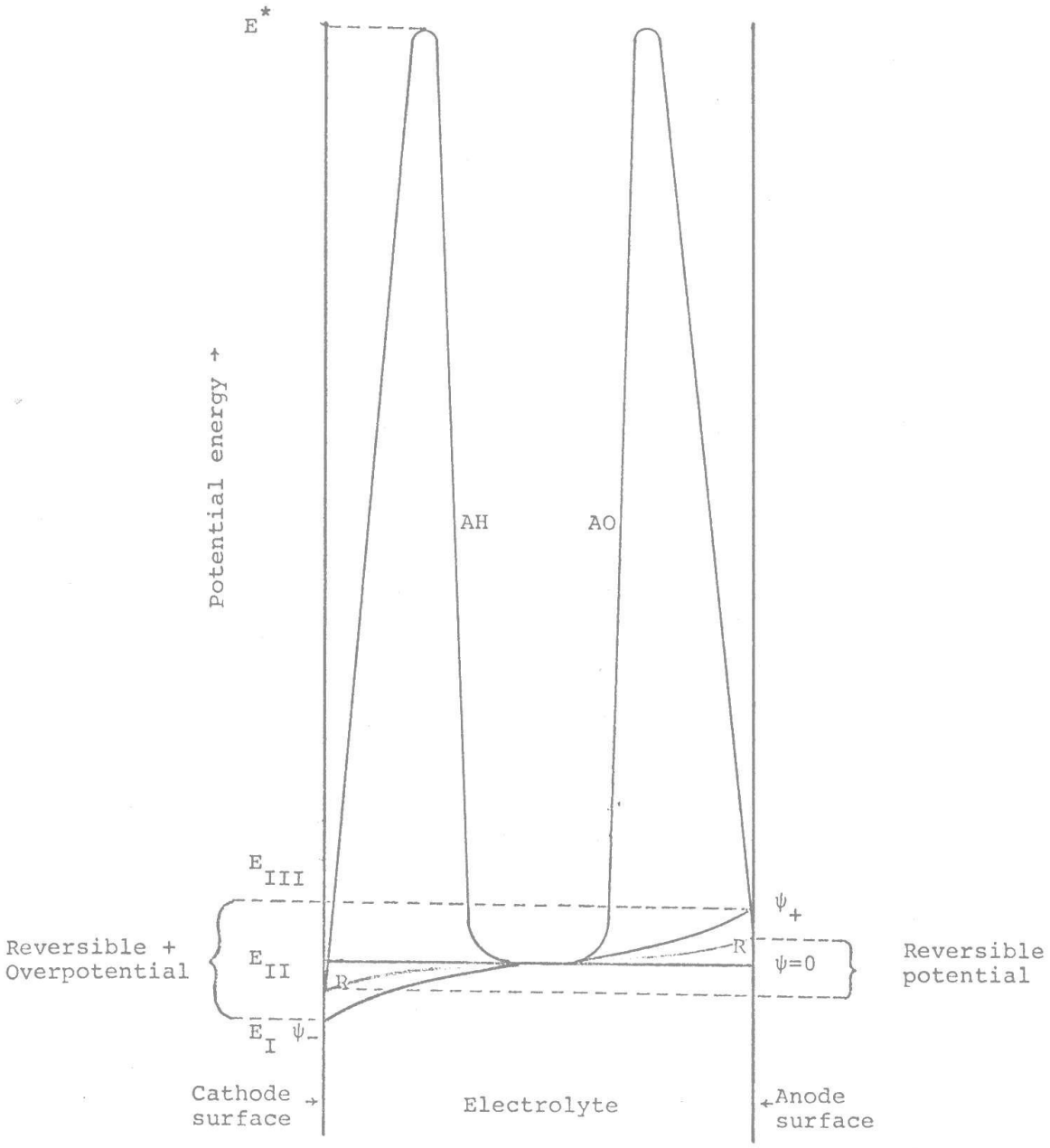

Fig. 17A- Energy changes for the entities taking part in an electrolytic process.

changes in energy levels of the entities taking part in an electrolytic process.

Let us consider first the hydrogen reduction at the cathode surface. The proton in the electrolyte, by means of the mechanism discussed earlier, will have its energy increased (up to the equivalent of 4,400°C) to the activation energy level (curve AH) assuming that the contribution of electron or proton tunnelling are small. At this point we have no more information except for the fact that the hydrogen atom formed is able to reduce the titanium oxide surface layer.

At the anode side, it was shown that the oxygen atom formed is able to oxidize titanium metal.

Since the system was kept constantly at room temperature this phenomenon can be explained in the following manner:

- the ion is activated up to an energy level at which an electron can escape from the solid state electrons valence cloud on the cathode metal surface and be attracted to orbit at the valence level around the ion forming a neutral atom (or viceversa). At this moment the newly formed atom is still at the activation energy level. However, when the atom reaches the electrode surface it is at the lowest energy level of the system. Thus, an amount of energy equal to the difference between the activation energy and the electrode surface energy levels must be dissipated during the atom's

advance from its initial to its final position on the surface, and then through the surface of the electrode. With electrodes having a low thermal conductivity, the dissipation of this Excess Energy will be slow, resulting in a build up of surface energy. When this surface energy has reached a value equivalent to the thermal energy required for the oxidation of the metal, anodic oxidation will take place.

For this reason it is possible to obtain titanium oxides in an electrolitic cell at 25°C.

CONCLUSIONS

1. The Excess Energy theory proves that newly neutralized atoms must have an energy level equivalent to a virtual temperature of several hundred degrees centigrade higher than the electrolytic cell system.

2. If the conductivity of the electrode metal is low, the dissipation of the Excess Energy will be slow and high virtual surface temperatures will be developed. At these temperatures anodic oxidation will take place.